



THE UNIVERSITY OF QUEENSLAND
A U S T R A L I A

Rock and Roll: The Effects of Centre of Mass Movement and Bicycle Lean on the Biomechanics of Cycling

Ross D. Wilkinson

BExSS(Hons)



<https://orcid.org/0000-0003-1439-7742>

*A thesis submitted for the degree of Doctor of Philosophy at
The University of Queensland in 2020
School of Human Movement and Nutrition Sciences*

Abstract

Cyclists frequently use a non-seated posture when accelerating, climbing steep hills, and sprinting, yet the biomechanical difference between seated and non-seated cycling remains unclear. The purpose of the first study incorporated within this thesis was to test the effects of posture (seated and non-seated) and cadence (70 rpm and 120 rpm) on joint power contributions, effective mechanical advantage, and muscle activity within the lower limb during very-high-power output cycling. Fifteen male participants rode on an instrumented ergometer at 50% of their individualised instantaneous maximal power ($10.74 \pm 1.99 \text{ W}\cdot\text{kg}^{-1}$; above the reported threshold for seated to non-seated transition) in different postures (seated and non-seated) and at different cadences (70 rpm and 120 rpm), whilst lower limb muscle activity, full body motion capture, and crank radial and tangential forces were recorded. A scaled, full-body musculoskeletal model was used to solve inverse kinematics and inverse dynamics to determine joint displacements and net joint moments. Statistical comparisons were made using repeated measure, two-way analyses of variance (posture–cadence). Our results showed significant main effects of posture and cadence on joint power contributions. A key finding was that the non-seated posture increased negative power at the knee, with an associated significant decrease of net power at the knee. The contribution of knee power decreased by 15% at both 70 and 120 rpm ($\sim 0.8 \text{ W}\cdot\text{kg}^{-1}$) when non-seated compared with seated. Subsequently, hip power and ankle power contributions were significantly higher when non-seated compared with seated at both cadences. In both postures, knee power was 9% lower at 120 rpm compared with 70 rpm ($\sim 0.4 \text{ W}\cdot\text{kg}^{-1}$). These results evidenced that the contribution of knee joint power to leg power was reduced by switching from a seated to non-seated posture during very-high-power output cycling; however, the size of the reduction is cadence dependent.

Previous research and field observations also suggest that when cyclists ride off the saddle, their centre of mass (CoM) appears to go through a rhythmic vertical oscillation during each crank cycle. Just like in walking and running, the pattern of CoM movement may have a significant impact on the mechanical power that needs to be generated and dissipated by muscle. To date, neither CoM movement strategies during non-seated cycling, nor the limb mechanics that allow this phenomenon to occur have been quantified. In our second study we estimated how much power can be contributed by a rider's body mass at each instant during the crank cycle by combining a kinematic and kinetic approach to measure CoM movement and joint powers of fifteen participants riding in a non-seated posture at three individualised power outputs (10%, 30%, and 50% of instantaneous maximal power output (P_{max})) at two different cadences (70 rpm and 120 rpm). Our analysis revealed that the peak-to-peak amplitude of vertical CoM displacement increased significantly with power output and with decreasing cadence. Accordingly, the greatest peak-to-peak amplitude of CoM displacement ($0.06 \pm 0.01 \text{ m}$) and change in total mechanical energy ($0.54 \pm 0.12 \text{ J}\cdot\text{kg}^{-1}$) occurred under the combination of high-power output and low cadence. At the same combination of high-power output and low

cadence, we found that the peak rate of CoM energy loss ($3.87 \pm 0.93 \text{ W}\cdot\text{kg}^{-1}$) was equal to 18% of the peak instantaneous crank power. Consequently, it appears that for a given power output, changes in CoM energy contribute to peak instantaneous power output at the crank, thus reducing the required muscular contribution. These findings suggest that the rise and fall of a rider's CoM acts as a mechanical amplifier during non-seated cycling, which has important implications for both rider and bicycle performance.

Building off the results of these first two studies we then investigated the effect of lateral bicycle dynamics on lower limb mechanics and rider CoM mechanical energy fluctuations during non-seated cycling. When riding off the saddle during climbing and sprinting, cyclists appear to coordinate the rhythmic, vertical oscillations of their CoM with the side-to-side lean of the bicycle. Is the coordination of these two motions merely a stability requirement, or could it also be a strategy to more effectively generate crank power? In our third study we again combined a kinematic and kinetic approach, this time to understand how different constraints on bicycle lean influence CoM movement and limb mechanics during non-seated cycling. Ten participants cycled in a non-seated posture at a power output of $5 \text{ W}\cdot\text{kg}^{-1}$ and a cadence of 70 rpm under three bicycle lean conditions: unconstrained on rollers (Unconstrained), under instruction to self-restrict bicycle lean on rollers (Self-Restricted) and constrained in a bicycle trainer (Trainer). Bicycle lean angle in the Unconstrained condition was greater than Self-Restricted and in the Trainer. Vertical CoM displacement, peak vertical crank force, and peak instantaneous crank power in the Unconstrained condition were greater than Self-Restricted but similar to in the Trainer. The amount and rate of energy lost and gained by the rider's CoM in the Unconstrained condition was greater than Self-restricted but similar to in the Trainer. The differences in joint power contributions to total joint power (hip, knee, ankle, and upper body) between conditions were inconclusive. We interpret these results as evidence bicycle lean plays an important role in facilitating the production of high crank force and power output during non-seated cycling by allowing a greater non-muscular contribution to crank power.

In summary, these investigations have established a fundamental but new understanding of the underlying mechanics and energetics of the phenomenon of non-seated cycling, while also pointing towards the potentially detrimental influence of self-restricting bicycle lean when cycling in a non-seated posture at high-power outputs. These findings should be of interest to the field of biomechanics, exercise physiology, and motor control, as well as those involved with optimising rider and bicycle performance.

Declaration by author

This thesis is composed of my original work, and contains no material previously published or written by another person except where due reference has been made in the text. I have clearly stated the contribution by others to jointly-authored works that I have included in my thesis.

I have clearly stated the contribution of others to my thesis as a whole, including statistical assistance, survey design, data analysis, significant technical procedures, professional editorial advice, financial support and any other original research work used or reported in my thesis. The content of my thesis is the result of work I have carried out since the commencement of my higher degree by research candidature and does not include a substantial part of work that has been submitted to qualify for the award of any other degree or diploma in any university or other tertiary institution. I have clearly stated which parts of my thesis, if any, have been submitted to qualify for another award.

I acknowledge that an electronic copy of my thesis must be lodged with the University Library and, subject to the policy and procedures of The University of Queensland, the thesis be made available for research and study in accordance with the Copyright Act 1968 unless a period of embargo has been approved by the Dean of the Graduate School.

I acknowledge that copyright of all material contained in my thesis resides with the copyright holder(s) of that material. Where appropriate I have obtained copyright permission from the copyright holder to reproduce material in this thesis and have sought permission from co-authors for any jointly authored works included in the thesis.

Publications included in this thesis

As per UQ policy (PPL 4.60.07 Alternative Thesis Format Options) the following section lists publications that have been included in this thesis.

1. **Wilkinson, Ross D.**, Glen A. Lichtwark, and Andrew G. Cresswell. 2020. The Mechanics of Seated and Nonseated Cycling at Very-High-Power Output: A Joint-Level Analysis. *Medicine & Science in Sports & Exercise* 52(7): 1584-94. doi: 10.1249/MSS.0000000000002285
2. **Wilkinson, Ross D.**, Andrew G. Cresswell, and Glen A. Lichtwark. 2020. Riders Use Their Body Mass to Amplify Crank Power during Nonseated Ergometer Cycling. *Medicine & Science in Sports & Exercise*: Publish Ahead of Print. doi: 10.1249/MSS.0000000000002408

Submitted manuscripts included in this thesis

1. **Wilkinson, Ross D.**, Andrew G. Cresswell, and Glen A. Lichtwark. 2020. Rock and Roll: The Influence of Bicycle Lean on the Mechanics of Non-Seated Cycling. *Journal of Biomechanics*: Under Review.

Other publications during candidature

Conference abstracts

1. **Wilkinson, R.D.** and Lichtwark, G.A., Measuring A Rider's Centre Of Mass Displacement During Non-seated Cycling Using A Single Inertial Measurement Unit. *Annual Meeting of the American-College-of-Sports-Medicine (ACSM)*, San Francisco, CA, United States, 26-30 May 2020.
2. **Wilkinson, R.D.**, Lichtwark, G.A., and Cresswell, A.G., Effect of lateral bicycle dynamics on rider biomechanics during non-seated cycling. *XXVII Congress of the International-Society-of-Biomechanics (ISB)*, Calgary, ON, Canada, 31 July - 4 August 2019.
3. **Wilkinson, R.D.**, Williams, J., Marcus, M., and Carver, T., Effect of chamois design on rider comfort and saddle pressure during sub-maximal cycling. *Annual Meeting of the American-College-of-Sports-Medicine (ACSM)*, Orlando, FL, United States, 28 May - 1 June 2019.
4. **Wilkinson, R.D.**, Lichtwark, G.A., and Cresswell, A.G., Mechanical energetics relating to rider centre of mass motion during non-seated cycling. *42nd Annual Meeting of the American-Society-of-Biomechanics (ASB)*, Rochester, MN, United States, 8-11 August 2018.

5. **Wilkinson, R.D.**, Lichtwark, G.A. and Cresswell, A.G., Stand and deliver: Muscle activity and mechanical energetics of the lower limb during cycling. *Annual Meeting of the American-College-of-Sports-Medicine (ACSM)*, Minneapolis, MN, United States, 29 May - 2 June 2018.
6. **Wilkinson, R.D.**, Lichtwark, G.A., and Cresswell, A.G., Sit, stand, rock and roll: Towards optimal pedalling posture. *Human-Movement-and-Nutrition-Sciences (HMNS) Post-Graduate Conference*, Brisbane, QLD, Australia, October 2018.
7. **Wilkinson, R.D.**, Lichtwark, G.A., and Cresswell, A.G., Sit v stand: Effect of cycling position on lower limb mechanics. *Human-Movement-and-Nutrition-Sciences (HMNS) Post-Graduate Conference*, Brisbane, QLD, Australia, October 2017.
8. **Wilkinson, R.D.**, Lichtwark, G.A., and Cresswell, A.G., Effect of bike sway and rider position on mechanical effectiveness and efficiency in cycling. *Human-Movement-and-Nutrition-Sciences (HMNS) Post-Graduate Conference*, Brisbane, QLD, Australia, October 2016.

Contributions by others to the thesis

Dr Glen A. Lichtwark and Dr Andrew G. Cresswell significantly contributed to the initial concept and ongoing design of the research project, the analysis and interpretation of experimental data, and the critical revision of written work.

Statement of parts of the thesis submitted to qualify for the award of another degree

No works submitted towards another degree have been included in this thesis.

Research involving human or animal subjects

Ethical approval was obtained from the School of Human Movement and Nutrition Sciences Ethics Committee at The University of Queensland (Approval Number(s): HMS16/1409, HMS17/0908). All methods were performed in accordance with the relevant ethical guidelines. Prior to data collection, written informed consent was obtained from all participants. Ethical approval forms can be found in Appendix D.

Financial support

Ross D. Wilkinson was supported by an Australian Government Research Training Program Scholarship.

Keywords

Cycling, biomechanics, non-seated, bicycle lean, standing, centre of mass, pedalling mechanics, joint power

Australian and New Zealand Standard Research Classifications (ANZSRC)

ANZSRC code: 110601, Biomechanics, 90%

ANZSRC code: 110602, Exercise Physiology, 5%

ANZSRC code: 110603, Motor Control, 5%

Fields of Research (FoR) Classification

FoR code: 1106, Human Movement and Sports Sciences, 100%

This work is dedicated to my parents, who sacrificed all they had for the sake of my sporting interests and education. To my family and friends - thank you for your love, endless support, and encouragement. To my mentors and colleagues - I wouldn't have made it this far without your wisdom, generosity, compassion, and patience. I hope this work stands as a testament to the belief that we can learn anything if we persevere.

Contents

Abstract	ii
Contents	ix
List of Figures	xiii
List of Tables	xvi
List of abbreviations and symbols	xvii
1 Introduction	1
2 Literature Review	3
2.1 Part I	3
2.1.1 Transmission and gearing	3
2.1.2 Phases of the crank cycle	4
2.1.3 Geometry of the bicycle	5
2.1.4 Muscle activity	6
2.1.5 Limb mechanics	7
2.1.6 Non-seated posture	14
2.2 Part II	16
2.2.1 Human power output during cycling	16
2.2.2 Centre of mass movement during cycling	17
2.2.3 The effect of changing power output and cadence on crank torque	19
2.3 Part III	21
2.3.1 Balance and steering	21
2.3.2 Lateral bicycle dynamics	22
2.3.3 Stability of a bicycle on treadmills and rollers	24
2.3.4 Effect of bicycle lean on the metabolic cost of cycling	25
3 The Mechanics of Seated and Non-Seated Cycling at Very-High-Power Output: A Joint-Level Analysis.	29

3.1 Abstract	29
3.2 Introduction	30
3.3 Methods	31
3.3.1 Experimental protocol	32
3.3.2 Data collection	33
3.3.3 Data analysis	34
3.3.4 Statistical analyses	36
3.4 Results	37
3.5 Discussion	44
4 Riders Use Their Body Mass to Amplify Crank Power During Non-Seated Ergometer Cycling	49
4.1 Abstract	49
4.2 Introduction	50
4.3 Materials and methods	51
4.3.1 Experimental design	51
4.3.2 Kinematics	53
4.3.3 External forces	53
4.3.4 Mechanical energy and power	54
4.3.5 Statistical analyses	55
4.4 Results	56
4.5 Discussion	64
5 The Effect of Bicycle Lean on the Mechanics of Non-Seated Cycling	69
5.1 Abstract	69
5.2 Introduction	69
5.3 Materials and methods	71
5.3.1 Experimental design	71
5.3.2 Kinematics	72
5.3.3 External forces	72
5.3.4 Mechanical energy and power	73
5.3.5 Statistical analyses	74
5.4 Results	75
5.4.1 Bicycle lean	75
5.4.2 CoM motion and energetics	75
5.4.3 Vertical force	77
5.4.4 Joint power	77
5.4.5 Crank power	77
5.5 Discussion	81

6 Discussion and Summary	85
6.1 Key findings	86
6.1.1 When cycling at high-power output, switching from a seated to a non-seated posture can reduce net mechanical power requirements at the knee joint.	86
6.1.2 When cycling at high-power output in a non-seated posture, raising and lowering the CoM during specific phases of the crank cycle can amplify crank power.	87
6.1.3 When cycling at high-power output in a non-seated posture, leaning the bicycle allows a greater non-muscular contribution to crank force and power.	88
6.2 Future work	89
6.2.1 Measuring CoM mechanics in ecologically valid conditions.	89
6.2.2 Contributions of the upper body to power production at the cranks. . . .	90
6.2.3 Non-muscular contributions to instantaneous crank power.	91
6.2.4 The influence of bicycle lean and vertical CoM displacement on gross efficiency and maximal power output during non-seated cycling.	92
6.2.5 The influence of bicycle lean and vertical CoM displacement on muscle function and mechanical work.	93
6.3 Potential Translation of Work and Thesis Reflections	94
Bibliography	97
A A Theoretical Comparison of the Effect of Bicycle Lean on the Travel Path of the Bicycle	111
A.1 Introduction	111
A.2 Theoretical evaluation of path length	111
A.3 Effect of path length on power output during uphill cycling	113
B A Method for Tracking Centre of Mass Displacement During Non-Seated Cycling Using an Inertial Sensor	117
B.1 Abstract	117
B.2 Introduction	118
B.3 Materials and methods	119
B.3.1 Participants	119
B.3.2 Experimental design	119
B.3.3 Optical motion capture	120
B.3.4 IMU	120
B.3.5 Musculoskeletal model	121
B.3.6 Statistical analysis	122
B.4 Results	125

B.4.1 Sensor Performance	125
B.4.2 IMU vs Optical motion capture	125
B.4.3 IMU vs Musculoskeletal model	125
B.5 Discussion	129
C Supplementary Figures	131
C.1 Supplementary figures for study in Chapter 3	131
C.2 Supplementary figure for study in Chapter 4	138
C.3 Supplementary figures for study in Chapter 5	139
D Ethical Approval Forms	143
D.1 Ethical approval for studies in Chapters 3 and 4, and Appendix B	144
D.2 Ethical approval for study in Chapter 5	145
E Copyright Permissions	147
E.1 Copyright permission for Figure 2.1	148
E.2 Copyright permission for Figure 2.2	149
E.3 Copyright permission for Figure 2.3	150
E.4 Copyright permission for Figure 2.4	151

List of Figures

2.1	Bi-articular muscle activation is extremely sensitive to changes in task demands.	7
2.2	Bi-articular muscles act to control the direction of external force at the pedal.	10
2.3	During seated cycling, joint power is redistributed away from the knee to the hip as power output increases.	13
2.4	Significant vertical displacement of a rider's CoM is likely to occur during non-seated cycling.	15
2.5	The effects of changing cadence and/or power output on crank torque are each unique depending on the power output and cadence you're riding at.	21
3.1	Switching to a non-seated posture shifts peak force production to later in the crank cycle	37
3.2	Joint power production occurs later in the crank cycle when in a non-seated posture compared to seated.	39
3.3	There was a significant main effect of posture at the hip, knee, and ankle during high-power output cycling.	40
3.4	The net mechanical power contribution at the knee was significantly reduced by switching to a non-seated posture.	41
3.5	Effective mechanical advantage at the knee was significantly increased by cycling in a non-seated posture at 70 rpm, but not 120 rpm.	43
3.6	Bi-articular hamstring activity was significantly reduced by cycling in a non-seated posture.	43
4.1	Calculations of instantaneous total joint power must account for any change in gravitational potential energy and kinetic energy of the rider's CoM relative to the reference frame of the bicycle.	56
4.2	Changes in kinetic energy of the rider's CoM had little impact on the overall total mechanical energy changes.	58
4.3	Net upward vertical handlebar forces decrease substantially as power output increases and are much lower at 70 rpm than 120 rpm.especially at 70 rpm.	59

4.4	Changes in CoM power are deliberately out of phase with crank power during the period of peak crank power production, meaning that peak joint power requirements are reduced.	61
4.5	Using a non-seated posture at high cadence resulted in theoretically costly periods of simultaneous power generation and dissipation by the lower body and upper body, respectively.	62
4.6	Riders use their upper body to contribute greater amounts of power as power output increases.	63
5.1	The group mean range of bicycle lean angle in the Unconstrained condition was 54% greater than Self-Restricted and 63% greater than in the Trainer	74
5.2	Riders self-restricted bicycle lean by reducing peak vertical forces at the crank by 15% on average.	76
5.3	The different constraints on bicycle lean appeared to alter the pattern of total joint power production during the crank cycle	78
5.4	Riders increased mean and peak CoM power when lateral bicycle dynamics were constrained by a trainer, but did the opposite when having to self-restrict bicycle lean.	79
5.5	The range of bicycle lean during the unconstrained condition was less than the values reported in previous studies of non-seated cycling in the field and on a treadmill	79
A.1	Leaning and steer of the bicycle increases the path length between two points.	112
A.2	Taking a wider path when climbing uphill could improve performance.	114
B.1	A single inertial sensor was used to estimate rider CoM displacement during non-seated cycling	121
B.2	The orientation of the sensor matched nicely with the attached marker cluster	124
B.3	The pattern of vertical IMU displacement matched well with the marker cluster and model's CoM	126
B.4	The IMU tracked the cluster with high accuracy, but overestimated the model's range of vertical CoM displacement	127
C.1	Peak crank power far exceeds peak power generated by the leg during seated and non-seated cycling, suggesting that additional power is generated by muscles in the upper body or the rider's CoM.	132
C.2	The hip, knee, and ankle extend later in the crank cycle and to a greater extent when non-seated compared to when seated.	134
C.3	Duty cycle of the knee increased at 70 rpm when non-seated compared to when seated, which also resulted in greater peak knee flexion velocity.	135
C.4	Peak hip extension moments and ankle plantar flexion moments increased when non-seated at 70 rpm, likely due to an increased redistribution of net joint moments by bi-articular muscles.	136

C.5	The period of EMG activity of most muscles within the lower limb was shifted later in the crank cycle when cycling in a non-seated posture.	137
C.6	Rider CoM displacement occurred predominantly in the vertical direction during non-seated cycling.	138
C.7	Riders appeared to dissipate power at the knee much earlier in the crank cycle when self-restricting bicycle lean.	140
C.8	Technical drawing of instrumented cranks used for study in Chapter 5.	141

List of Tables

5.1 Self-restricting bicycle lean had a large effects on vertical crank force and CoM energetics	80
A.1 Leaning the bicycle at low velocity increases path length more so than at high velocity.	113
A.2 Taking a wider path around uphill corners can reduce the amount of torque required.	116
B.1 Notation, reference coordinates, and definitions used in this study.	122
B.2 The sensor performance was excellent across all conditions	126
B.3 There was good agreement between the IMU and cluster, but not between the IMU and model	128
C.1 Peak knee extension moments decreased, while range of motion at the knee increased when non-seated at 70 rpm compared to when seated.	133

List of abbreviations and symbols

Abbreviations	
BDC	Bottom Dead Centre
BoS	Base of Support
b.w.	body weight
CoM	Centre of Mass
EMG	Bipolar surface electromyography
EMA	Effective Mechanical Advantage
ES	Hedge's g_{av} corrected effect size
MA	Mechanical Advantage
MAD	Median Absolute Deviations
P_{CoM}	Centre of mass power
P_{lb}	Lower body joint power
$P_{max.i}$	Instantaneous maximal power output
P_{tot}	Total joint power
P_{ub}	Upper body joint power
PCSA	Physiological Cross-Sectional Area
rad	Radians
rpm	Revolutions Per Minute
SD	Standard Deviation
TDC	Top Dead Centre

Symbols	
η_G^2	Generalised eta squared
\pm	Plus minus
\circ	Degrees of rotation
\cdot	Dot product
Δ	Change in
Σ	Sum of

Chapter 1

Introduction

The bicycle is a masterful piece of engineering. The combination of wheels and the additional lever system of the drive train decouple the conditions under which muscles generate power from the forward velocity of the system. By removing the link between the foot and the ground, a bicycle significantly reduces the cost of transport compared to walking and running and allows the system to coast across the ground, similar to a bird soaring through the air or a fish gliding through water (Cavagna 2017).

Typically we cycle in a seated posture, whereby the saddle supports much of our bodyweight against the force of gravity. An intriguing aspect of cycling is that, under certain circumstances, riders choose to forego bodyweight support at the saddle and seemingly use their body mass to help produce force on the pedals. Presumably, we learn this technique by cycling in a seated posture under various natural conditions and experiencing perturbations relating to resistance, such as increasing slope and air resistance (Loeb 1995). Thus, depending on the nature and motivation of the task, we eventually learn to spontaneously transition from a seated to non-seated posture (commonly referred to as standing on the pedals). This transition becomes instinctive, to the point where most of us struggle to explain why we do it. A simple explanation may be that it moves our mass over the pedal, but we don't always do it because producing force to support a larger portion of bodyweight costs energy (Kram and Taylor 1990). So what triggers this transition response in each of us? Perhaps there is a certain level of external torque, or power, or a combination of both that becomes unsustainable when we're seated or just unfavourable compared to a non-seated posture. This topic was addressed in our first study where we uncovered some clues about the biomechanics that underlie the transition response by making people cycle in a seated posture under conditions where they would typically prefer to be non-seated. This study is incorporated as **Chapter 3 - The Mechanics of Seated and Non-seated Cycling at Very-High-Power Output: A Joint-level Analysis**.

Once a rider has transitioned to a non-seated posture, they begin to periodically lean the bike from side to side and move their centre of mass (CoM) up and down during each crank cycle. Once again, we may presume that riders learn these movement strategies through the

experience of cycling in a non-seated posture under different natural conditions. Similar to the transition response from a seated to non-seated posture, the coordination of CoM movement and bicycle lean seemingly becomes instinctive. Indirect evidence suggests that the magnitude of a rider's vertical CoM displacement and bicycle lean increases at higher power outputs (Soden and Adeyefa 1979; Hull, Beard, and Varma 1990). However, the magnitude and pattern of CoM movement has not been directly quantified under different task demands. This gap was addressed in our second study, which is incorporated as **Chapter 4 - Riders Use Their Body Mass to Amplify Crank Power during Non-seated Ergometer Cycling**. Based on these findings, there appears to be more to the story than just balance. Perhaps CoM movement and bicycle lean work together to optimise the biomechanics of power production during non-seated cycling. One option to test whether a link exists between these two phenomena and how they may help us to optimise cycling performance would be to compare the CoM movement and limb mechanics of riders cycling in a non-seated posture while different constraints are placed on bicycle lean. This was the premise of our third study, which has been incorporated as **Chapter 5 - Rock and roll: The influence of bicycle lean on the mechanics of non-seated cycling**.

The scope of this thesis is to answer the general questions of how the biomechanics of seated and non-seated cycling differ under various task demands and whether bicycle lean has a biomechanical effect on how a rider generates power. Thus, a fundamental understanding of the laws that govern lateral bicycle dynamics and how power is generated by the rider is covered briefly within the following literature review.

Chapter 2

Literature Review

This literature review is broken up into three parts (I, II, and III), each one providing relevant information pertaining to the aims of the respective investigation incorporated as Chapters 2, 3, and 4. The aim of the investigation incorporated as Chapter 2 was to compare the distribution of joint powers, muscle activity, and effective mechanical advantage between seated and non-seated postures during high power output cycling. Thus, Part I of the literature review will focus on the geometry and drivetrain of the bicycle, typical patterns of muscle activity and limb mechanics during cycling, and what is currently known about the non-seated posture. The aim of the investigation incorporated as Chapter 3 was to understand the implications of mechanical energy changes of the rider's CoM on crank power output and limb mechanics during non-seated cycling at different power outputs and cadences. Thus, Part II will focus on why mechanical energy changes of the CoM may influence the total power output a rider must generate during cycling, and the unique influence that changing power output and cadence have on torque requirements during cycling. The aim of the investigation incorporated as Chapter 4 was to understand how different constraints on lateral bicycle dynamics effect CoM movement and limb mechanics during non-seated cycling. Thus, Part III will focus on lateral bicycle dynamics, the effect of bicycle lean on the balance and stability of the bicycle, and the difference between riding outdoors, on a treadmill, and on rollers.

2.1 Part I

2.1.1 Transmission and gearing

A machine achieves ideal mechanical efficiency when there is no loss of power during transmission (Simón Mata et al. 2016). A bicycle is an intricate example of excellent mechanical efficiency. The teeth of the front chain ring and rear sprocket, linked by a chain, send power produced by the rider to the rear wheel. A well-maintained bicycle will only lose approximately 2.3% of power during transmission (Martin et al. 1998). These small power losses are due to the

combination of friction, deformation, and wear within the frame and components.

The mechanical advantage (MA) of the system dictates whether this power will then produce force or displacement at the rear wheel. The definition of MA is the ratio between the output force and the input force (Simón Mata et al. 2016). Four components of the bicycle contribute to its MA. They are the rear wheel (including the tyre), rear sprocket, front chain ring, and crank arm. A change in the radii of any of these components will cause a change in MA. Because the crank arm rotates in a circular path around its spindle, a change in its length is equal to a change in radius. These four components act around two axes of rotation, each with two gears. We can use the radii of these four components to calculate a bicycles MA as shown in Equation 2.1 (Sharp 1977).

$$MA = \frac{\text{Crank arm length (mm)} \cdot \text{Sprocket size (teeth)}}{\text{Rear wheel radius (mm)} \cdot \text{Chain ring size (teeth)}} \quad (2.1)$$

You can conceptualise MA as the ease at which you can pedal. If you ride a bike with a high MA on a flat surface it will feel very easy to pedal. The lower the MA the harder it is to pedal. Travelling at a certain velocity using an “easy” gear requires a higher cadence (measured in pedal revolutions per minute (rpm)) than using a “hard” gear. This is because the MA value dictates how much pedal displacement will occur per unit of rear wheel displacement. The inverse of MA is the gear ratio. In Equation 2.1 we can see that an increase in crank arm length and/or rear sprocket size will increase MA as will a decrease in rear wheel radius and/or front chain ring size, thus, increasing the distance that the pedal must travel per unit of rear wheel displacement. In this scenario the rider trades displacement of the system for maximising force output. An example of this occurs when a rider cycles up a steep hill. The rider shifts the chain onto a smaller front chain ring or a larger rear sprocket to decrease the force required at the pedal. For instance, modern road bicycles commonly have a total of 22 gears, made up of two front chain rings and 11 rear sprockets. The MA of these modern road bicycles will range from 0.1 to 0.5. Riders can choose to alter the range and spacing of gears to suit the cycling event and their strengths.

The other important aspect of a bicycle’s MA is the ratio of angular velocity between the wheels and the crank. Low MA allows the rear wheel to reach angular velocities that are unattainable by the rider at the pedal (Sharp 1977). This is most helpful during flat sections, downhill descents, and fast sprint finishes. Altering the MA of the transmission allows a rider to achieve their desired power output using any combination of torque and angular velocity that the gearing and terrain allows. A later section on human power generation will discuss why riders choose certain combinations of torque and cadence.

2.1.2 Phases of the crank cycle

“Crank cycle” is one term used to describe when the pedal completes a 360°revolution of the crank axis (Fonda and Sarabon 2012). Top dead centre (TDC, 0°) refers to the point in which

the pedal is at its highest point during the crank cycle if the bicycle is on a level surface. TDC defines the start and end point of the crank cycle (0-360°). If the bicycle is on a level surface, then TDC will coincide with a vertical crank position, however, when on a slope the change in angular position of TDC will be equal to the slope of the riding surface. Bottom dead centre (BDC, 180°) is a term used to define the halfway point of the crank cycle. BDC also defines the end of the first phase, known as the downstroke (0-180°) and the start of the second phase, known as the upstroke (180-360°). These reference points allow spatial and temporal comparisons of biomechanical parameters during cycling.

2.1.3 Geometry of the bicycle

The geometry and configuration of the bicycle dictate rider position during seated cycling (Müller and Hofmann 2008). Depending on the goals of the rider, the configuration will aim to maximise performance, comfort, or a blend of each (Too and Landwer 2003). We can adjust five parts of the bicycle to position the legs: saddle height, saddle setback, crank length, spindle width, and cleat position (Hayot et al. 2012). The position of the upper body will then rely on the position of the handlebars in relation to the saddle.

The effects of saddle height (Bini, Hume, and Kilding 2014), saddle setback (Rankin and Neptune 2010), crank length (Barratt et al. 2016), and cleat position (Straw and Kram 2016) have all been thoroughly investigated. Yet, it has been difficult to isolate the effects of each variable due to the complex interaction between one another (Rankin and Neptune 2010). For example, a change in crank length will also alter the angle and distance between the saddle and pedal during the crank cycle. Thus, it is understandable that research into these variables has yielded mixed results.

The influence of saddle height on lower limb kinematics during cycling is more consistent (Bini, Hume, and Croft 2011). Research shows that saddle height has a significant effect on knee and ankle kinematics (Nordeen-Snyder 1977). A 5% decrease in saddle height can decrease extension of the knee by 35% (Nordeen-Snyder 1977). This will impact the length, rate of length change, and moment arm of knee extensor muscles (Bini, Hume, and Croft 2011). Thus, pelvis to pedal distance may play an important role in joint mechanics and energetics during cycling (Hull, Beard, and Varma 1990).

An important consideration is that altering any of these variables may cause a change in both the horizontal and vertical position of the rider's CoM relative to the pedal. It may be that changing the position of the CoM relative to the pedal is a confounding variable that underlies any differences in metabolic energy expenditure or performance caused by changing these variables.

2.1.4 Muscle activity

Due to the constraint of the pedal trajectory during cycling, the basic phasing of functional muscle groups in the lower limb remains similar across different task demands (Raasch and Zajac 1999). Riders will tend to concentrate their muscular effort during the downstroke to match the optimal force and power producing capabilities of the lower limb (Ericson et al. 1986a; Yamaguchi et al. 1990). Hip extensors, knee extensors, and ankle plantar flexors produce the majority of work to move the pedal from TDC to BDC (Ericson et al. 1986a). During the latter stages of the downstroke, knee flexors activate even though the knee continues to extend (Hug and Dorel 2009). This hamstring activity during concurrent knee extension is known as Lombard's Paradox (Gregor, Cavanagh, and Lafontaine 1985). Activating a knee flexor during knee extension would seem to be inefficient, however, the activation of bi-articular hamstring muscles (i.e. biceps femoris) is able to contribute to power output during the second half of the downstroke by redirecting the external force produced on the pedal (Gregor, Cavanagh, and Lafontaine 1985). Thus, the coordinated activity of uni- and bi-articular muscles partially avoids the inefficiency of uni-articular muscles having to actively lengthen and absorb power during the downstroke, thereby increasing the efficiency of steady-state cycling (Kuo 2001).

It is also clear that the nervous system quickly adapts this paradoxical activity in response to changing task demands (Connick and Li 2013). For example, it has been shown that the specific timing of bi-articular hamstring activity is sensitive to changes in both saddle height and cadence (Connick and Li 2013). Knee extensors activate close to TDC in preparation for the downstroke. The activation of knee extensors continues through the downstroke to around 120°. This creates a large and effective knee extensor moment to drive the pedal. Hip extensors also activate around TDC and then peak at about 60°. This coincides with the pedal moving downward away from the hip joint. This hip extension moment continues through the downstroke to BDC. The ankle plantar flexors activate for a shorter period compared to hip and knee extensors; beginning after TDC, peaking at approximately 90° and ending after BDC. The transition to the upstroke then begins. Far less muscle activity occurs during the upstroke compared to the downstroke. Typically, the hip flexors, knee flexors, and ankle dorsiflexors produce relatively small amounts of work to return the pedal from BDC to TDC. The amount of effective tangential force applied to the pedal during the upstroke is minimal compared to the levels of flexor muscle activity (Hug and Dorel 2009). This is because the pedal is raised predominantly by the action of the contralateral leg, which drives the opposite pedal downward from TDC to BDC. Thus, the hip flexors and knee flexors act predominantly to lift the leg during the upstroke to minimise counter-productive tangential pedal force.

Figure 2.1 shows the electromyographical (EMG) activity measured in six lower limb muscles while cycling under three conditions: 1) seated on a level treadmill (LS), 2) seated on an inclined treadmill (US), and 3) non-seated on an inclined treadmill (ST) (Li and Caldwell 1998). It appears that changing incline has little effect on the pattern of lower-limb muscle activity, while there are large effects due to the change in posture; especially within the primary hip extensor,

gluteus maximus, and the primary knee extensor, vastus lateralis.

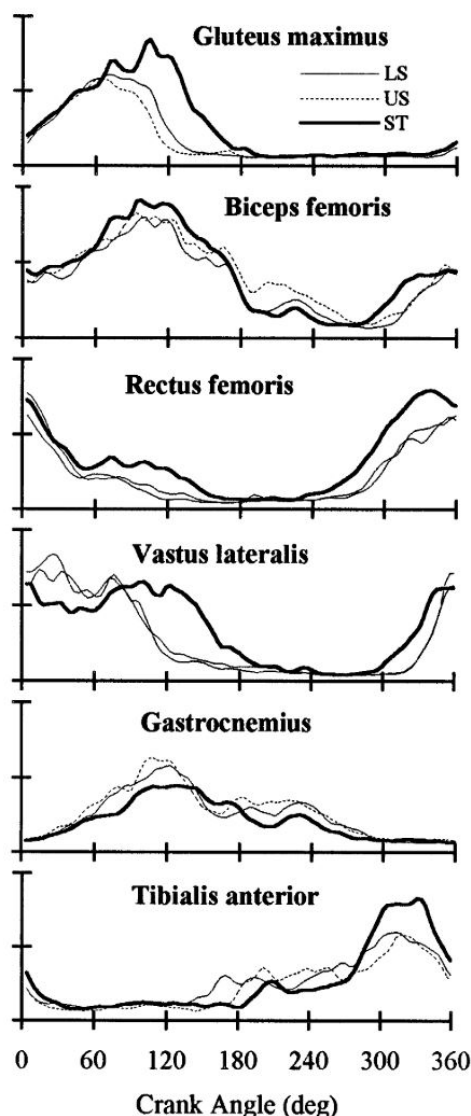


Figure 2.1: Bi-articular muscle activation is extremely sensitive to changes in task demands. Shown here is muscle activity within the lower limb during seated cycling on a level treadmill (LS), seated on an inclined treadmill (US), and non-seated on an inclined treadmill (ST). Note the altered pattern of rectus femoris activity due to the change in posture. *Adapted [reprinted] with permission from Li L, Caldwell GE. Muscle coordination in cycling: effect of surface incline and posture. J Appl Physiol. 1998;85(3):927-34. Copyright ©1998 by American Physiological Association.*

2.1.5 Limb mechanics

Muscle mechanics

During cycling, the rider assumes the role of an engine for the bicycle. The only mechanical structure in humans that can generate net positive mechanical power is muscle. Thus, we must consider the properties which govern a muscle's ability to generate power. Peak power and

efficiency of a muscle are an extension of its force producing capabilities in relation to length and the rate of length change (velocity) (Hill 1922).

If a muscle is fully activated, then the force a muscle exerts is primarily dependent on its size (physiological cross-sectional area (PCSA)), fascicle length, and the speed at which it contracts. During cycling, it is important to consider the collective force-length curve of a group of synergistic muscles rather than each muscle in isolation. The muscle group that contributes the most power during steady-state cycling is the knee extensor group (Ericson et al. 1986a; Elmer et al. 2011). The knee extensor group contains the bi-articular rectus femoris muscle, which means that the knee extensor strength curve is dependent on hip angle. The dependence of the knee extensor strength curve on hip angle will be proportional to the contribution of rectus femoris, which has a PCSA 92% the size of vastus lateralis and is larger than vastus medialis (128%) and vastus intermedius (144%) (Herzog, Hasler, and Abrahamse 1991). A comparison of theoretical and experimental knee extensor strength curves by Herzog et al. (1991) showed that at a hip angle of 180°(lying with a straight leg) rectus femoris will produce maximal force at a knee angle of approximately 155°. With the hip fully extended, the rectus femoris will be the major contributor of knee extensor force at knee joint angles ranging from about 135°to full knee extension. At a hip angle of 90°(sitting) rectus femoris will produce maximal force at a knee angle of approximately 60°(full knee extension = 180°), and a complete loss of active force production due to the loss of overlap of the myofilaments within the sarcomeres will likely occur at a knee angle of approximately 135°. Furthermore, the rectus femoris will likely become the major contributor to knee extensor force at knee joint angles ranging from 80°to full knee flexion (Herzog, Hasler, and Abrahamse 1991). Hence, it is important for cyclists to consider both their hip joint angle and knee joint angle when adjusting their riding posture and bicycle geometry in order to “optimize” the strength curve of the knee extensor group.

Muscles convert chemical energy to mechanical energy at an efficiency of around 20-25% (Wilkie 1950), but this efficiency can drop to zero if an external force is so large that the muscle cannot move it. Thus, to utilise the greatest efficiency of muscle, we must match the force and velocity of movement to produce the most power. Peak efficiency occurs at approximately 50% of peak force and approximately 25% of peak shortening velocity (Wilkie 1960b), but peak power production will occur at higher shortening velocities than that of peak efficiency (Wilkie 1960b).

Human potential for mechanical power output decays exponentially as a function of activity duration (Wilkie 1960a; Harrison 1970), which affects the the optimal force and velocity of movement (Too and Landwer 2003). For instance, maximal power output occurs at a cadence of approximately 120 rpm (McCartney, Heigenhauser, and Jones 1983; Gardner et al. 2007). As power output decrease over time, so too does the cadence that maximises power output (MacIntosh, Neptune, and Horton 2000). At sub-maximal power outputs, elite cyclists tend to cycle at a higher cadence than that which is most metabolically efficient (Marsh and Martin 1993). Yet, these higher cadences lead to a greater time to exhaustion (Nickleberry and Brooks

1996). Surprisingly, it is only when cycling uphill that riders tend to reduce their preferred cadence closer to that which is most efficient (Lucia, Hoyos, and Chicharro 2001). Research suggests that preferred cadence may be related to a number of factors including joint-moment minimisation, muscle power, and gross efficiency (Marsh, Martin, and Sanderson 2000), but it remains unclear which factor is being prioritised by the rider and whether this changes under different task constraints.

Segmental energy transfer

During cycling, muscles create pedal force through the proximal-to-distal transfer of segmental energy (Enoka 2008; Kautz and Neptune 2002). Thus, the leg muscles are required to produce, absorb, and redistribute energy. The type of contraction that the muscle undergoes will dictate the ratio of energy distributed from one connected segment to another. A concentric (shortening) contraction produces mechanical work. This means that an accelerated segment will gain more energy than that lost by the connected decelerated segment. The opposite will occur for an eccentric (lengthening) contraction, which will absorb energy. An isometric (fixed length) contraction will redistribute an equal amount of energy between segments (Zajac, Neptune, and Kautz 2002).

The synergy of muscle activity in the lower limb can increase the amount of force produced on the pedal. For example, the synergistic activity of the triceps surae redistributes work done by the gluteals and vastii on the thigh and shank, respectively, to the pedal. This enables the transfer of energy across the ankle to the pedal. Without this activity the angular momentum of the thigh and shank would force the ankle into dorsiflexion (Zajac, Neptune, and Kautz 2002). Bi-articular muscles and the co-activation of muscles on opposing sides of the joint complicate the transfer of energy between segments. This makes it difficult to categorise muscles as having distinct functional roles during cycling. Nevertheless, comparing the magnitude and patterns of muscle activity under different cycling conditions can reveal important insights into the pattern of segmental energy transfer and the role of particular muscles during cycling.

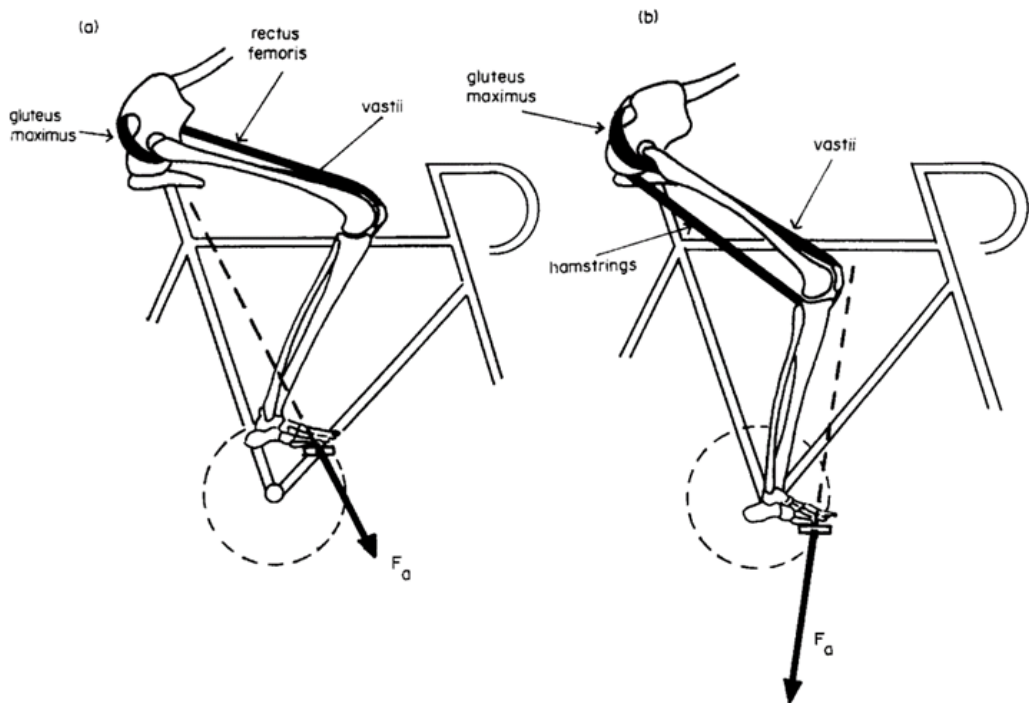


Figure 2.2: Bi-articular muscles act to control the direction of external force at the pedal. Depiction of how bi-articular muscles act to control the direction of the external force vector. Rectus femoris can act to transfer hip extension power to the knee, while biceps femoris long head can transfer knee extension power to the hip. F_G , Pedal reaction force. Adapted [reprinted] with permission from Van Ingen Schenau GJ, Boots PJM, de Groot G, Snackers RJ, and van Woensel WW. *The constrained control of force and position in multi-joint movements*. *Neuroscience*. 1992;46(1):197-207. Copyright ©1992 by Elsevier.

Directing external force output

Cycling is an interesting example of an “open-chain kinetic exercise” (Enoka and Duchateau 2019) whereby pedalling efficiency relies on both the magnitude and direction of pedal force. Thus, coordinating the intensity and timing of muscle activity in the lower limb is crucial to the task. The resultant pedal force is made up of both tangential and radial force; the direction of which are perpendicular and parallel to the crank, respectively. The circular trajectory of the pedal means that only tangential force is effective in producing forward motion (Gregor and Childers 2011). The primary force producing muscles of the lower limb alone cannot produce an effective force throughout the pedal cycle (Zajac, Neptune, and Kautz 2002). Thus, there is a need for co-contraction of uni- and bi-articular muscles to control the size and direction of the pedal force vector (van Ingen Schenau et al. 1990). For example, the production of an effective force at the start of the downstroke requires a large net knee extensor moment. During the second half of the downstroke, hip extensor, knee flexor, ankle plantar flexor moments act to direct the pedal force vector perpendicular to the crank.

Muscle activity can also lead to the production of radial force. Although radial force is not effective at turning the crank, the theory that reducing the ratio of radial to tangential force (often referred to as “force effectiveness”) will increase efficiency and performance is fundamentally flawed (Kautz and Hull 1993). The main oversight in this theory is that radial

force is often generated by non-muscular forces such as momentum of the lower limbs (Neptune and Herzog 2000). This means that any attempts to offset this non-muscular force would require greater muscular effort to decelerate the lower limb segments (Kautz and Hull 1993). It is likely that attempting to control the momentum of the segments in this manner would place a greater demand on muscle and decrease a rider's time to task failure at a given mechanical power output (Enoka and Duchateau 2019).

Effective mechanical advantage

Postural changes can affect the required muscle force during many forms of terrestrial locomotion (Alexander 1991; Kram and Dawson 1998; Kipp, Grabowski, and Kram 2018), which subsequently affects metabolic cost (Biewener et al. 2004). These postural changes can affect the amount of muscular force needed by altering the MA of the lower limb (Biewener 1989). The MA of a muscle is calculated as the ratio of the reaction force moment arm to the muscle moment arm, known as “effective mechanical advantage” (EMA) (Biewener 1989). The muscle moment arm is the perpendicular distance from the muscle-tendon insertion to the joint centre. The reaction force moment arm is the perpendicular distance from the projection of the ground reaction force to the joint centre.

Research has shown that runners are able to minimize their energetic cost by increasing the overall EMA of the lower limb (McMahon, Valiant, and Frederick 1987). They achieve this through a reduction in the ground reaction force moment arm. During stance phase, runners align the ground reaction force vector with the longitudinal axis of the support leg (Chang et al. 2000). A key difference between running and cycling is that a saddle supports the majority of a cyclist's bodyweight. This will reduce the effect of bodyweight on the magnitude and direction of the pedal reaction force. This means that transition from a seated to a more vertically aligned non-seated posture is likely to increase EMA of the lower limb during cycling. To the best of our knowledge, no data currently exists on EMA during cycling in either a seated or non-seated posture.

Joint-specific power

The biomechanics of cycling are typically studied under power outputs associated with steady-state exercise or maximal endurance performance (Bini, Hume, and Kilding 2014). Yet, cycling events are usually interspersed with brief but important periods of high power output, such as accelerations, climbing, and sprinting (Lucia, Earnest, and Arribas 2003). Thus, many gaps still remain pertaining to the biomechanics of cycling at high power outputs. Knee extensors contribute the most power during the pedal cycle at low to moderate power outputs (Ericson et al. 1986b). However, hip extensors become the largest contributor at high power outputs (Martin and Brown 2009; Elmer et al. 2011). This redistribution of joint power may occur due to an increase in knee flexor moments, which reduce the knee extensor moment and subsequent

net knee power, or the ability of hip extensors to produce higher maximal joint moments than the knee extensors (Anderson, Madigan, and Nussbaum 2007). Figure 2.3 shows the patterns of joint-specific power in response to increasing power output at a cadence of 90 rpm. As expected, all joint powers increase with an increase in power output, but the relative increase in peak hip power is much larger than at the knee or ankle. These results may provide a clue as to why cyclists spontaneously transition from a seated to a non-seated posture at high power outputs. If joint power is redistributed away from the knee when cycling in a seated posture as power output increases, then it is possible that this re-distribution of joint power could be linked to the transition response of riders. To date, joint-specific power during non-seated cycling has not been published. Further consideration should also be given to the effects of changing cadence on joint-specific power during seated and non-seated cycling.

The time that the lower limb and each joint spends in extension was also shown to increase at high power outputs (Elmer et al. 2011). This increases the time spent using stronger anti-gravity muscles to generate power (Yamaguchi et al. 1990). The ratio of time a joint spends extending relative to flexing is known as the duty cycle. Thus, it is proposed that an increase in duty cycle is an essential strategy for producing maximal power. To date, duty cycle values during non-seated cycling have not been published.

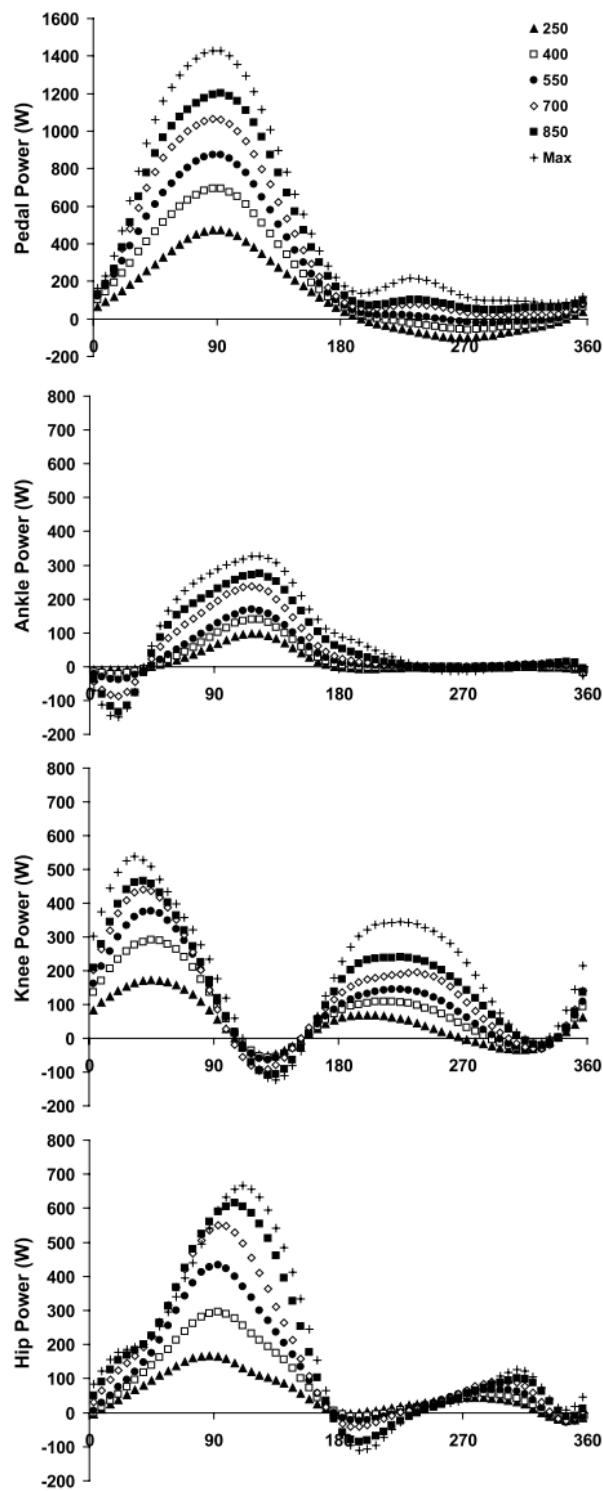


Figure 2.3: During seated cycling, joint power is redistributed away from the knee to the hip as power output increases. Shown here are the patterns of joint-specific power within the lower limb during seated cycling at 90 rpm as power output is increased from 250 Watts, through 850 Watts, to Maximum. Adapted [reprinted] with permission from Elmer SJ, Barratt PR, Korff T, and Martin JC. Joint-specific power production during sub-maximal and maximal cycling. MSSE. 2011;43:1940-1947. Copyright ©2011 by Wolters Kluwer Health, Inc.

2.1.6 Non-seated posture

During short, intensive bouts of cycling, many riders choose to ride out of the saddle (Harnish, King, and Swensen 2007). Single-day or multi-stage road races can often end with enthralling high-speed or steep uphill sprints to the finish. In some cases, two riders will go head-to-head while in two different postures; one seated while the other is not. It is a fascinating scenario, which leads one to ask whether the choice of posture is a key factor in the result. This question has led many researchers to try and understand the effects of the non-seated posture on cycling performance (Tanaka et al. 1996; Li and Caldwell 1998; Millet et al. 2002; McLester, Green, and Chouinard 2004; Poirier, Do, and Watier 2007; Hansen and Waldeland 2008; Turpin et al. 2016).

It has been shown that recreational cyclists will transition to a non-seated posture at a power output of approximately 567 Watts at a cadence 90 rpm (Costes et al. 2015). Yet, it has been proposed that cyclists should transition well before this power output to increase performance (Hansen and Waldeland 2008). One group of researchers compared time to exhaustion between the seated and non-seated posture at different power outputs (Hansen and Waldeland 2008). This study had elite cyclists ride to exhaustion on a treadmill set with a 10% gradient in either a seated or non-seated posture. Different intensities were set relative to the highest power output the subject could sustain for one minute (W_{max}). Most riders in this study achieved a greater time to exhaustion using a non-seated posture at their W_{max} intensity or above. W_{max} equated to a power output of 441 Watts for this subject group. Thus, it is possible that a non-seated posture may enhance performance fatigability (Enoka and Duchateau 2019) within lower-limb muscles when cycling at power outputs above the preferred transition power. Based on their findings, the authors recommended that cyclists should use the non-seated posture when riding above 94% of W_{max} . However, previous research has found no difference in gross efficiency between a seated and non-seated posture at power outputs equivalent to only 75% of W_{max} (Millet et al. 2002).

There is also a difference in the preferred cadence used during seated and non-seated cycling (Hansen and Waldeland 2008). At W_{max} subjects dropped their cadence from 97 rpm when seated to 71 rpm in a non-seated posture. Other research supports this finding, showing that highly trained and elite cyclists prefer to use a lower cadence when in the non-seated posture (Harnish, King, and Swensen 2007; Lucia, Hoyos, and Chicharro 2001). More recent research observed a much higher transition point of 567 Watts when controlling cadence at 90 rpm (Costes et al. 2015). The discrepancy between this result and that of previous research suggests that cadence likely affects the preferred transition power. It must be noted that many other constraints may explain the difference in these results including slope, riding experience, rider mass, ergometer type, activity duration, and fatigue. Further consideration should be given to the task constraints that may affect the preferred seated to non-seated transition power in cycling.

Forward modelling of cycling has shown that the instantaneous power output at the pedal can exceed that of muscular power capabilities (Neptune and Bogert 1998). This would suggest

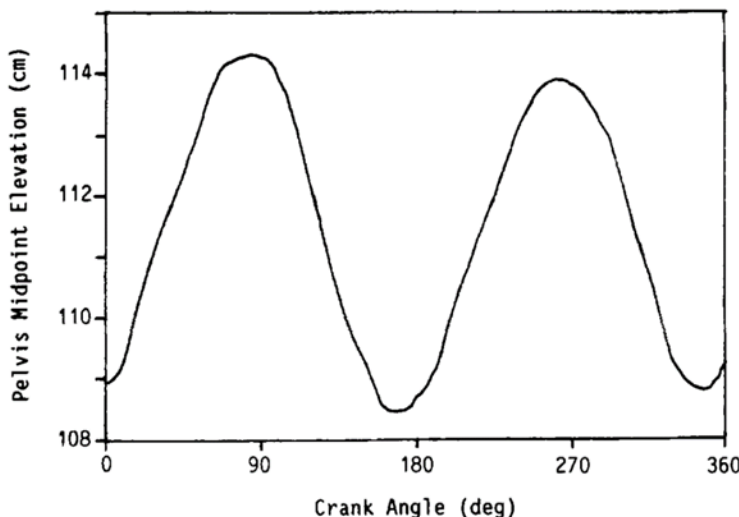


Figure 2.4: Significant vertical displacement of a rider's CoM is likely to occur during non-seated cycling. Indirect evidence of vertical CoM displacement during non-seated cycling via the measurement of a pelvis marker. *Adapted [reprinted] with permission from Hull ML, Beard A, Varma H. Goniometric measurement of hip motion in cycling while standing. J Biomech. 1990;23(7):687-703. Copyright ©1990 by Elsevier.*

that lower-limb muscles are able to transfer energy of lower- and upper-body segments to the pedal. Pioneering research using cine film showed a sinusoidal pattern of vertical lower back displacement during over-ground non-seated cycling (Soden and Adeyefa 1979). This finding was later confirmed by a study (Hull, Beard, and Varma 1990) on pelvis motion during non-seated cycling on a treadmill. Figure 2.4 shows the results of pelvis midpoint elevation over one crank cycle. The vertical fluctuations of the pelvis indicate that substantial amounts of mechanical energy could also be gained and lost by the torso. Note the double cycle pattern of peak elevation and downward acceleration occurring during the downstroke. These results suggest that mechanical energy of the upper body may be transferred to the crank during non-seated cycling. More recent research using modern motion capture techniques have shown vertical motion of the trunk and hips increases with power output even when cycling in a seated posture (Costes et al. 2015). Vertical displacement of the rider's CoM and the associated mechanical energy changes may affect the kinematics, kinetics, and energetics of the lower limb during both seated and non-seated cycling.

A rider's CoM moves forward and upward when transitioning from a seated to a non-seated posture (Caldwell et al. 1999). Evidence suggests that this leads to a phase shift of muscle activity and crank torque to later in the crank cycle (Li and Caldwell 1998). Fore-aft CoM displacement will change the ratio of bodyweight supported at the pedals versus the handlebar. The force vector due to gravity acting on the mass of the body is always directed towards the centre of the earth, which means any fore-aft movement of the CoM will change the moment arm between the CoM and the axis of crank rotation. Presumably, this change in moment arm could increase the contribution of a rider's body mass to pedal force, and subsequently increase

time to exhaustion during high-power output cycling (McLester, Green, and Chouinard 2004; Hansen and Waldegaard 2008). It may also explain why cyclists report a lower perceived rate of exertion in the lower limb during non-seated cycling (Tanaka et al. 1996). There is a need to test whether these measures relate to either an increase in peak maximal power or a decrease in peak total joint power generated by the rider during non-seated cycling.

When in a non-seated posture, the bodyweight of the rider is supported by the pedals and handlebar. Partitioning out the separate metabolic costs of supporting bodyweight and accelerating body mass during running has provided important insights into running performance (Kipp, Grabowski, and Kram 2018). However, quantifying the energy cost of producing force to support bodyweight seems to be far more complex when pedalling a bicycle than when on solid ground. Nevertheless, applying a similar approach to non-seated cycling may provide important insights into how muscle simultaneously supports bodyweight and generates net positive mechanical work to propel the bicycle during non-seated cycling.

Both efficiency and maximal power output are important aspects of cycling performance. Depending on the goal of the cycling task a rider may choose to prioritise one or the other. For instance, during very short sprints and climbs the priority may be to produce maximal power no matter the energetic cost. In this case, research shows that the non-seated posture is superior to the seated posture for producing maximal power (Millet et al. 2002). It is also likely in this case, for chemical energy to be liberated primarily through anaerobic metabolism. Thus, comparisons of aerobic energy expenditure between the seated and non-seated posture are unlikely to reveal any advantage to the non-seated posture under steady-state conditions (Ryschon and Stray-Gundersen 1991). Rather, comparisons of lower-limb mechanics between the two postures may provide more insight into the preference for a non-seated posture.

2.2 Part II

2.2.1 Human power output during cycling

Both internal and external forces impede forward motion of the bicycle. Positive power generated by muscle is dissipated to the environment (excluding gravity), to conservative forces (including gravity and the stretching of elastic elements), and to non-conservative forces such as friction and drag (van Ingen Schenau and Cavanagh 1990). To start moving forward, the rider must produce enough thrust to overcome resistance due to aerodynamic drag, rolling resistance, wheel-bearing friction, changes in potential energy, and changes in kinetic energy (Martin et al. 1998). The portion of resistance attributed to these sources varies depending on the riding scenario. In most cases when riding on a flat surface, the main resistance will be due to aerodynamic drag. Atmospheric sources of drag include air density as well as the direction and velocity of wind. The total amount of drag experienced by the bicycle-rider system will depend on the velocity relative to wind, frontal surface area, and shape. The force needed to overcome aerodynamic

drag increases to the square of velocity (Martin et al. 1998; Müller and Hofmann 2008). Thus, optimising shape and frontal surface area will decrease the power required per unit of velocity. For example, when travelling at a constant velocity of $30 \text{ km}\cdot\text{h}^{-1}$ ($8 \text{ m}\cdot\text{s}^{-1}$) on a flat surface into a $2 \text{ m}\cdot\text{s}^{-1}$ head wind, approximately 75% of power production is needed to overcome aerodynamic drag (Martin et al. 1998). At speeds above $50 \text{ km}\cdot\text{h}^{-1}$, drag increases to $>90\%$ of the total resistive force (Faria, Parker, and Faria 2005). During steep uphill cycling the main resistance becomes the rate at which the rider gains potential energy due to gravity. When accelerating from a standstill on flat ground the main resistance is the rate of change in kinetic energy. Hence, a rider's choice of riding posture often depends on the type and magnitude of external resistance.

Typically it is assumed that the rider's CoM travels parallel to the riding surface, meaning that the change in potential and kinetic energy of the rider's CoM is reflected by the change in the potential and kinetic energy of the system. Under this assumption power measured at the cranks will be equivalent to the total power output generated by the rider. However, this assumption does not account for any movement of the rider's CoM relative to the reference frame of the bicycle. Evidence suggests that this is particularly important when cycling in a non-seated posture as the rider's CoM is raised and lowered periodically during the crank cycle (Soden and Adeyefa 1979; Hull, Beard, and Varma 1990). Thus, the total power generated by the rider (P_{tot}) will be equivalent to power measured at the cranks (P_{cranks}) plus the rate of energy gained and lost by their CoM (P_{CoM}) as shown in Equation 2.2

$$P_{tot} = P_{cranks} + P_{CoM} \quad (2.2)$$

$$P_{lb} + P_{ub} = P_{cranks} + P_{CoM} \quad (2.3)$$

Typically, P_{cranks} is calculated as the summed dot product of torque and angular velocity measured at each crank. P_{CoM} is calculated using inverse kinematic results as the sum of the change in potential energy (E_p) and kinetic energy (E_k) of each segment divided by the change in time. P_{tot} can also be thought of as the sum of lower body and upper body joint power as shown in Equation 2.3. Lower body joint power (P_{lb}) can be calculated using inverse dynamic results as the summed dot product of net joint moments and joint angular velocities at the hip, knee, and ankle of each leg. Upper body power (P_{ub}) can be assumed to be the difference between P_{tot} and P_{lb} , which can be attributed to the net power generated by muscles crossing the joints within the arms and trunk. It is far less common for studies to directly measure P_{ub} . The limitation of this is that it cannot be identified whether power is being simultaneously generated and dissipated within the upper body.

2.2.2 Centre of mass movement during cycling

Contrary to popular belief, the CoM of the rider does not travel parallel to the riding surface even during seated cycling (Costes et al. 2015). The measurement of rider kinematics during seated

cycling shows that a rider's CoM is displaced in all three axes (Telli et al. 2016). The vertical component of this displacement may have a significant energetic cost due to the energy required to raise the body's mass against gravity. As pedal torque increases the vertical displacement of the trunk also increases (Costes et al. 2015). Limiting CoM displacement has been proposed as an optimal strategy during walking and running (Saunders, Inman, and Eberhart 1952). Yet, adapting gait to constrain CoM movement can be even more costly than allowing CoM movement, as evidenced by "Groucho" running (McMahon, Valiant, and Frederick 1987). If you can imagine walking with similar knee flexion angles used in seated cycling it may look like what has been termed "Groucho" running. This unusual gait was adopted by runners who were under instruction to run while limiting CoM movement. Subjects chose to run in a crouched posture with a compliant knee. This resulted in greater knee flexion angles than a preferred gait. This happened to be an excellent strategy for limiting CoM movement, however, this gait came at a higher energetic cost due to the increase in work required at the knee joint (Gordon, Ferris, and Kuo 2009). These increased knee flexion angles led to an increase in knee extensor moments compared to a preferred gait. A similar concept could be tested during cycling, by instructing riders to limit CoM movement during non-seated cycling.

Vertical acceleration of the rider's CoM during seated and non-seated cycling would mean that the full bodyweight of the rider is not always supported by the saddle and handlebars. There is evidence of this during seated cycling, where it was shown that, at a power output of 682 ± 111 W and a cadence of 90 rpm, the amount of bodyweight supported at the saddle was measured to be as low as $7 \pm 5\%$ (Costes et al. 2015). Due to the flexed position of the leg during seated cycling, the loss of saddle support to this extent could significantly increase the force and work requirements of anti-gravity muscles. Presumably a more flexed hip and knee would decrease EMA, which would increase the muscle force required to support the greater portion of bodyweight at the pedals.

Measuring a rider's CoM position while cycling on an ergometer, treadmill, or over-ground can be done using an optical motion capture system. However, there are limitations to each of these experimental setups. Although ergometers allow multiple cycles to be collected per trial, they constrain the lateral dynamics of the bicycle, which changes the preferred movement pattern of the rider and may affect performance. Treadmills can provide a solution to ecological validity, but performing maximal sprinting is problematic due to the danger of matching the belt velocity to the rapid acceleration and high velocity of the bicycle wheels. Over-ground cycling can be captured, but the calibrated volume of the camera system will limit the number of cycles that can be collected. Thus, a method for tracking a rider's CoM motion when motion capture is not feasible would make it possible to examine the preferred movement pattern of cyclists outside of the laboratory. A possible solution to this problem is presented in Appendix B, where we undertook an additional study to assess the validity of an inertial measurement unit (IMU) mounted near the sacrum for measuring vertical CoM displacement and associated energy changes of cyclists while riding in a non-seated posture by comparing

the derived vertical displacement of the IMU to an attached marker cluster tracked with an optical motion capture system and to a kinematic estimate of vertical CoM displacement using a full-body musculoskeletal model.

Currently we can only speculate about the role of CoM movement during cycling. Research on this matter may shed light on whether the seated posture becomes unfavourable compared to a non-seated posture due to the bodyweight of the rider becoming unsupported at the saddle. Presumably as power output increases at a particular cadence, so too will the vertical component of pedal force. The upward accelerations of the CoM due to vertical pedal force may be detrimental for external power production if they occur during the downstroke, as this would require additional power to that generated on the crank. Transitioning to a non-seated posture could be an optimal strategy for generating high power outputs as the rider may be able to use their arms more effectively to resist upward accelerations of their CoM (Baker et al. 2002).

2.2.3 The effect of changing power output and cadence on crank torque

During cycling, the combination of power output and cadence dictates the amount of torque a rider must produce on the crank. Figure 2.5 shows a surface plot of the crank torque required at a wide range of power output (50-1000 Watts) and cadence (20-160 rpm) combinations. Equation 2.4 shows how crank torque is calculated from power output and cadence.

$$T = \frac{P}{\omega} \quad (2.4)$$

Where T is the mean torque over a crank cycle in Newton·metres, P is the mean power output over a crank cycle in Watts, and ω is the mean angular velocity over a crank cycle in $\text{rad}\cdot\text{s}^{-1}$. In Figure 2.5 angular velocity (ω) has been converted to cadence in revolutions per minute (rpm) using Equation 2.5.

$$\text{Cadence (rpm)} = \frac{\omega \cdot 60}{2\pi} \quad (2.5)$$

Note the decrease in cadence while keeping power output constant results in an exponential increase in torque required per crank cycle. Conversely, increasing power output while maintaining the same cadence shows a linear increase in torque required per crank cycle will occur. Furthermore, we can see that the effect of changing cadence or power output on crank torque is unique to each power output or cadence that is being used. The unique effect of changing power output at each cadence can be seen by the differences in the rate of change between each exponential curve as you move from 20-160 rpm. The unique relationship of changing cadence at each power output can be seen by the difference in slope between each cadence as you move from 50-1000 Watts.

This surface plot of torque can help explain the conflicting evidence on the preferred cadence of cyclists and the effects of changing cadence and power output on metabolic and mechanical

efficiency (Ansley and Cangley 2009). Force production and moving the lower limbs accounts for the majority of metabolic demand during locomotion (Taylor et al. 1980; Gottschall and Kram 2005; Kipp, Grabowski, and Kram 2018). Thus, the lower rate of increase in torque in response to increasing power output at higher cadences compared to lower cadences should correspond with a lower rate of increase in metabolic demand as power output increases at higher cadences compared to lower cadences. Consistent with this theory, it has been shown that delta efficiency, the ratio of change in external work to the change in total energy expenditure, is greater as cadence increases (Chavarren and Calbet 1999). However, this finding is misleading in the sense that it does not reflect gross efficiency, the ratio of total external work to total energy expenditure, of cycling at each particular cadence, which may be more relevant to sub-maximal cycling performance.

Exercise duration adds another layer of complexity to this topic (Wilkie 1960a), however, it is evident that the effect size of changing cadence will depend on the specific level of power output and vice versa. This varying interaction between torque, cadence, and power output seems consistent with the load-dependent nature of preferred cadence (Coast and Welch 1985; MacIntosh, Neptune, and Horton 2000), whereby rider's increase their preferred cadence in response to increasing power output. An apparent paradox in cycling is that preferred cadence is typically higher than that which is shown to be energetically optimal (Marsh and Martin 1993). More recent evidence suggests that other physiological and biomechanical factors have a greater influence on preferred cadence (Brennan et al. 2018, 2019). Specifically, riders appear to choose their preferred cadence based on a balance of maximising efficiency and power generation within specific muscles such as vastus lateralis (Barclay, Constable, and Gibbs 1993; Brennan et al. 2019). Thus, a rider's preferred riding posture and amount of vertical CoM displacement may also be a strategy to balance efficiency and power generation at a muscular level. There is evidence that at the same power output preferred cadence is significantly lower when non-seated compared to when seated (Lucia, Hoyos, and Chicharro 2001). This would suggest that the conditions under which the muscles must generate power and the contribution of non-muscular power influences a rider's choice of posture and preferred cadence. Further investigations of muscle mechanics and energetics during non-seated cycling at preferred cadences would provide important insights into the choice of posture during cycling. Furthermore, it is likely that a trade-off may exist between the energetic cost of producing positive work to raise the CoM against the benefit of increasing the momentum of the CoM to amplify tangential crank force. In fact it may be necessary to incur this cost to overcome the threshold of force production within the lower limb (Chang et al. 2000) as crank torque requirements increase. If the assumption that raising and lowering the CoM can be used to amplify tangential crank force production is correct, then the amplitude of CoM displacement may be linked to the amount of torque required at the crank, which means that the amplitude of vertical CoM displacement during non-seated cycling could be mapped as a function of power output and cadence similar to torque.

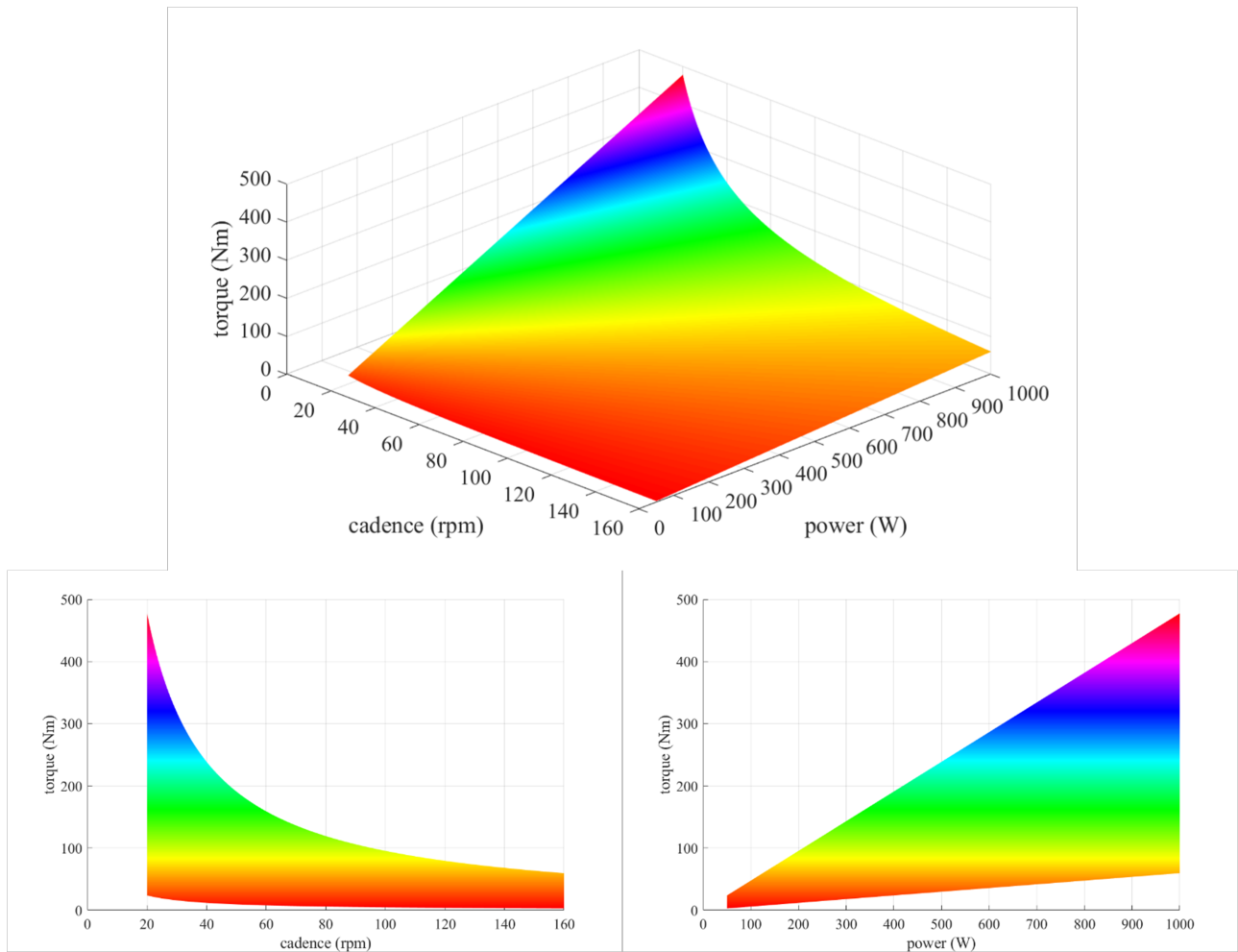


Figure 2.5: The effect of changing cadence or power output on torque requirements during cycling are each unique depending on the power and cadence you’re riding at. Top: A surface plot of torque as a function of power and cadence. Bottom left: Torque as a function of cadence. Bottom right: Torque as a function of power. The effect of changing power output on torque requirements is linear, but greater at low cadence than high cadence as can be seen by the increased slope. The effect of changing cadence on torque requirements is exponential, but increases at a greater rate as you increase power output from 50-1000 Watts. *Data calculated using Equation 2.4.*

2.3 Part III

2.3.1 Balance and steering

Maintaining balance is essential to any cycling task. Luckily, many of us gained the ability to balance a bicycle early in our childhood. Thus, the ease of performing the task later in life can mask its complexity. The principles that govern the stability of the bicycle are far from simple. Precise rider inputs must harmonise with the self-stabilising mechanisms of the bicycle (Jones 1970). To achieve balance, the bicycle and rider act as one system. The contact points between the road and the two tyres create the system’s base of support (BoS). This provides a large lengthwise BoS, but a very small lateral BoS. During dynamic balance, the position and velocity of a system’s CoM relative to its BoS is key (Hof, Gazendam, and Sinke 2005). If the

CoM falls outside the BoS, we are able to use force to redirect the momentum of the CoM back towards the BoS. You could liken this to a gymnast moving their arms and trunk to restore balance on a beam.

Recent research has quantified the skill of balancing on a bicycle (Cain, Ashton-Miller, and Perkins 2016). Subjects rode an instrumented bicycle on training rollers. Rollers constrain forward motion of the bicycle, but allow lateral movement and lean of the bicycle. Thus, a rider maintains balance by pedalling, steering, and leaning, similar to riding outdoors (Dressel and Papadopoulos 2012). This research compared the control strategies of experienced cyclists and non-cyclists. They graded performance on the correlation between the lateral position of CoM and the centre of pressure. At high speeds, experienced riders showed a higher correlation compared to novice riders. Meaning that experienced cyclists made small corrections to their CoM position rather than steering angle to achieve superior performance.

These researchers also measured the angle of bicycle lean in the frontal plane. This showed a negative correlation between rider lean and bicycle lean. This means that riders tend to counteract lean of the bicycle by shifting their CoM laterally or vice versa. Amplification of this motion occurs when a cyclist rides out of the saddle to climb or sprint. As the rider's produce peak force on each pedal, the bicycle steers and leans from side to side underneath the rider to shift the BoS and maintain dynamic balance of the system.

2.3.2 Lateral bicycle dynamics

Lateral bicycle dynamics involve changes in the net torque acting around the longitudinal axis of the bicycle-rider system's line of support. If the equilibrium of torque is disrupted, often referred to as a toppling torque (Loram, Maganaris, and Lakie 2004; Day, Lichtwark, and Cresswell 2013), then the system will either fall over or turn towards the fall. If the system has forward motion, then turning corners is achieved by maintaining a toppling torque on one-side of the BoS. Maintaining a straight path is achieved by continual adjustment of the toppling torque back to equilibrium.

Greater amounts of bicycle lean seem to occur when cyclists produce high pedal forces while in a non-seated posture (Duc et al. 2008) and appears to have an important role in balancing the torque around the longitudinal axis of the bicycle-rider system. Besides its apparent role during dynamic balance, little is known about how bicycle lean affects efficiency or maximal power output during cycling.

One aspect of non-seated cycling performance that should be considered is the increase in path length that is caused by the greater amplitudes of steering angle and bicycle lean. Theoretically, increasing deviations away from the straight line path between two points should increase the time it takes to complete the journey. Thus, a comparison of the effects of bicycle lean on the path length travelled during sprinting and climbing was undertaken. The results of this comparison are presented in Appendix A.

When the bicycle leans, the position of the pedals change in relation to the rider. Thus, it seems reasonable to suggest that this could change the kinematics of the rider's lower limbs. Early research using cine-film showed that the greatest angle of bicycle lean occurred when the cranks were in a vertical position (Soden and Adeyefa 1979). This coincided with the lowest vertical position of the lower back relative to the bike frame. It was surprising that the authors of this study concluded that these motions were of little consequence to cycling performance.

As the cranks are attached to the bicycle frame, the angle of lean must be the same for both. This could result in the pedal trajectory becoming elliptical rather than circular relative to the global reference frame and viewed in the sagittal plane. Very few studies have focused on the effects of bicycle lean on performance or the underlying physiological or biomechanical factors during non-seated cycling. One study tested the effect of bicycle lean on lower limb muscle activity by comparing non-seated cycling on a treadmill against cycling in a stationary ergometer which constrains bicycle lean. Their results showed that the sum of lower limb muscle activity was greater when riding the ergometer compared to using a preferred amount of lean on the treadmill (Duc et al. 2008). Thus, bicycle lean may benefit performance by changing the conditions under which muscles must produce force and power.

Bicycle lean angles were also found to increase as the slope of the ground increased (Duc et al. 2008). The authors conclude that this is "in order to achieve a better balance". However, it is hard to ascertain what is meant by "better balance" and what aspect of slope would cause a greater demand on lateral stability if cadence and power output are kept constant. A more thorough analysis of this finding coupled with the knowledge of lateral bicycle dynamics (Kooijman and Schwab 2009) may help to explain these findings. When we steer and the lean the bicycle, the imaginary line between the contact point of the front and rear wheel rotates like a horizontal pendulum (Dong et al. 2014). The projection of the rider's CoM must remain over this imaginary line of support or have a velocity in the direction of this line of support in order to maintain dynamic balance. As slope increases, the vertical projection of the bicycle's wheel base decreases. The vertical projection of the rider's CoM down to the surface of the Earth must always be in line with gravity. Therefore, the projection of the rider's CoM will move further towards the rear wheel unless the rider moves their CoM forward towards the handlebar. If the projection of the CoM moves further back in the wheel base, then an important change occurs regarding the amount of steering and lean that is required to bring the line of support underneath the CoM. As slope increases, the same lateral shift of the CoM will require greater and greater angular changes to the line of support. Hence, a greater amount of steering and subsequent lean would be required. An investigation of rider CoM position during non-seated cycling on increasing slopes would be necessary to show the relationship between slope, balance requirements, and bicycle lean angles. In such a study it would be necessary to measure the following: 1) the slope of the ground, 2) the fore-aft position of CoM within the bicycle's wheelbase, 3) the height of the rider's CoM above the ground, 4) the heading angle of the bicycle's line of support, and 5) the roll angle of the bicycle.

Leaning the bicycle also causes a vertical displacement of the bicycle's CoM. It is conceivable that the magnitude and timing of bicycle lean could decrease the vertical displacement of the bicycle-rider system's CoM. Out-of-phase vertical displacement between the rider and bicycle's CoM could play an important role in sprint cycling performance. Evidence for the benefit of this decoupling motion comes from research on the modern racing position of jockeys (Pfau et al. 2009). This research shows that adopting the modern riding technique allows jockeys to reduce the system's CoM movement in a global reference frame by moving their CoM out-of-phase with the horse's CoM. To do this the jockey performs a high amount of negative mechanical work with their legs (Pfau et al. 2009). This dissipation of energy compensates for the gain in potential energy of the horse. The result is that the horse no longer needs to perform work to raise and lower the mass of the jockey during each stride. The adoption of this technique over the first decade of the 20th century led to a greater improvement of race times in one decade than that of the following century (Pfau et al. 2009). It remains unclear whether a similar out-of-phase motion between the rider and bicycle's CoM occurs during non-seated cycling and whether it can provide any performance advantages.

2.3.3 Stability of a bicycle on treadmills and rollers

As outlined by Meijaard et al. (2011) in their "Historical Review of Thoughts on Bicycle Stability", there are many common beliefs about the stability of bicycles that are in contrast to reality. For example, neither the "gyro effect" nor trail of the front wheel behind the steering axis are necessary for a bicycle to self-stabilise. Instead, their findings highlight a complex interaction of many other terms. Specifically, they concluded that the location of the front-assembly CoM relative to the system CoM and steer axis was the one variable that had the greatest effect on self-stability. These findings have particular significance for conducting experiments on treadmills and rollers. An assumption that pervades cycling research is that lateral dynamics of a bicycle are different when riding on a treadmill compared to riding outdoors. However, rigorous experimental findings (Kooijman and Schwab 2009) together with the principle of Galilean invariance (Dressel and Papadopoulos 2012) show that at constant velocity, riding a bicycle on a treadmill is mechanically identical to riding on fixed, level ground. The original example used to illustrate that the laws of motion hold true in all inertial reference frames was that of a passenger below the deck of a ship travelling at constant velocity without rocking (Galilei 1967). In the passenger's frame of reference the ship appears to be stationary, thus they would be unable to distinguish whether the ship had a velocity or was stationary. It is obvious in this example that the passenger's frame of reference has no bearing on the laws of motion acting on the ship. Similarly, the frame of reference of a rider or an observer during treadmill cycling has no bearing on the laws of motion acting on the bicycle.

There are however subtle differences between riding on rollers compared to riding on a treadmill and fixed ground (Dressel and Papadopoulos 2012). First, the curved surface of the

rollers means that the contact patch of a tyre on rollers is less than on a flat treadmill belt. Secondly, there is a “*complex geometric interaction between the front wheel and the upper surface of the front roller as the bicycle steers and yaws*”, which requires further investigation to be fully understood. Finally, “*the moments about a vertical axis exerted on the rear wheel by lateral forces*” differs from treadmill cycling as the rear wheel is in contact with two rollers rather than a flat belt.

Beyond the mechanics there are alterations to psychological factors and motion perception that pertain to riding on both a treadmill and rollers that may increase the difficulty of the task. First, the narrow width of the belt or rollers constrain the rider to an unusually narrow path and may induce a cognitive dissonance between the expectation or sense of moving forward and the stationary visual field. The presence and magnitude of these effects is still unknown, however it must be considered when attempting to generalise findings from studies on treadmills and rollers to riding on a fixed surface.

2.3.4 Effect of bicycle lean on the metabolic cost of cycling

Literature on this topic is sparse, however it has been proposed by one group of authors that cyclists may be able to decrease the metabolic cost of cycling in a non-seated posture by self-restricting the amount of lateral bicycle lean that occurs during each crank cycle (Bouillod et al. 2018). This theory was proposed after finding that both metabolic cost and bicycle lean velocity increased during uphill cycling in a non-seated posture versus a seated posture. The obvious flaw in this theory is the confounding effect of posture. The non-seated posture increases both metabolic energy expenditure and bicycle lean velocity. Thus, this spurious correlation provides no evidence of any relationship between bicycle lean velocity and metabolic cost. Furthermore, this investigation had a number of methodological flaws. First, metabolic measures were taken during 30-s intervals of cycling where riders immediately switched from a seated to non-seated posture. To illustrate the problem of inferring the metabolic cost during interval type training sessions, consider measuring metabolic cost on someone performing alternating 30-s bouts of cycling at 100 W and 300W in the same posture. The well-known delay between mechanical power production and oxygen uptake (Astrand et al. 2003) means that we could make erroneous conclusions about the metabolic cost of each intensity as a washout period occurs during each 30-s interval. Secondly, the RER values in this experiment were >1 , meaning that the ratio of CO₂ exceeded that of O₂. This invalidates any conclusions about metabolic energy expenditure, as the predominant fuel source was supplied through anaerobic metabolism during all conditions (Astrand et al. 2003). Finally, as mentioned, there was no direct comparison between a non-seated posture with and without the use of bicycle lean. Therefore, the spurious correlation between bicycle lean velocity and metabolic energy expenditure is likely due to differences between the seated and non-seated posture. To the best of our knowledge, no other evidence has been published regarding the direct effect of

self-restricting bicycle lean on the mechanics or energetics of non-seated cycling.

The following published manuscript has been incorporated as Chapter 2.

Wilkinson, Ross D., Glen A. Lichtwark, and Andrew G. Cresswell. 2020. The Mechanics of Seated and Nonseated Cycling at Very-High-Power Output: A Joint-Level Analysis. *Medicine & Science in Sports & Exercise* 52(7): 1584-94. doi: 10.1249/MSS.0000000000002285

Contributor	Statement of contribution	%
Wilkinson, R.D.	writing of text study design and concept data collection data analysis statistical analysis preparation of figures revision of written work supervision, guidance	80 20 90 90 90 80 40 0
Lichtwark, G.A.	writing of text study design and concept data collection data analysis statistical analysis preparation of figures revision of written work supervision, guidance	10 40 5 5 5 10 30 50
Cresswell, A.G.	writing of text study design and concept data collection data analysis statistical analysis preparation of figures revision of written work supervision, guidance	10 40 5 5 5 10 30 50

Chapter 3

The Mechanics of Seated and Non-Seated Cycling at Very-High-Power Output: A Joint-Level Analysis.

3.1 Abstract

Cyclists frequently use a non-seated posture when accelerating, climbing steep hills, and sprinting; yet, the biomechanical difference between seated and non-seated cycling remains unclear. **Purpose:** To test the effects of posture (seated and non-seated) and cadence (70 rpm and 120 rpm) on joint power contributions, effective mechanical advantage, and muscle activation within the leg during very-high-power output cycling. **Methods:** Fifteen male participants rode on an instrumented ergometer at 50% of their individualised peak maximal power ($10.74 \pm 2 \text{ W}\cdot\text{kg}^{-1}$; above the reported threshold for seated to non-seated transition) in different postures (seated and non-seated) and at different cadences (70 rpm and 120 rpm), whilst lower limb muscle activity, full body motion capture and crank radial and tangential forces were recorded. A scaled, full-body model was used to solve inverse kinematics and inverse dynamics to determine joint displacements and net joint moments. Statistical comparisons were made using a repeated measure, two-way analysis of variance (posture x cadence). **Results:** There were significant main effects of posture and cadence on joint power contributions. A key finding was that the non-seated posture increased negative power at the knee, with an associated significant decrease of net power at the knee. The contribution of knee power decreased by 15% at both 70 and 120 rpm ($\sim 0.8 \text{ W}\cdot\text{kg}^{-1}$) when non-seated compared to seated. Subsequently, hip power and ankle power contributions were significantly higher when non-seated compared to seated at both cadences. In both postures, knee power was 9% lower at 120 rpm compared to 70 rpm ($\sim 0.4 \text{ W}\cdot\text{kg}^{-1}$). **Conclusion:** These results evidenced that the non-seated posture

significantly decreases net mechanical power requirements at the knee when cycling at high power outputs, however the effect is cadence dependent.

3.2 Introduction

Cyclists often transition from a seated to a non-seated posture during short, intensive bouts of climbing, accelerating and sprinting (Costes et al. 2015). An increased understanding of the biomechanical differences between the seated and non-seated posture has practical importance for cycling performance and equipment design (Hansen and Waldeland 2008), as well as injury prevention and rehabilitation (Stone and Hull 1993). The non-seated posture is typified by cyclists raising their pelvis off the saddle, which results in a more extended hip and knee angles, an alteration of the direction of the resultant crank force (Caldwell et al. 1998) and an effective use of body mass to generate positive power at the crank during the downstroke (Stone and Hull 1995). Although it is known that the non-seated posture is more effective than the seated posture for peak maximal power production (Millet et al. 2002; Reiser II et al. 2002) cyclists often transition off the saddle well before their limit of power production is reached (Costes et al. 2015; Poirier, Do, and Watier 2007). For example, using an incremental testing protocol within a laboratory setting it was determined that non-cyclists spontaneously transitioned to a non-seated posture at 568 ± 93 Watts ($7.9 \pm 1.4 \text{ W}\cdot\text{kg}^{-1}$) when pedalling at a cadence of 90 rpm (Costes et al. 2015), well below the 6-sec maximal power production measured in a similar untrained population of 813 ± 137 W ($12.43 \pm 1.34 \text{ W}\cdot\text{kg}^{-1}$) (Vandewalle et al. 1987).

Field testing (Hansen and Waldeland 2008) has shown that competitive cyclists can increase their time to exhaustion during uphill cycling by using the non-seated posture when the required power output is at or above 419 ± 30 Watts ($5.6 \pm 0.4 \text{ W}\cdot\text{kg}^{-1}$). In the same study, it was shown that preferred cadence decreased from 92 ± 2 rpm when seated to 74 ± 3 rpm when non-seated. This preference for a lower cadence when non-seated implies that cyclists favour generating power at the crank by increasing crank torque and reducing crank angular velocity. Thus, if we assume the range of motion at each lower limb joint to be similar between postures, one of the possible benefits of the transition could be that it alters the conditions under which the muscles perform work or allows cyclists to redistribute the work requirements to different muscles. Currently no methods exist to directly measure this redistribution at a muscular level, however the integration of inverse dynamics and electromyography (EMG) may provide indirect evidence of these changes.

Joint-level analyses of seated cycling have shown that the distribution of total lower limb power among the hip, knee and ankle is sensitive to the torque and angular velocity demands (Elmer et al. 2011; Lieber and Bodine-Fowler 1993). For example, Elmer et al. (Elmer et al. 2011) reported that as net crank power increased from 250 to 850 Watts at a constant cadence of 90 rpm (i.e. increasing torque demand), the contribution of knee extension power decreased, whereas the contribution of knee flexion power increased. A similar analysis of seated maximal

sprint cycling by McDaniel et al. (McDaniel et al. 2014) found that as cadence increased from 60 rpm to 180 rpm the contribution of hip extension power and knee flexion power increased, while the contribution of knee extension power did not change. These findings provide an indication of how joint power is likely to be redistributed in response to changes in power output and cadence, however it is not known whether a similar redistribution of joint power will occur when non-seated, or if the initial distribution of total lower limb power is similar to when seated.

EMG analyses have provided insight into the sources of power generation during non-seated cycling (Li and Caldwell 1998; Turpin et al. 2016), however fundamental mechanical differences between the seated and non-seated posture remain unresolved. These gaps exist as previous research has primarily focused on either performance (Reiser II et al. 2002; Hansen and Waldeland 2008) or physiological economy differences (Millet et al. 2002; Tanaka et al. 1996; Harnish, King, and Swensen 2007) between the two postures. Thus, biomechanical assessments of the non-seated posture remain incomplete and allow only speculation of the underlying mechanical interaction of muscles and body segments. It seems likely that the kinematic differences between the seated and non-seated posture; notably the anterior shift in the rider's CoM and more extended hip and knee position, will impact the pattern of power production and absorption within the lower limb, especially at the knee. Yet to date, no study has determined whether the distribution of lower limb power among the hip, knee and ankle differs between the seated and non-seated postures.

The present study was designed to compare the distribution of joint powers between seated and non-seated postures during high power output cycling at two different cadences. Effective mechanical advantage and muscle activity in the lower limb was also compared between the postures under these same cadence and power conditions. It was predicted that at a constant external power output, the net contribution of knee power would be lower in the non-seated posture compared to seated at each cadence and that the redistribution of this power would be cadence dependent. It was also predicted that a decrease in both the peak knee extension moment and net knee power in the non-seated posture would be associated with improved effective mechanical advantage at the knee compared to when seated.

3.3 Methods

Participants

Fifteen active and healthy males (age 30 ± 8 years, height 179 ± 5 cm; mass 74 ± 9 kg) volunteered to participate in this study. The athletic background of the participant group was varied. Eight of the participants were cyclists who competed weekly at club level, while the remainder regularly engaged in a variety of competitive or recreational sports. All participants gave their written informed consent prior to participating in this study according to the procedures approved by the Human Ethics Committee of The University of Queensland and in

accordance with the general principles expressed in the Declaration of Helsinki.

3.3.1 Experimental protocol

Participants performed five 3-s all-out seated sprints to determine their peak instantaneous maximal power ($P_{max,i}$) followed by four sub-maximal trials at 50% of their individual $P_{max,i}$ under different combinations of posture (seated or non-seated) and cadence (70 rpm or 120 rpm); outlined below.

Ergometer setup

Once the participants were deemed fit for testing, their body mass, height, inside leg length, torso length, arm length and shoe size were measured. These measures were then used to fit the participants to the cycling ergometer, which was used for all trials (Excalibur Sport, Lode BV, Groningen, The Netherlands). Seat tube angle was standardised to 73° with respect to horizontal and knee angle was standardised to 150° of extension when the right pedal was at its lowest position. This angle was measured using a goniometer with the participant in a static, seated posture on the ergometer. Knee angle was determined from the bisection of two lines connecting markers placed on the greater trochanter, lateral femoral condyle and lateral malleolus. The saddle height and fore-aft position of the saddle were incrementally adjusted until the desired combination of knee angle and seat tube angle were achieved. Torso angle was standardised to 70°, with arms slightly bent at the elbow and hands placed in the drops of the handlebar. Torso angle was defined with respect to horizontal by the line connecting markers placed on the acromion process and greater trochanter. Some minor adjustments to this fitting were allowed based on participant preference. Crank length was constant at 175 mm. Participants wore a standardised model of cleated cycling shoe (SH-R070, Shimano, Osaka, Japan) that clipped into the pedals (SH-R540, Shimano, Osaka, Japan).

Maximal power output test ($P_{max,i}$)

Participants began with a 5-min cycling warm-up at 100 W at their preferred cadence. Participants then performed five maximal sprints of 3-s duration in a seated posture to determine their individual $P_{max,i}$. The ergometer was set to “Linear” mode, which ensured that power was coupled to cadence. It was expected that participants would achieve $P_{max,i}$ at a cadence of approximately 120 rpm (Gardner et al. 2007; Dorel et al. 2005; Dorel 2018a). Thus, the linear resistance was increased or decreased for each subsequent trial based on whether the participant achieved a peak cadence above or below 120 rpm. $P_{max,i}$ was successfully determined within five trials for all participants and was calculated as the highest “instantaneous” power that occurred during a crank cycle. Participants were given 3 min of rest between trials to reduce any potential fatigue effects.

Sub-maximal trials

A 20-min period of rest was given after the $P_{max.i}$ test before commencing the four sub-maximal trials. The constant power output and cadence (70 rpm or 120 rpm) conditions for the sub-maximal trials were chosen with the intention to create two scenarios where cyclists would prefer to ride in a non-seated position. This assumption was based on the reported seated to non-seated transition power at 90 rpm (Costes et al. 2015), and that this transition power is dependent upon the amount of torque required per crank cycle. Thus, the power output had to be high enough for riders to still want to ride off the saddle at 120 rpm, while low enough that it was still achievable at 70 rpm in both postures. Pilot testing revealed that 50% of individual $P_{max.i}$ measured at approximately 120 rpm would be appropriate for this purpose. The two cadence conditions of 70 rpm and 120 rpm were chosen primarily to provide a contrast in the amount of torque required per cycle, however they also happen to be approximately equal to preferred cadences used during climbing (Lucia, Hoyos, and Chicharro 2001) and sprinting (Gardner et al. 2007), respectively. It should be noted that the selected power output and cadences were not intended to simulate the exact conditions of sprinting or climbing. Participants performed the combinations of posture and cadence in a randomised order and were required to maintain the target cadence and power output for a minimum period of 10-sec. The ergometer was set to ‘Hyperbolic’ mode, which ensures that the power output remains constant independent of cadence, thus riders were required to maintain the specific set cadences using feedback from the visual display on the ergometer. To test for the presence of any exercise-induced fatigue, an additional 3-s maximal sprint was performed following the sub-maximal trials. Inclusion required the participants to be able to match ($\pm 5\%$) their previously tested $P_{max.i}$ in this additional trial. Kinematics, kinetics and EMG were recorded during the sub-maximal trials.

3.3.2 Data collection

All analogue signals were acquired using a 16-bit analogue-to-digital (A/D) conversion board (USB-2533, Measurement Computing Corporation, Norton, MA) using Qualisys Track Manager software (Qualisys AB, Gothenburg, Sweden).

Motion capture

An eight camera, opto-electronic motion capture system (Oqus, Qualisys, AB, Sweden) was used to measure the three-dimensional (3D) position of 45 passive reflective markers at 200 Hz. Markers were secured using double-sided tape over the suprasternal notch, vertebrae C7, sacrum, and bilaterally over the acromion processes, lateral epicondyles of the humerus, styloid processes of the radius, iliac crests, anterior superior iliac spines, posterior superior iliac spines, greater trochanters, medial and lateral condyles of the femur, medial and lateral malleoli, calcanei, heads of the 1st and 5th metatarsals and the 2nd distal phalanxes (marker placements are shown in Figure 3.1). Lightweight rigid clusters of four markers were also secured bilaterally to

the lateral mid-thighs and lateral mid-shanks using double-sided tape and self-adhesive bandage. Prior to the sub-maximal trials, marker positions were captured with the participant standing in a standard anatomical posture. This static trial was later used for scaling purposes during data processing. The heading (yaw) angle of the ergometer was determined relative to the motion capture global coordinate system by placing two passive reflective markers on the rear support legs of the ergometer. These markers were used to establish a local coordinate system for the ergometer, which accounted for any discrepancy with the global coordinate system between trials.

Crank angle and forces

Tangential and radial forces to the left and right crank, and crank angle were recorded at 100 Hz using pre-calibrated, wireless, instrumented cranks (Axis, SWIFT Performance, Brisbane, Australia). Digital signals were transmitted wirelessly to a base receiver and then converted to an analogue signal through the A/D Board. The digital sampling frequencies of the crank (100 Hz) and EMG (2k Hz) were matched to the motion capture (200 Hz) sampling frequency using the internal sampling factor within the Qualisys Track Manager software. A multi-axis, dynamic calibration of each crank was performed in-house by the fabricating company (Swift Performance, Australia). In addition and prior to testing, voltage offsets for tangential and radial force signals were determined by hanging a known mass of 2.5 kg from each pedal spindle with the cranks in a horizontal and vertical position, which allowed any discrepancy in the offset to be removed post-processing. The crank angle signal was zeroed with the right crank at top dead centre (TDC).

Electromyography

Surface EMG signals of gluteus maximus (GMax), rectus femoris (RF), long head of biceps femoris (BF), vastus lateralis (VL), gastrocnemius medialis (MG) and soleus (SOL) were recorded wirelessly from the right leg at 2 kHz (Myon AG, Baar, Switzerland). Before electrode application, the skin at each recording site was shaved, abraded and cleaned to reduce impedance. Bipolar electrodes (Ag/AgCl, Covidien, Mansfield, MA) were then placed according to SENIAM recommendations, except for SOL which was placed medial to the muscle belly and parallel to its fibre pennation angle. Each signal was then checked for clarity and strength during an attempted isolated contraction. All cables and electrodes were then secured to the skin using a combination of adhesive tape and self-adhesive bandage to minimise movement artefact.

3.3.3 Data analysis

Joint power

3D motion capture marker trajectories were labelled and exported with all analogue data (EMG, crank force and angle) to MATLAB (R2017a, Mathworks Inc., USA) where they were processed

using custom scripts. Crank force signals and marker trajectories were zero-lag low-pass filtered at 12 Hz using a digital second order Butterworth filter (Kristianslund, Krosshaug, and Van den Bogert 2012). The position (angle) signal collected for the right crank was used to create an anti-phase signal which was used as the angle of the left crank. These angle signals were converted to the global coordinate system and then used to convert the respective crank forces (tangential and radial) into their horizontal and vertical components with respect to the same global coordinate system. These force components, along with the marker trajectories, were then rotated into the ergometer coordinate system using 2D and 3D rotation matrices, respectively. The origin of the resultant force was determined by creating a virtual marker at the centre of the cleat attachment. This approximation was determined using the crank angle, three-dimensional shoe orientation and shoe size and then verified against a second approximation using the bottom bracket position, crank length, crank angle and pedal spindle length.

Inverse kinematics and inverse dynamics were calculated using OpenSim software (Delp et al. 2007). First, a previously developed generic full-body musculoskeletal model (Rajagopal et al. 2016), was scaled to each participant's anthropometry. Segment length of the upper limbs, torso and lower limbs were scaled in all three axes using the distance between nominated marker pairs. Scaling factors were calculated by comparing these distances to that of the generic model. The mass of the participant was then used in combination with these scaling factors to distribute segment masses. This scaled model as well as the kinematic and kinetic data collected during the sub-maximal trials were used to run inverse kinematics and inverse dynamics via the Application Programming Interface between OpenSim and MATLAB. The inverse kinematics tool within OpenSim calculates joint angles at each time step by using a weighted least squares fit to minimise errors between the experimental markers and model markers. These results are then combined with external loads applied to the model, in this case reaction forces at the left and right crank, to determine the net joint moment at the ankle, knee and hip joints. Joint power was calculated as the dot product of the net joint moment and joint angular velocity. Flexor moments and flexion velocity were defined as positive. Joint powers were then summed and integrated to calculate joint work. Net joint work was the integral of all joint power values over a complete crank cycle starting and finishing at TDC. Total positive and negative work were the integral of all positive and negative powers, respectively, over the same range (Winter 1990). Individual joint work contributions to total work were calculated by dividing individual net joint work by the summed net joint work of the hip, knee and ankle. Data from the sub-maximal trials were averaged across five cycles of the right crank where the participant was able to match the target power ($\pm 5\%$) and cadence ($\pm 5\%$). If the participant failed to simultaneously match the target power and cadence the data was excluded from the analysis. The minimum number of crank cycles used to average participant data in this study was two.

Muscle activity

DC offset was removed from the raw EMG signal for each muscle prior to band-pass filtering between 20-400 Hz. The signals were then rectified and low pass filtered at 15 Hz using a fourth order zero-lag digital Butterworth filter. The resulting EMG signals were interpolated to 360 data points per cycle to enable a mean signal to be calculated over 5 crank cycles. The mean signals were then normalised to the peak EMG RMS value from the trial in which the participant achieved $P_{max,i}$. Due to movement artefact a number of trials for specific recording sites were discarded. Results for GMax, RF and VL were averaged across 14 participants, MG and SOL were averaged across 12 participants and BF was averaged across 10 participants.

Effective Mechanical Advantage

As defined by Biewener (Biewener 1989), “effective mechanical advantage (EMA) is the ratio of the extensor muscle moment arm (r) to the moment arm of the ground reaction force (R) acting about the joint.” In cycling the reaction force on the crank takes the place of the ground reaction force for this ratio. Hence, closer alignment of the joint centre of rotation to the crank reaction force vector will increase a muscle group’s EMA. Extensor muscle moment arms (r) of the right hip, knee and ankle were calculated within OpenSim software using the moment arms of gluteus maximus as the hip extensor moment arm, vastus lateralis for the knee and soleus for the ankle. In each condition, EMA of hip extensors, knee extensors and ankle plantar flexors were calculated at the time of the peak resultant crank force.

3.3.4 Statistical analyses

A two-way repeated-measures ANOVA was performed to test for main effects of posture and cadence and interaction effects (posture-cadence) on relative joint power, EMA and mean EMG RMS. The alpha level for main and interaction effects was set at 0.037 prior to statistical analysis. This alpha level was based on a desired false positive risk of < 5%, a prior probability for a real effect of 0.5, sample size of fifteen and an estimated effect size of 1 (Colquhoun and Longstaff). Whenever a main or interaction effect was found, multiple comparisons were used to detect the effect of the factor/s in each condition. The alpha level was corrected for family-wise multiple comparisons using the Sidak method. As per recommendations (Bakeman 2005; Lakens 2013), the F-value (F), p-value (ρ), and generalised eta squared (η_G^2) are provided for main and interaction effects. For multiple comparisons the t-statistic (t), adjusted p-value (ρ), 95% confidence intervals (95%CI [Low-High]), and corrected effect size known as Hedge’s g_{av} (ES) are provided. The η_G^2 for each variable was assessed against the benchmarks of trivial (<0.0099), small (0.0099-0.0588), moderate (0.0588-0.1379), and large effect (>0.1379)(29). The ES for each variable was assessed against the commonly used benchmarks of small (0.1-0.3), moderate (0.3-0.5) and large effect (≥ 0.5) (Bakeman 2005). All values are reported as mean \pm SD.

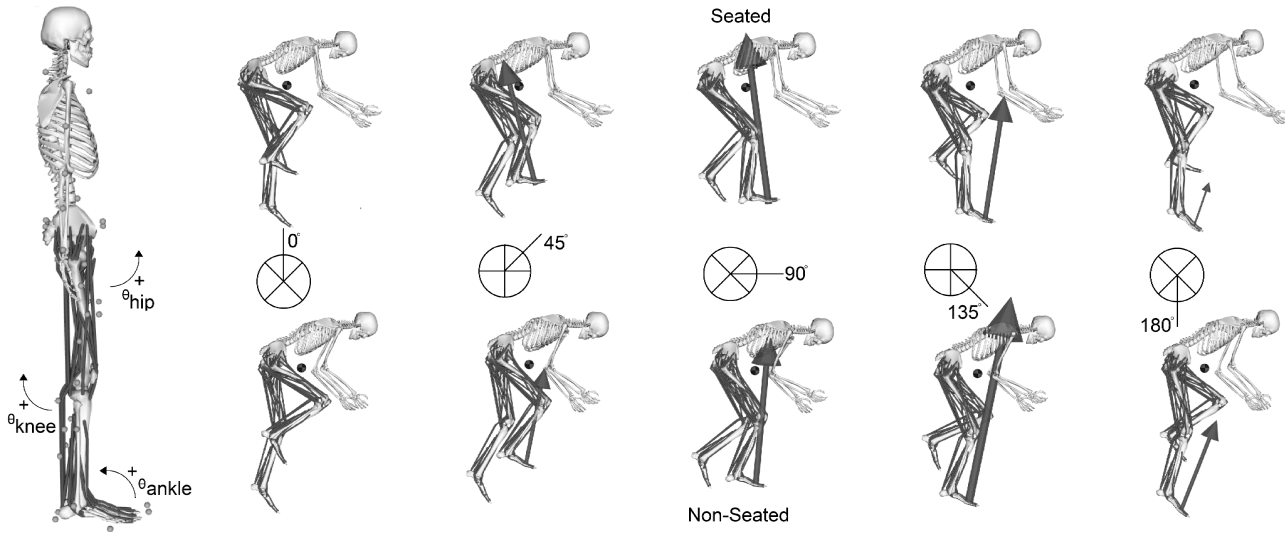


Figure 3.1: Switching to a non-seated posture shifts peak force production to later in the crank cycle. Sagittal-plane images of a representative participant during a static trial (left) showing the definition of hip, knee and ankle joint angles and marker positions; and during seated and non-seated cycling at 70 rpm for five selected crank positions during the downstroke (0° , 45° , 90° , 135° , 180°). Arrows represent the magnitude and direction of the resultant crank reaction force vector. Grey and black circle represents the participant’s CoM position. n.b.: The clockwise shift in force production when non-seated compared to seated.

3.4 Results

The mean $P_{max,i}$ across the participant group was 1605 ± 368 W (21.5 ± 4 W·kg $^{-1}$), giving a mean power output of 10.74 ± 2 W·kg $^{-1}$ for the sub-maximal trials. We individualised the mean crank power output over a complete crank for the sub-maximal trials (10.74 ± 1.99 W·kg $^{-1}$) as 50% of each participant’s $P_{max,i}$ recorded during the maximal power output test. Thus, the power output for the sub-maximal trials was $\sim 85\%$ of each participant’s mean maximal power output ($P_{max,m}$) recorded during the maximal power output test (See Table 3.3). Furthermore, due to the effect of cadence on maximal power production it is likely that the sub-maximal power output was near maximal during the 70 rpm conditions. There was good agreement between the target power and cadences, with power and cadences measured at the crank during each sub-maximal trial (See Table 3.3). Group mean crank torque, velocity and power curves with respect to crank angle during the $P_{max,i}$ and sub-maximal trials have been provided as supplementary information (See Figure, Appendix C.1). There was a clear rightward phase shift in crank resultant force, velocity and power when non-seated compared to seated, as well as a large difference between crank power and lower limb power during the downstroke, as has previously been demonstrated (Elmer et al. 2011).

Mean power production at the hip, knee and ankle with respect to crank angle are shown in Figure 3.2, from which clear effects of posture and cadence can be seen. At 70 rpm, power curves for all joints are phase shifted to the right when non-seated, however this phase shift is less pronounced at 120 rpm. In all conditions the crank cycle begins with power being generated predominantly through knee extension. At 70 rpm, this contribution is much greater in the

seated posture, but similar between postures at 120 rpm. The power generation phase at the knee is followed by an absorption phase, which occurs simultaneously with hip extension and ankle plantar flexion power. During this period the hip contributes significantly more power at 120 rpm than at 70 rpm. At 70 rpm, the ankle begins the crank cycle with a small period of negative plantar flexion power in both postures, after which its positive power steadily increases. Positive power contributions at the hip and knee during the second half of the crank cycle are clearly visible.

All statistics (F-value (F), p-value (p), generalised eta squared (η_G^2), t-statistic (t), adjusted p-value (p), 95% confidence intervals (95%CI [Low-High]), and corrected effect size (ES)) relating to the effects of posture and cadence on joint power contributions have been provided in Table 3.3. This analysis revealed main effects of posture on net joint power contributions, which resulted in a moderate increase in hip power, a large decrease in knee power and a large increase in ankle power in the non-seated compared to seated posture (Figure 3.4A). At both cadences, knee power in the non-seated posture was 15% ($0.8 \text{ W}\cdot\text{kg}^{-1}$) less than when seated. At 70 rpm, hip power increased by 10% ($0.55 \text{ W}\cdot\text{kg}^{-1}$) and ankle power by 5% ($0.26 \text{ W}\cdot\text{kg}^{-1}$) in the non-seated compared to seated posture. At 120 rpm, hip power increased by 12% ($0.78 \text{ W}\cdot\text{kg}^{-1}$) and ankle power by 3% ($0.25 \text{ W}\cdot\text{kg}^{-1}$) in the non-seated compared to seated posture. Interestingly, net knee power was lower than net hip and ankle power in all conditions. There was also a main effect of cadence on the power contributed at each joint, which resulted in a large increase in hip power, a moderate decrease in knee power, and a large decrease in ankle power when cycling at 120 rpm compared to 70 rpm (See Table 3.3).

The contribution of each joint to both positive and negative power is shown in Figure 3.4 (B-D). In all conditions the knee contributed positive power in the first and third quarter of the crank cycle, however, this was offset by large amounts of negative power during the second quarter. There was a 21.5% increase in negative power during knee extension when non-seated ($-0.8 \text{ W}\cdot\text{kg}^{-1}$) compared to seated ($-0.6 \text{ W}\cdot\text{kg}^{-1}$) at 70 rpm and a 22.4% increase in negative power during knee extension when non-seated ($-0.9 \text{ W}\cdot\text{kg}^{-1}$) compared to seated ($-0.7 \text{ W}\cdot\text{kg}^{-1}$) at 120 rpm. Hip flexion power accounted for $24 \pm 6\%$ ($1.1 \cdot\text{kg}^{-1}$) of positive hip power when non-seated at 120 rpm compared to $20 \pm 9\%$ ($0.8 \cdot\text{kg}^{-1}$) when seated. When seated at 70 rpm, knee flexion power accounted for $32 \pm 8\%$ ($0.6 \cdot\text{kg}^{-1}$) of positive knee power compared to $27 \pm 13\%$ ($0.4 \cdot\text{kg}^{-1}$) when non-seated. At 120 rpm, knee flexion power accounted for $44 \pm 11\%$ ($0.8 \cdot\text{kg}^{-1}$) of positive knee power compared to only $34 \pm 10\%$ ($0.5 \cdot\text{kg}^{-1}$) when non-seated.

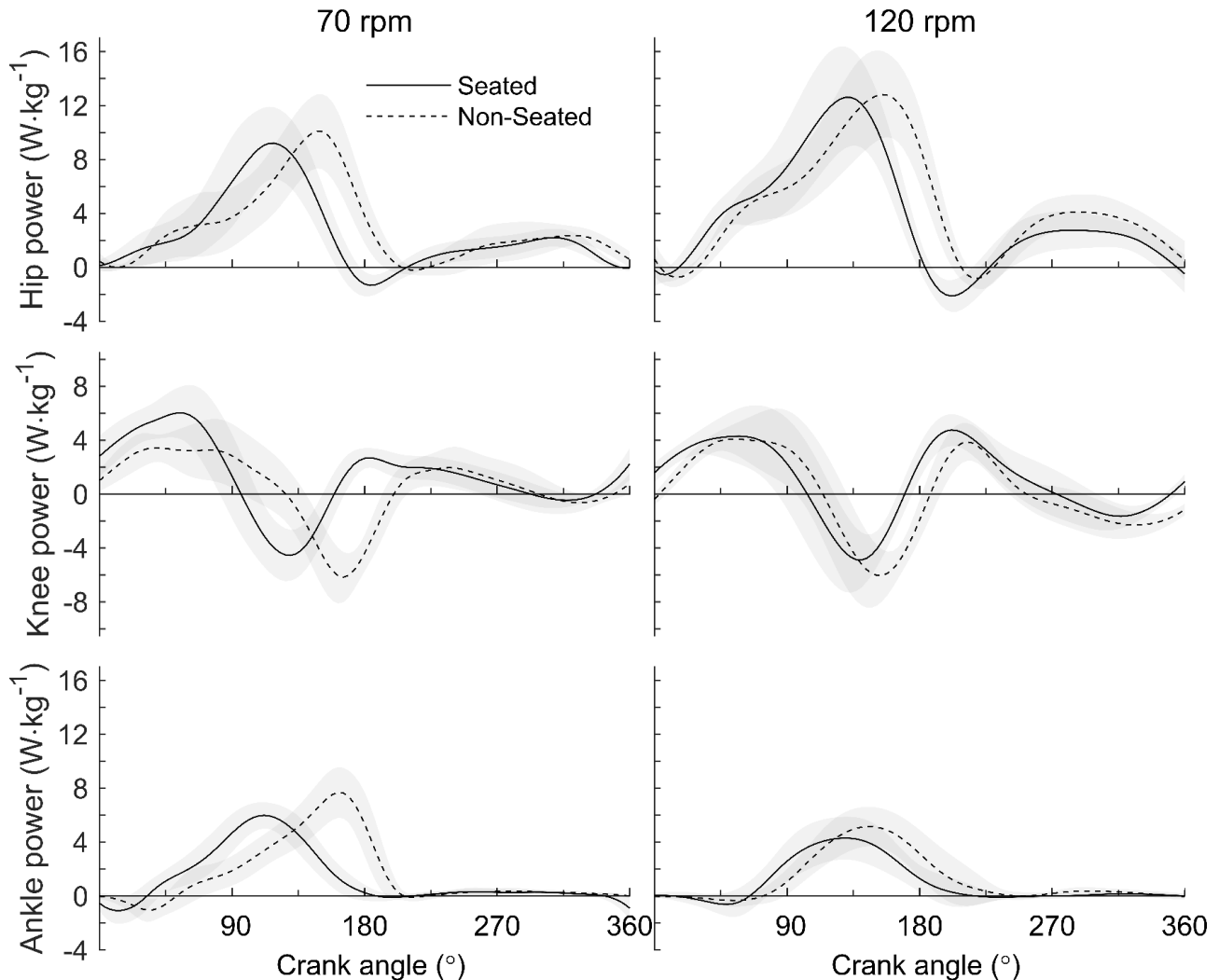


Figure 3.2: Joint power production occurs later in the crank cycle when in a non-seated posture compared to seated. Comparison of group mean (\pm SD; shaded area) hip, knee and ankle power in the right lower limb between the seated (solid lines) and non-seated (dashed lines) posture during high-power output cycling at 70 rpm and 120 rpm. n.b.: Power curves are visibly phase shifted to the right when non-seated, particularly at 70 rpm. Knee power curves are characterised by a significant period of negative power during the downstroke.

TABLE 1. Group mean \pm SD crank power ($\text{W}\cdot\text{kg}^{-1}$), cadence (rpm), and joint power ($\text{W}\cdot\text{kg}^{-1}$) during the maximal sprint and submaximal trials.

	Maximal Sprint		70 rpm		120 rpm		Two-Way ANOVA (Posture–Cadence)	
	Seated	Seated	Seated	Nonseated	Seated	Nonseated	Main and Interaction Effects	
Cadence	120 \pm 2	70 \pm 3	71 \pm 3		118 \pm 4	119 \pm 4	No main or interaction effects	
Crank power								
Peak instantaneous ($P_{\text{max,i}}$)	21.48 \pm 3.97	15.67 \pm 1.28	17.94 \pm 2.12		17.29 \pm 2.48	18.34 \pm 2.79	(–)	
% $P_{\text{max,i}}$	100 \pm 0	75 \pm 12	85 \pm 14		81 \pm 8	86 \pm 10	(–)	
Mean								
Both cranks ($P_{\text{max,m}}$)	13.52 \pm 2.53	11.27 \pm 1.45	11.45 \pm 1.62		11.23 \pm 1.56	11.36 \pm 1.50	(–)	
% $P_{\text{max,i}}$	63 \pm 4	53 \pm 5	54 \pm 6		53 \pm 5	54 \pm 5	(–)	
% $P_{\text{max,m}}$	100 \pm 0	85 \pm 11	86 \pm 12		84 \pm 9	85 \pm 11	(–)	
% Target power	(–)	106 \pm 11	108 \pm 12		106 \pm 9	107 \pm 10	(–)	
Right crank	6.94 \pm 0.66	5.67 \pm 0.67	5.82 \pm 0.86		5.65 \pm 0.81	5.74 \pm 0.80	Posture ($F=9.5$, $P=0.008$, $\eta_G^2 = 0.006$ [trivial])	
% Both cranks	51 \pm 1	50 \pm 1	52 \pm 2		50 \pm 2	51 \pm 2	(–)	
Joint power								
Right leg	(–)	4.92 \pm 0.34	4.95 \pm 0.60		5.47 \pm 0.69	5.67 \pm 0.69	Cadence ($F=56$, $P<0.001$, $\eta_G^2 = 0.24$ [large])	
% Right crank	(–)	87 \pm 7	86 \pm 7		97 \pm 7	99 \pm 9	(–)	
Hip	(–)	2.39 \pm 0.80	2.94 \pm 0.87		3.62 \pm 1.03	4.40 \pm 0.99	Posture ($F=37$, $P<0.001$, $\eta_G^2 = 0.12$ [moderate]); Cadence ($F=278$, $P<0.001$, $\eta_G^2 = 0.36$ [large])	
% Right leg	(–)	49 \pm 15	59 \pm 16		66 \pm 18	78 \pm 15	(–)	
Knee	(–)	1.26 \pm 0.71	0.48 \pm 0.74		0.89 \pm 1.00	0.06 \pm 0.86	Posture ($F=80$, $P<0.001$, $\eta_G^2 = 0.20$ [large]); Cadence ($F=13$, $P<0.003$, $\eta_G^2 = 0.055$ [small])	
% Right leg	(–)	26 \pm 15	9 \pm 15		16 \pm 19	1 \pm 15	(–)	
Ankle	(–)	1.27 \pm 0.28	1.53 \pm 0.30		0.96 \pm 0.32	1.21 \pm 0.32	Posture ($F=26$, $P<0.001$, $\eta_G^2 = 0.16$ [large]); Cadence ($F=34$, $P<0.001$, $\eta_G^2 = 0.23$ [large])	
% Right leg	(–)	26 \pm 6	31 \pm 5		17 \pm 5	21 \pm 6	(–)	
Residual*	(–)	0.81 \pm 0.52	0.87 \pm 0.49		0.18 \pm 0.39	0.07 \pm 0.54	(–)	
% Right crank	(–)	13 \pm 7	14 \pm 7		3 \pm 7	1 \pm 9	(–)	

*Residual power was calculated as the difference between right crank power and right leg power, which provides an estimate of the net power contributed by muscles in the upper limbs. NB: Target power for the submaximal trials was $10.74 \pm 1.99 \text{ W}\cdot\text{kg}^{-1}$. η_G^2 , generalized eta-squared; ES, Hedges' g_{av} corrected ES. (–) indicates that either data were not calculated or statistical analysis was not performed.

Figure 3.3: There was a significant main effect of posture at the hip, knee, and ankle during high-power output cycling. Group mean (\pm SD) right crank power, right leg power and joint-specific power relative to body mass during seated and non-seated cycling at 70 rpm and 120 rpm.

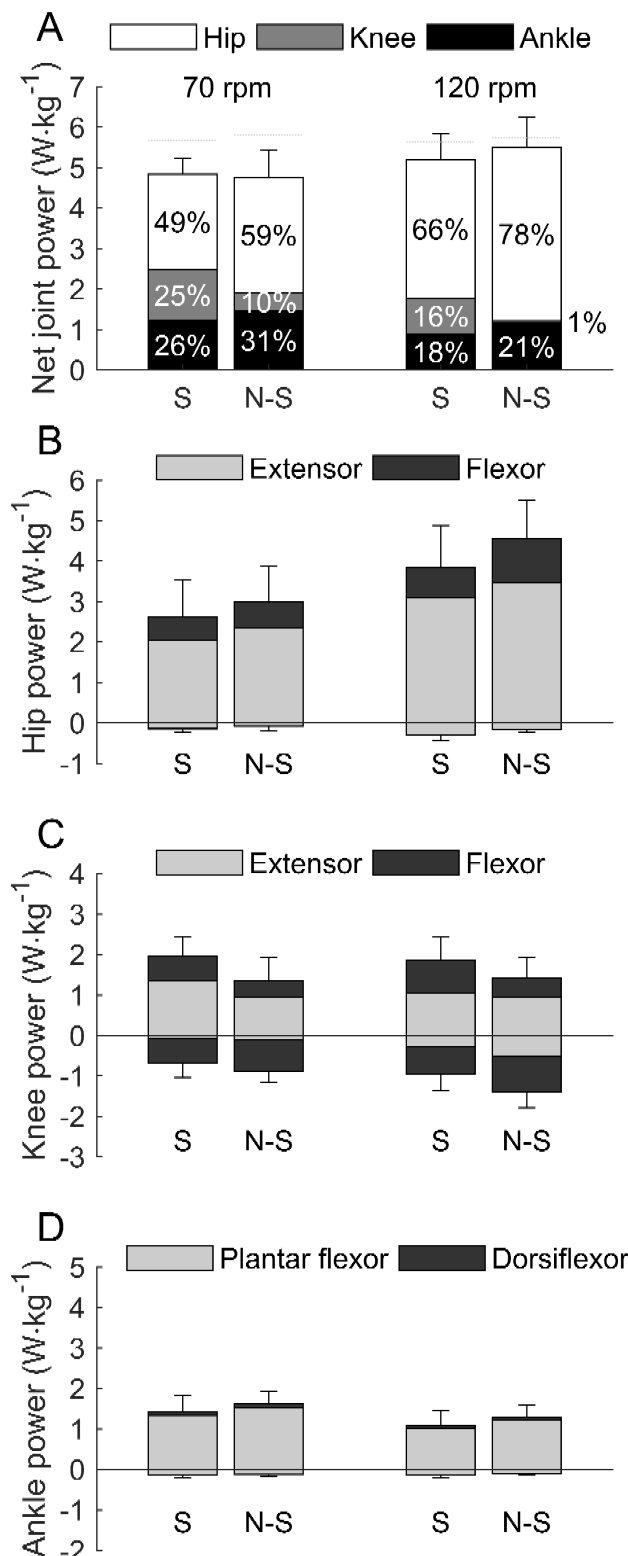


Figure 3.4: The net mechanical power contribution at the knee was significantly reduced by switching to a non-seated posture. A. Total lower limb joint power (mean \pm SD) per cycle during seated (S) and non-seated (N-S) cycling at 70 rpm and 120 rpm. Stacked bars show the net power contribution (%) at the hip, knee and ankle to total lower limb power. The breakdown of joint power into positive and negative contributions during net flexor and extensor muscle moments is shown for the hip (B), knee (C) and ankle (dorsiflexor/ plantar flexor) (D). n.b.: The reduction in net knee power is the result of large amounts of positive and negative power at the knee.

An unsurprising, but noteworthy result was the discrepancy in power between the ergometer, cranks, and lower limb. Power measured at the crank was marginally greater than power measured by the ergometer which was likely due to power losses in the drivetrain. Lower limb power was significantly lower than crank power in all conditions except for when in the non-seated posture at 120 rpm, likely due to contributions of the upper body to crank power. At 70 rpm, lower limb power accounted for $82 \pm 5\%$ of crank power when non-seated and $86 \pm 5\%$ when seated. At 120 rpm, lower limb power accounted for $96 \pm 9\%$ when non-seated and $92 \pm 6\%$ when seated. Previous research (Turpin et al. 2016) has shown that muscle activity within the upper limbs and handlebar forces increase significantly during high power output cycling. Thus, it seems plausible that greater contributions of power from the upper body and upper limbs occur when higher crank force is required, especially when in the non-seated posture.

EMA at the knee was significantly greater when non-seated compared to seated at the time of peak resultant force production ($F=103$, $p<.001$, $\eta_G^2=0.27$) (Figure 3.5). The moderate interaction effect between posture and cadence ($F=9.4$, $p=.008$, $\eta_G^2=0.1$) meant that the increase in EMA at the knee when non-seated was greater at 70 rpm ($S=0.34 \pm 0.09$ vs. Non-S= 0.52 ± 0.15 , $t=6.1$, $p<.001$, 95%CI [0.1-0.3], ES=1.4) than at 120 rpm ($S=0.29 \pm 0.07$ vs. Non-S= 0.35 ± 0.08 , $t=3.5$, $p=.004$, 95%CI [0.02-0.1], ES=0.7). In both postures, there was a moderate increase in EMA at the hip ($F=8.9$, $p=.01$, $\eta_G^2=0.08$) and a small decrease in EMA at the ankle ($F=17$, $p=.001$, $\eta_G^2=0.04$) at 70 rpm compared to 120 rpm.

BF was the only muscle to show a main effect of posture on mean EMG RMS (Figure 3.6). At both cadences, there was a large decrease in BF activity in the non-seated compared to seated posture ($F=92$, $p<.001$, $\eta_G^2=0.6$). Predictably the mean EMG RMS signal of all muscles was higher at 70 rpm than at 120 rpm ($p<.001$) due to the increase in torque required to maintain the set power output, which was likely to be closer to a quasi-maximal power output for each participant at the cadence of 70 rpm (Gardner et al. 2007; Dorel et al. 2005).

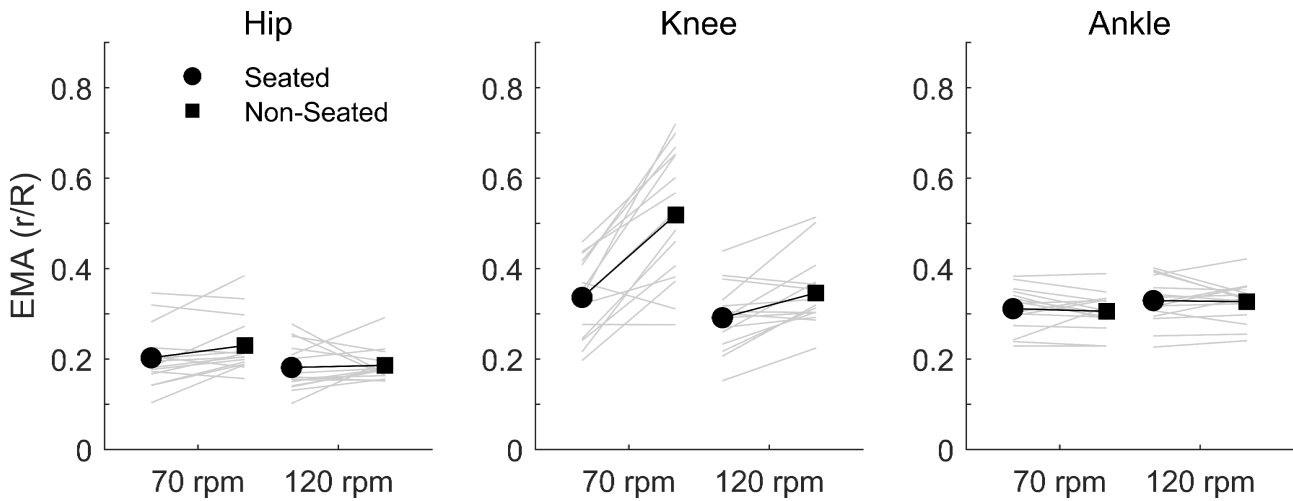


Figure 3.5: Effective mechanical advantage (EMA) at the knee was significantly increased by cycling in a non-seated posture at 70 rpm, but not 120 rpm. EMA of the hip, knee and ankle at the time of peak resultant crank force production in the seated (S) and non-seated (N-S) posture at 70 rpm and 120 rpm. Data for each participant (grey lines) is shown along with the group mean (black lines).

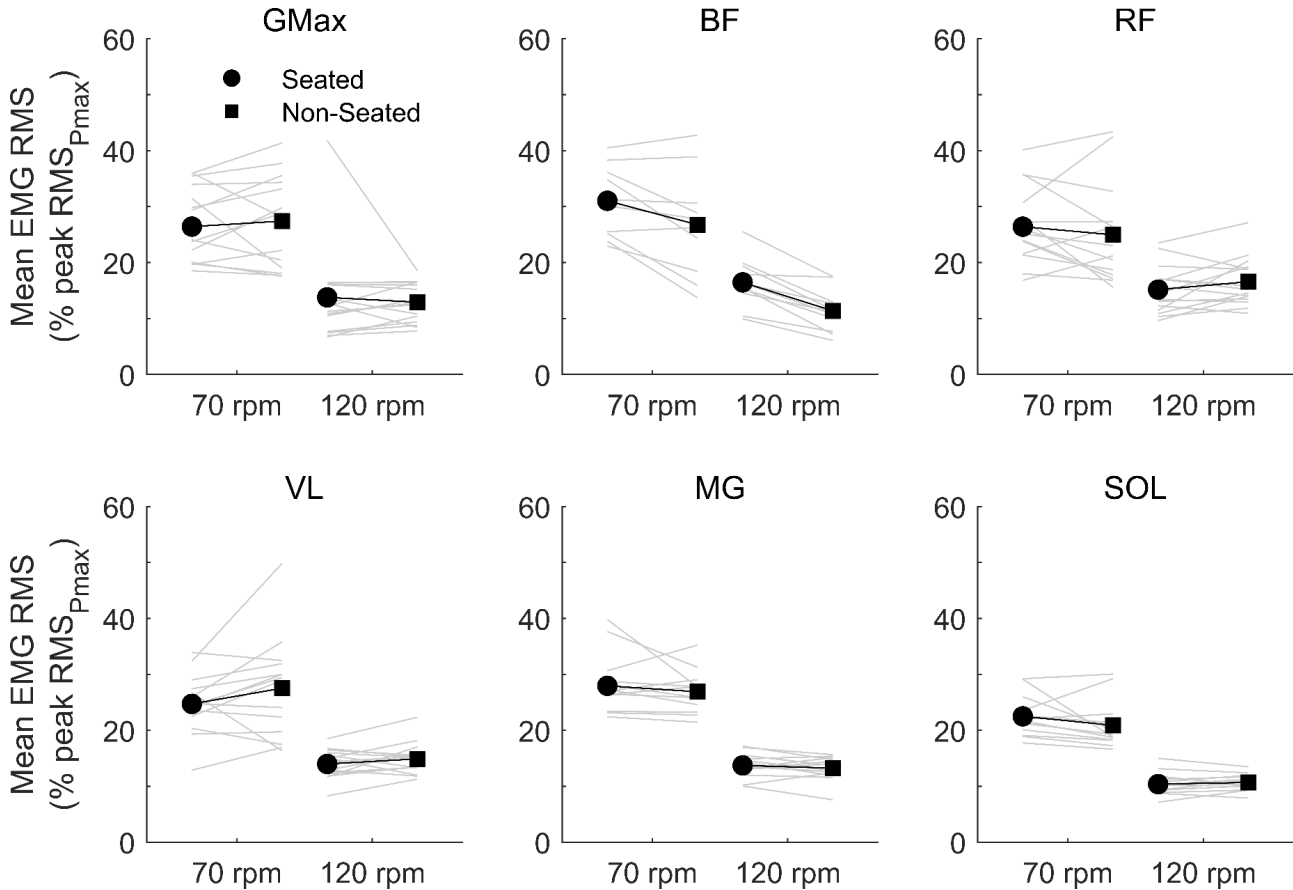


Figure 3.6: Bi-articular hamstring activity was significantly reduced by cycling in a non-seated posture. Mean muscle activity (EMG RMS across the crank cycle, normalised to each muscle's peak RMS activity during the maximal sprint trial) for the gluteus maximus (GMax), rectus femoris (RF), biceps femoris (BF), vastus lateralis (VL), medial gastrocnemius (MG) and soleus (SOL) in seated (S) and non-seated (N-S) cycling at 70 rpm and 120 rpm. n.b.: Due to the increase in torque required per crank cycle, muscle activity was significantly greater at 70 rpm and 120 rpm for all muscles. Data for each participant (grey lines) is shown along with the group mean (black lines).

Statistical analysis was also performed on the magnitude and timing of peak joint angles, velocities and moments (See Table, Appendix C.1, which summarises the significant main and interaction effects of posture and cadence). Of note is the $0.33 \text{ Nm}\cdot\text{kg}^{-1}$ reduction in the peak knee extension moment when non-seated at 70 rpm and the significant increase in peak knee extension angle when non-seated at 70 rpm (9°) and 120 rpm (12°) compared to when seated. Angular displacement, velocity and moments at the hip, knee and ankle with respect to crank angle have also been provided (See Figures, Appendix C.2, C.3, and C.4) as well as EMG RMS signals with respect to crank angle (See Figure, Appendix C.5).

3.5 Discussion

The aim of this experiment was to compare power production across the hip, knee, and ankle between seated and non-seated cycling postures. This comparison was made when cycling at a very-high-power output (above the reported seated to non-seated threshold) at two different cadences (70 rpm and 120 rpm). The results support our primary hypothesis that joint power would be distributed away from the knee joint when cycling in a non-seated posture compared to when seated. In partial support of our second hypothesis, the redistribution of knee power due to the change in posture was different at each cadence, however, it was not re-distributed solely to the hip and ankle as we predicted. Cycling in a non-seated posture at 70 rpm resulted in 14% of crank power being re-distributed away from the knee to the hip (+8%) and ankle (+4%) compared to when seated. Cycling in a non-seated posture at 120 rpm resulted in 15% of crank power being re-distributed away from the knee to the hip (+13%) and ankle (+4%) compared to when seated. The discrepancy between the change in knee power relative to the summed change in hip and ankle power suggests there was a net gain in upper body power when cycling in a non-seated compared to seated posture at 70 rpm and a net loss in upper body power when cycling in a non-seated posture at 120 rpm compared to when seated. Cycling in a non-seated posture at 70 rpm also appears to increase the effectiveness of ankle power production, as higher levels of ankle power were produced without an increase in plantar flexor (MG, SOL) activity. At 120 rpm, hip power increased using similar levels of muscle activation in GMax and RF as at 70 rpm, but with lower levels of activation in BF, which may indicate that cyclists are more effective at producing hip power when in the non-seated posture.

A key result of this study was that the non-seated posture increased negative power at the knee, which resulted in decreased net power at the knee. The increase in negative knee power, while the knee was extending, provides evidence that greater amounts of knee extension power are transferred away from the knee joint when non-seated. It is well understood that the coordinated activity of mono- and bi-articular muscles can serve to transfer energy across joints and orient the crank reaction force during the downstroke (Dorel 2018b). In light of this, it is important to note the individual muscle-joint designs of BF and MG (Lieber and Ward 2011; Kuo 2001). For example, BF's moment arm is larger at the hip than at the knee, which

means that co-contraction of VL and BF can transfer knee extension power to the hip. MG's moment arm is larger at the ankle than at the knee, which means co-contraction of VL and MG can transfer knee extension power to the ankle. Thus, shifting to a non-seated posture appears to utilise the ability of BF and MG to transfer knee extension power to the hip and ankle, respectively.

In line with previous research (Caldwell et al. 1999), joint moments at the hip, knee and ankle were significantly altered by the change in posture which suggests that transitioning to the non-seated posture when high crank forces are required can provide significant mechanical benefits. When non-seated at 70 rpm, peak extension moments at the hip, knee and ankle contributed to the resultant crank force being more closely aligned to the knee joint centre. As such, EMA at the knee was 53% higher in the non-seated posture (0.52 ± 0.15) compared to when seated (0.34 ± 0.09) at 70 rpm. Net torque requirements at the knee were reduced when non-seated, however mean RMS activity of the knee extensors (VL, RF) was similar between postures. Given the cautious assumption that the measured EMG in VL and RF provides an indication of the active muscle volume within the knee extensors (Enoka 2008), it appears that when in the non-seated posture, riders were able to support their bodyweight while also fulfilling the external power requirement at the cranks using a similar active volume of knee extensor muscle.

It may also be the case that switching to a non-seated posture at 70 rpm increases the force producing capability of knee extensor muscles. The peak knee extension angle and range of motion increased significantly in the non-seated posture, however, the increased range of motion did not lead to an increase in the mean extension velocity. This is because a greater portion of the crank cycle was spent extending the knee. For example, when non-seated at 70 rpm, the period of knee extension was so great (59%) that the mean knee extension velocity was actually 5.8% lower than when seated. As supported by the findings of Brennan et al. (Brennan et al. 2018), the reduction in mean knee extension velocity in the non-seated ($181 \text{ deg}\cdot\text{s}^{-1}$) compared to seated ($192 \text{ deg}\cdot\text{s}^{-1}$) posture at 70 rpm would bring the fascicle shortening velocity of VL closer to its optimum for both efficiency and force production. Thus, it appears that rider's use extra degrees of freedom afforded in the non-seated posture to increase the force producing capabilities of knee extensor muscles.

Power generated during hip flexion and knee flexion played a critical role in the differences in positive hip and knee power between postures. Interestingly, when in the non-seated posture at 120 rpm almost half of the 12% increase in the contribution of positive hip power was due to hip flexion power. We only measured the activity of one hip flexor muscle (RF) making it difficult to provide insight into this finding as other hip flexor muscles such as iliacus, psoas, and sartorius were likely responsible for this increase. At both cadences, a large portion of the 15% increase in positive knee power when seated compared to non-seated was due to knee flexion power. The increase in knee flexion power was not reflected by any difference in BF activity during the period of knee flexion power production between postures. Thus, the most likely

explanation is other knee flexor muscles were responsible for this increase. Another explanation is the greater mean knee flexion angle when seated compared to non-seated may have shifted the fascicle operating lengths of the knee flexors closer to optimal and hence been more favourable for generating power (Brennan et al. 2018). On the whole, it appears there is a greater reliance on knee flexors to contribute power when seated, while there is a greater reliance on hip flexors to produce power when non-seated at 120 rpm.

The limitations inherent to inverse dynamics (Zelik and Kuo 2012; Hicks et al. 2015) and quantifying surface EMG (Enoka 2008) must be acknowledged when attempting to understand function and performance from an energetic perspective. One must consider that individual muscle force and power contributions cannot be inferred from joint-level analyses, nor can the level of neural drive to muscle be fully inferred from surface EMG. A further limitation pertains to the questionable ecological validity of ergometer cycling due to the constraint of frontal plane bicycle dynamics (Meijaard et al. 2007). It has been shown that when bicycling in a non-seated posture in the field, cyclists sway the bike laterally underneath their body (Soden and Adeyefa 1979), which might impact the power generating profile of different joints. Finally, accurate conclusions were unable to be made about which technique would be more economical, as metabolic cost (oxygen consumption) was not measured. However, due to the high power output and short duration of the conditions tested here, it is unlikely that the rate of metabolic energy expenditure with respect to time or per unit distance was the variable being optimised in either posture.

In summary, the contribution of knee joint power to total leg power was reduced by switching from a seated to non-seated posture during very-high-power output cycling. The decrease in net knee power when in the non-seated posture is likely the result of power produced by knee extensors being transferred by bi-articular muscles to the hip and ankle. This coordination strategy and increase in EMA at the knee joint means it is likely that both non-muscular and muscular power is more effectively transferred to the crank compared to when seated. These results highlight important differences in joint power contributions during seated and non-seated cycling, which may be a fundamental aspect of why cyclists choose to frequently use a non-seated posture when needing to produce very-high levels of crank torque and power.

The following published manuscript has been incorporated as Chapter 3.

Wilkinson, Ross D., Andrew G. Cresswell, and Glen A. Lichtwark. 2020. Riders Use Their Body Mass to Amplify Crank Power during Nonseated Ergometer Cycling. *Medicine & Science in Sports & Exercise*: Publish Ahead of Print. doi: 10.1249/MSS.0000000000002408

Contributor	Statement of contribution	%
Wilkinson, R.D.	writing of text study design and concept data collection data analysis statistical analysis preparation of figures revision of written work supervision, guidance	80 20 90 90 100 80 40 0
Lichtwark, G.A.	writing of text study design and concept data collection data analysis statistical analysis preparation of figures revision of written work supervision, guidance	10 40 5 5 0 10 30 50
Cresswell, A.G.	writing of text study design and concept data collection data analysis statistical analysis preparation of figures revision of written work supervision, guidance	10 40 5 5 0 10 30 50

Chapter 4

Riders Use Their Body Mass to Amplify Crank Power During Non-Seated Ergometer Cycling

4.1 Abstract

When cyclists ride off the saddle, their centre of mass (CoM) appears to go through a rhythmic vertical oscillation during each crank cycle. Just like in walking and running, the pattern of CoM movement may have a significant impact on the mechanical power that needs to be generated and dissipated by muscle. **Purpose:** To date, neither the CoM movement strategies during non-seated cycling, nor the limb mechanics that allow this phenomenon to occur, have been quantified. **Methods:** Here we estimate how much power can be contributed by a rider's CoM at each instant during the crank cycle by combining a kinematic and kinetic approach to measure CoM movement and joint powers of fifteen participants riding in a non-seated posture at three individualised power outputs (10%, 30%, and 50% of peak maximal power) and two different cadences (70 rpm and 120 rpm). **Results:** The peak-to-peak amplitude of vertical CoM displacement increased significantly with power output and with decreasing cadence. Accordingly, the greatest peak-to-peak amplitude of CoM displacement (0.06 ± 0.01 m) and change in total mechanical energy (0.54 ± 0.12 J·kg $^{-1}$) occurred under the combination of high-power output and low cadence. At the same combination of high-power output and low cadence, we found that the peak rate of CoM energy loss (3.87 ± 0.93 W·kg $^{-1}$) was equal to 18% of the peak crank power. **Conclusion:** Consequently, it appears that for a given power output, changes in CoM energy contribute to peak instantaneous power output at the crank, thus reducing the required muscular contribution. These findings suggest that rise and fall of a rider's CoM acts as a mechanical amplifier during non-seated cycling, which has important implications for both rider and bicycle performance.

4.2 Introduction

When cyclists ride off the saddle during climbing and sprinting, their centre of mass (CoM) appears to go through a rhythmic vertical oscillation during each crank cycle. Early analyses of non-seated cycling from the late 1970's (Soden and Adeyefa 1979) and early 1990's (Hull, Beard, and Varma 1990) showed significant vertical oscillations of the rider's pelvis, providing indirect evidence that the CoM may follow a similar pattern. To date, no studies have quantified rider CoM movement, nor its impact on limb mechanics and crank power during non-seated cycling. Knowledge of CoM movement strategies during non-seated cycling is of importance as it may have a direct impact on the peak force and power that must be contributed by muscle during cycling, which in turn is a potential limiting factor to cycling performance.

The movement pattern of an animal's CoM has a significant impact on the mechanical power that their muscles must generate or dissipate during locomotion (Cavagna, F. P. Saibene, and Margaria 1963; Cavagna, Franco P. Saibene, and Margaria 1964). For instance, when humans and many other terrestrial animals walk, run, or trot, they perform substantial amounts of mechanical work to redirect the CoM velocity during each step-to-step transition (Cavagna 2017). Although performing work to raise the CoM requires muscles to consume metabolic energy, this rise and fall of the CoM can save energy during locomotion through the storage and release of lost kinetic and potential energy as elastic strain energy in spring-like tendons (Alexander 1991). Likewise, we propose that when riding a bicycle off the saddle, vertical displacement of the CoM is important from both a mechanical and metabolic perspective. As evidenced during treadmill cycling, raising the CoM appears to benefit the rider by allowing a greater range of motion at the hip joint and is likely to alter the relative contribution of muscular and non-muscular sources to pedal force (Caldwell et al. 1998). However, these benefits may be offset as raising the mass of the body against gravity requires additional energy to that which creates propulsion at the crank (van Ingen Schenau and Cavanagh 1990). Although net zero mechanical work is typically performed on the CoM over a complete crank cycle, at each instant within the crank cycle the interchange between gravitational potential energy and kinetic energy will dictate the total mechanical energy of the CoM; which in turn influences how much energy muscles need to generate and/or dissipate (Cavagna 2017). Determining the phasing and magnitude of changes in CoM mechanical energy may provide evidence that energy can be transferred between the CoM and the crank, which may reveal why riders choose to perform mechanical work to raise their CoM during non-seated cycling.

Previous research provides a strong indication that the gravitational and inertial components of pedal force are greater during non-seated compared to seated cycling (Stone and Hull 1993; Caldwell et al. 1998). Removing the saddle as a base of support means that a greater portion of bodyweight must be supported at the pedal (Caldwell et al. 1998), while vertical motion of the pelvis suggests that the inertial contribution to pedal force is significantly higher than when seated (Soden and Adeyefa 1979; Hull, Beard, and Varma 1990). Riders appear to utilise this

non-muscular contribution to crank force by lowering their preferred cadence compared to when seated (Harnish, King, and Swensen 2007; Lucia, Hoyos, and Chicharro 2001). Furthermore, joint-level comparisons of seated and non-seated cycling at very high-power outputs suggest that the non-seated posture can increase the force-producing capabilities of the lower limb (Wilkinson, Lichtwark, and Cresswell 2020). To date, the relative contribution of muscular and non-muscular sources to crank force and power during non-seated cycling have not been quantified.

Quantifying the contribution of non-muscular sources to crank force and power may help to explain why the non-seated posture is the most effective solution during certain sprinting and climbing scenarios. For example, in a group of highly trained cyclists ($n=11$, 4F/7M), maximal power output was 8% higher in a non-seated posture compared to seated (1567 vs. 1447 Watts) during a 5-s sprint at a cadence of 128 rpm on a level-ground ergometer ()(Hug et al. 2011). It has also been shown that during a 30-s Wingate test against a fixed resistance, competitive college cyclists ($n=12$) produced a mean power output of $11.0 \pm 0.4 \text{ W}\cdot\text{kg}^{-1}$ at a cadence of $127 \pm 5 \text{ rpm}$ when non-seated compared to $10.4 \pm 0.6 \text{ W}\cdot\text{kg}^{-1}$ at a cadence of $121 \pm 6 \text{ rpm}$ when seated (Reiser II et al. 2002). Furthermore, the non-seated posture appears to significantly increase time to exhaustion during treadmill cycling on a 10% incline at power outputs approaching $9.6 \pm 0.7 \text{ W}\cdot\text{kg}^{-1}$ (Hansen and Waldeland 2008). Further biomechanical analyses are required to shed light on the mechanisms that underpin the increase in sprinting and climbing performance when non-seated compared to seated.

Here we combined a kinematic and kinetic approach to measure CoM movement and joint power of fifteen participants riding in a non-seated posture at a range of individualised but controlled power outputs (10%, 30%, and 50% of instantaneous maximal power output ($P_{max.i}$) at two different cadences (70 rpm and 120 rpm). Our first prediction was that additional power to that measured at the crank would be generated by the rider to raise the CoM during the crank cycle. Secondly, the phasing and magnitude of CoM motion would change with power output and cadence due to the different magnitude, direction, and duration of forces, and thirdly that the potential energy gained by raising the CoM would be used to amplify positive crank power; making raising and lowering of the CoM potentially useful.

4.3 Materials and methods

4.3.1 Experimental design

We tested 15 men (age 30 ± 8 years, height $1.79 \pm 0.05 \text{ m}$, and mass $74.4 \pm 8.5 \text{ kg}$); eight of whom were cyclists who competed weekly at club level, while the others regularly engaged in a variety of competitive or recreational sports. The recruitment of roughly equal numbers of cyclists and non-cyclists was not intentional nor a focus of the study. Post-hoc analysis confirmed that cycling experience did not significantly affect instantaneous maximal power

output capability between the two groups (cyclists=22.6 \pm 5 W·kg $^{-1}$ vs. others=20.6 W·kg $^{-1}$, $p=0.35$). All participants gave their written informed consent prior to participating in this study according to the procedures approved by the Human Ethics Committee of The University of Queensland and in accordance with the general principles expressed in the Declaration of Helsinki. For the regular cyclists, we matched the seat height and handlebar position of the ergometer (Excalibur Sport, Lode BV, Groningen, The Netherlands) to their accustomed cycling position. For the remaining participants, we standardised fitting to an internal knee angle of 150° and torso angle (trunk relative to horizontal) of 70°. Based on each cyclist's preference, we made minor adjustments to this fitting. Crank length was set to 175 mm. Participants wore cleated cycling shoes (SH-R070, Shimano, Osaka, Japan) that clipped into the pedals (SH-R540, Shimano, Osaka, Japan).

The test session began with a 5-min cycling warm-up at 100 W at their preferred cadence. To individualise power output in the sub-maximal trials we first determined each participant's instantaneous maximal power output ($P_{max.i}$) by having them perform five maximal sprints of 3 s duration in a seated posture. We calculated $P_{max.i}$ as the highest "instantaneous" power that occurred during a crank cycle. The ergometer was set to "Linear" mode, which ensured the coupling of power output and cadence. Participants were given a familiarisation trial before performing the test. For all sprints, the participant began with the crank and flywheel stationary. The initial resistance was based on $P_{max.i}$ results from pilot testing three individuals. We expected that participants would achieve $P_{max.i}$ at a cadence close to 120 rpm (Dorel 2018a). Thus, we increased or decreased the linear resistance of the ergometer for the subsequent trial based on whether the participant achieved a cadence above or below 120 rpm. A 3-min rest period was given between trials to reduce any potential fatigue effects. For all participants, it took five or less sprint trials to determine the resistance which elicited their $P_{max.i}$.

A rest period of 20-min was given after the $P_{max.i}$ test before beginning the six sub-maximal trials. Participants performed combinations of power output (10%, 30%, and 50% of $P_{max.i}$) and cadence (70 rpm and 120 rpm) in a randomised order. Participants were required to maintain the target cadence and power output for a minimum period of 10 s. The ergometer was set to 'Hyperbolic' mode, which ensured that power output remained constant independent of cadence. Thus, participants were required to maintain the target cadence using feedback from the visual display on the ergometer. Post-hoc analyses confirmed that the target cadences were met across all trials in each cadence condition (70 rpm=71.9 \pm 0.5 rpm, 120 rpm=120.7 \pm 2.0 rpm). Following the sub-maximal trials, the presence of exercise-induced fatigue was assessed by asking each participant to perform an additional 3-s maximal sprint. Inclusion required the participant to match, within \pm 5%, their previously tested $P_{max.i}$ in this added maximal sprint. For each sub-maximal trial, we acquired crank angle and force signals synchronously with motion capture using a 16-bit A/D conversion board (USB-2533, Measurement Computing Corporation, Norton, MA) and Qualisys Track Manager Software (Qualisys AB, Gothenburg, Sweden).

4.3.2 Kinematics

The three-dimensional (3D) positions of 45 passive reflective markers were collected at 200 Hz using an eight camera, opto-electronic motion capture system (Oqus, Qualisys, AB, Sweden). Reflective markers were secured to the skin using double-sided tape over the suprasternal notch, C7 spinous process, sacrum, and bilaterally over the acromion processes, lateral epicondyles of the humerus, styloid processes of the radius, iliac crests, anterior superior iliac spines, posterior superior iliac spines, greater trochanters, medial and lateral condyles of the femur, and medial and lateral malleoli. Markers were secured to the cycling shoe over the calcanei, heads of the 1st and 5th metatarsals and the 2nd distal phalanxes. Lightweight, rigid clusters of four markers were also secured bilaterally to the lateral mid-thighs and lateral mid-shanks using double-sided tape and self-adhesive bandage. A static trial was collected with the participant standing in a standard anatomical posture before commencing the sub-maximal trials. This trial was used for kinematic model scaling. The heading (yaw) angle of the ergometer was determined within the motion capture global coordinate system by placing two markers on the rear support legs of the ergometer. These markers were used to create a local coordinate system for the ergometer, which accounted for any discrepancy with the global coordinate system between trials.

4.3.3 External forces

We recorded tangential and radial forces at the left and right crank, as well as crank angle at 100 Hz using pre-calibrated, wireless, instrumented cranks (Axis, SWIFT Performance, Brisbane, Australia). Digital signals were transmitted wirelessly to a base receiver before being converted to an analogue signal through the A/D Board. The internal sampling factor within Qualisys Track Manager Software matched the digital sampling frequencies of the crank (100 Hz) to the motion capture (200 Hz) sampling frequency. Each crank was independently calibrated by performing a multi-axis, dynamic calibration. In addition, and prior to testing, we calibrated the output voltage for the tangential and radial force by suspending a 2.5 kg mass from each pedal spindle with the cranks in both horizontal and vertical positions. A spirit level was used to zero the crank angle of the right crank at top dead centre (TDC).

Equations 4.1 and 4.2 show how the net force acting at the handlebar (F_{hb}) was calculated by comparing the total vertical force (F_z) required to cause the measured accelerations of the rider's CoM (a_{com}) with the sum of vertical force at the left (F_{cl}) and right (F_{cr}) cranks. The remainder is an estimate of the net vertical force acting on the hands of the rider at the handlebar (F_{hb}). Thus, a net positive vertical handlebar force pertains to the reaction force induced by a net downward pushing force from the arms/body and a negative vertical reaction force pertains to a net upward pulling force from the arms/body. A limitation to the calculation of net F_{hb} is that it cannot identify whether simultaneous pushing and pulling forces are being

generated. A diagram of the net vertical forces acting on the rider are displayed in Figure 4.1A.

$$F_z = m \cdot (g + a_{com}) \quad (4.1)$$

$$F_{hb} = F_z - (F_{cr} + F_{cl}) \quad (4.2)$$

4.3.4 Mechanical energy and power

Motion capture marker trajectories, crank forces, and crank angles were processed using custom scripts in MatLab (R2018b, Mathworks Inc., USA). These scripts filtered crank force signals and marker trajectories with a zero-lag, second-order, low-pass Butterworth filter with a cut-off frequency of 12 Hz (Kristianslund, Krosshaug, and Van den Bogert 2012). The measured angular position of the crank was rotated into the global coordinate system to transform the respective crank forces (tangential and radial) into their horizontal and vertical components. The force components and marker trajectories were then rotated into the ergometer coordinate system. The origin of the resultant force was determined by creating a virtual marker at the centre of the cleat. This approximation was determined using the crank angle, three-dimensional shoe orientation, and shoe size. We then verified this first approximation against a second approximation using the bottom bracket position, crank length, crank angle, and pedal spindle length.

OpenSim software (Delp et al. 2007) was used to create participant-specific models by scaling segment lengths and segment masses of a previously developed generic full-body musculoskeletal model (Rajagopal et al. 2016) based on each participant's anthropometry. Inverse kinematic analysis was used to calculate joint kinematics (Seth et al. 2011). Inverse dynamic analysis was used to calculate hip, knee, and ankle net joint moments by combining the inverse kinematics results with external loads applied to the model, in this case reaction forces at the left and right crank (Seth et al. 2011). Joint power was calculated as the dot product of the net joint moment and joint angular velocity. Flexor moments and flexion velocity were defined as positive and joint work as the integral of joint power with respect to time. Inclusion of data required the cyclist to simultaneously match the target power ($\pm 5\%$) and cadence ($\pm 5\%$) at the right crank for a minimum of five consecutive crank cycles.

In cycling, positive power generated by muscle is dissipated to the environment (excluding gravity), conservative forces (including gravity and the stretching of elastic elements), and non-conservative forces such as friction and drag (van Ingen Schenau and Cavanagh 1990). More specifically, the rider imparts motion to the rider-bicycle system by overcoming aerodynamic drag, rolling resistance, wheel bearing friction, the rate of change of potential and kinetic energy, and friction in the drive train (Martin et al. 1998). Typically, it is assumed that the rider's CoM travels parallel to the riding surface, meaning that the change in potential and kinetic energy of the rider's CoM is reflected by the change in the potential and kinetic energy of the system.

Under this assumption power measured at the cranks will be equivalent to the total power output generated by the rider. However, this assumption does not account for any movement of the rider's CoM relative to the reference frame of the bicycle. Evidence suggests that this is particularly important when cycling in a non-seated posture, where it appears that the rider's CoM is raised and lowered periodically during the crank cycle (Soden and Adeyefa 1979; Hull, Beard, and Varma 1990). Thus, the total joint power generated by the rider (P_{tot}) at each instant during the crank cycle will be equivalent to power measured at the cranks (P_{cranks}) plus energy lost or gained by the rider's CoM with respect to time (P_{CoM}) as shown in Equation 4.3.

$$P_{tot} = P_{cranks} + P_{CoM} \quad (4.3)$$

$$P_{lb} + P_{ub} = P_{cranks} + P_{CoM} \quad (4.4)$$

In this study, P_{cranks} was calculated as the summed dot product of torque and angular velocity measured at each crank. P_{CoM} was calculated using the inverse kinematic results as the sum of the change in potential energy (E_P) and kinetic energy (E_k) of each segment divided by the change in time. Kinetic energy of motion (a scalar quantity) was accounted for in all axes by using the square of the resultant velocity of the CoM in x, y, and z axes multiplied by half mass. Kinetic energy due to angular motion of the CoM was deemed negligible. P_{tot} can also be thought of as the sum of lower body and upper body joint power as shown in Equation 4.4. Lower body joint power (P_{lb}) was calculated using inverse dynamic results as the summed dot product of net joint moments and joint angular velocities at the hip, knee, and ankle of each leg. Upper body power (P_{ub}) was assumed to be the difference between P_{tot} and P_{lb} , which can be attributed to the net power generated by muscles crossing the joints within the arms and trunk. A limitation of this calculation of P_{ub} is that it cannot identify whether power is being simultaneously generated and dissipated within the upper body. To illustrate these calculations, a plot of P_{tot} with respect to crank angle is shown in Figure 4.1B split into its components of P_{cranks} and P_{CoM} and its components of P_{lb} and P_{ub} (right).

4.3.5 Statistical analyses

We performed repeated measures, two-way analyses of variance (ANOVAs) to test for main effects of power and cadence and interaction effects (power x cadence) on the peak-to-peak amplitude of CoM displacement and energy, peak CoM power, net lower body power, and net upper body power. The alpha level for main and interaction effects was set at 0.037 prior to statistical analysis. This alpha level was based on a desired false positive risk of <5%, a prior probability for a real effect of 0.5, sample size of fifteen, and an estimated effect size of 1 (Colquhoun and Longstaff). Whenever a main or interaction effect was found, multiple comparisons were used to detect the effect of the factor/s in each condition. The alpha level was corrected for family-wise multiple comparisons using the Sidak method. The F-value (F),

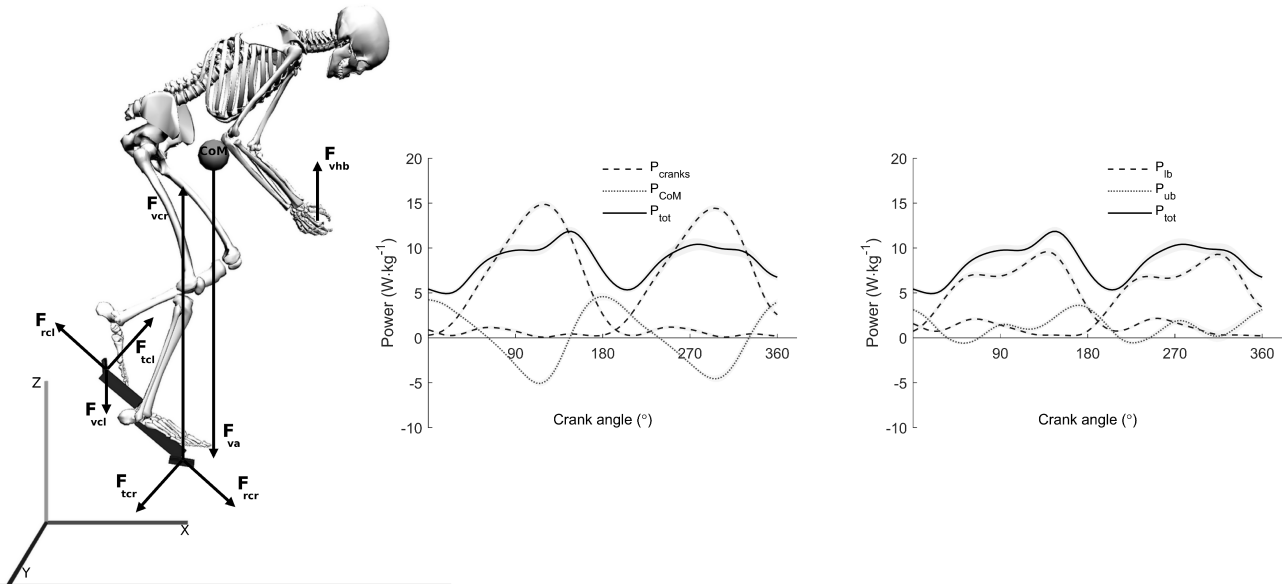


Figure 4.1: Calculations of instantaneous total joint power must account for any change in gravitational potential energy and kinetic energy of the rider's CoM relative to the reference frame of the bicycle. A. Diagram of vertical forces acting on the rider during non-seated cycling. The measured vertical accelerations of the rider's CoM must be in equilibrium with the sum of vertical interaction force between the rider and the bicycle. F_{va} represents the net vertical force that must be counteracted to cause the measured acceleration of the rider's CoM; F_{vcr} and F_{vcl} are, respectively, the measured vertical components of the reaction force impressed by each foot on the right and left crank, and F_{vhb} is the vertical component of the net reaction force at the handlebar, calculated as the difference between F_{va} and the sum of F_{vcr} and F_{vcl} . B. Total joint power generated by the rider normalised to body mass (P_{tot}) separated into the measured power at the left and right crank (P_{cranks}) and the rate of energy gained and lost by the rider's CoM (P_{CoM}). C. Total joint power generated by the rider (P_{tot}) separated into the calculated power in the left and right lower limb (P_{lb}) and the net power generated on, and by, the upper body (P_{ub}). Data shown is the mean \pm one standard deviation (shaded area) of one subject over 15 crank cycles during non-seated cycling at 30% $P_{max,i}$ ($8.5 \text{ W}\cdot\text{kg}^{-1}$) and 70 rpm.

p-value (ρ), and generalised eta squared (η_G^2) are provided for main and interaction effects. For multiple comparisons the t-statistic (t), adjusted p-value (ρ), 95% confidence intervals (95%CI [Low-High]), and corrected effect size, known as Hedge's g_{av} (ES), are provided. The η_G^2 for each variable was assessed against the benchmarks of trivial (<0.0099), small (0.0099-0.0588), moderate (0.0588-0.1379), and large effect (>0.1379) (Lakens 2013). The ES for each variable was assessed against the commonly used benchmarks of small (0.1-0.3), moderate (0.3-0.5) and large effect (>0.5). All values are reported as mean \pm standard deviation.

4.4 Results

We first sought to quantify rider CoM kinematics and associated mechanical energy changes during non-seated cycling under six combinations of power output and cadence. The group mean CoM displacement in 3D space highlighted that CoM displacement occurred predominantly in

the vertical (Z) axis (See Figure, Appendix C.6, which shows 3D plots of CoM displacement in each condition). The peak-to-peak amplitude of CoM displacement, velocity, and acceleration increased significantly with increasing power output at each cadence (See Figure, Appendix C.6, which shows CoM displacement, velocity, and acceleration with respect to crank angle in each condition). Figure 4.2 shows the group mean change in potential, kinetic, and total CoM mechanical energy with respect to crank angle for each condition.

In support of our first hypothesis, substantial increases in potential energy of the CoM occurred predominantly in the first half of each leg's down-stroke (0-90°) without an equal decrease in kinetic energy, confirming that work performed by muscle was required to raise the rider's CoM. Likewise, substantial decreases in potential energy occurred during the second half of each leg's downstroke (90-180°) without an equivalent decrease in kinetic energy, meaning energy of the CoM was most likely transferred to the crank. Importantly, the timing of CoM energy changes with respect to crank angle showed that the CoM was raised from its lowest height to its peak height using predominantly forces that did not impede crank power (i.e. radial forces), while the lowering of the CoM occurred when the rider's mass could most effectively contribute to tangential force, and hence power at the crank.

The group mean maximal peak power output was 1605 ± 368 W (21.5 ± 4 W·kg $^{-1}$), meaning that the individualised power outputs of 10%, 30%, and 50% of $P_{max,i}$ corresponded to 2.1 ± 0.4 , 6.4 ± 1.2 and 10.7 ± 2.0 W·kg $^{-1}$, respectively. At each power output, regular oscillations of the total CoM mechanical energy (E_{tot}) occurred within each crank cycle, with only minor in-phase and out-of-phase exchanges of kinetic energy (E_k) and gravitational potential energy (E_p) (See Figure 4.2). Maximum and minimum E_{tot} occurred earlier in the crank cycle at the lower cadence and shifted progressively earlier as power output increased for both cadence conditions. E_{tot} reached a single maximum value during the power phase for each leg (i.e. twice per 360°cycle of the right crank as seen in Figure 4.2). After reaching peak height at a crank angle of approximately 45°, the CoM lowered to a minimum height at a crank angle of approximately 135°. Thus, it is possible that the majority of energy lost by the CoM (E_{tot}) during this phase contributed to positive work at the crank. Peak downward velocity of the CoM occurred between crank angles of 90°and 135°(See Figure, Appendix C.6) and were coincident with vertical forces being equal to bodyweight (F_{va}) (See Figure 4.2). Vertical forces greater than bodyweight acted to decrease the downward velocity of the CoM during the later stages of the downstroke and then to accelerate the CoM back to a maximum height ready for the power phase of the opposite leg. In all conditions, the downstroke leg ($\sim 135\text{-}225^\circ$) produced the majority of vertical force to raise the CoM from its lowest position to its highest ($60 \pm 9\%$), followed by the handlebars ($25 \pm 6\%$), and the opposite leg ($\sim 315\text{-}45^\circ$) ($16 \pm 4\%$). A greater portion of bodyweight was supported at the handlebar across the crank cycle at 120 rpm (10% $P_{max,i}=36 \pm 8\%$, 30% $P_{max,i} =29 \pm 16\%$, 50% $P_{max,i} =20 \pm 26\%$) compared to 70 rpm (10% $P_{max,i}=32 \pm 9\%$, 30% $P_{max,i} =16 \pm 19\%$, 50% $P_{max,i} =1 \pm 28\%$) at each power output. At both cadences, the portion of bodyweight supported at the handlebar decreased as

power output increased.

In support of our second hypothesis, increasing power output and lowering cadence each increased the peak-to-peak amplitude of rider CoM displacement. Statistical analyses showed large main effects of power output ($F=21$, $\rho=<0.001$, $\eta_G^2=0.25$) and cadence ($F=268$, $\rho=<0.001$, $\eta_G^2=0.73$) and a moderate interaction effect ($F=8.1$, $\rho=0.002$, $\eta_G^2=0.06$) on the peak-to-peak amplitude of CoM displacement. The peak-to-peak amplitude of changes in E_{tot} increased significantly with power output at 70 rpm (10% = 0.34 ± 0.10 , 30% = 0.44 ± 0.09 , and 50% = 0.54 ± 0.12 $J \cdot kg^{-1}$) and at 120 rpm (10% = 0.12 ± 0.04 , 30% = 0.14 ± 0.06 , and 50% = 0.22 ± 0.10 $J \cdot kg^{-1}$) and were significantly greater at 70 rpm than at 120 rpm at each power output (See Figure 4.2). Although not tested statistically, the peak-to-peak amplitude of changes in E_{tot} appears to increase roughly linearly with power output under both cadence conditions, but the rate of increase is seemingly greater at low cadence compared to high cadence.

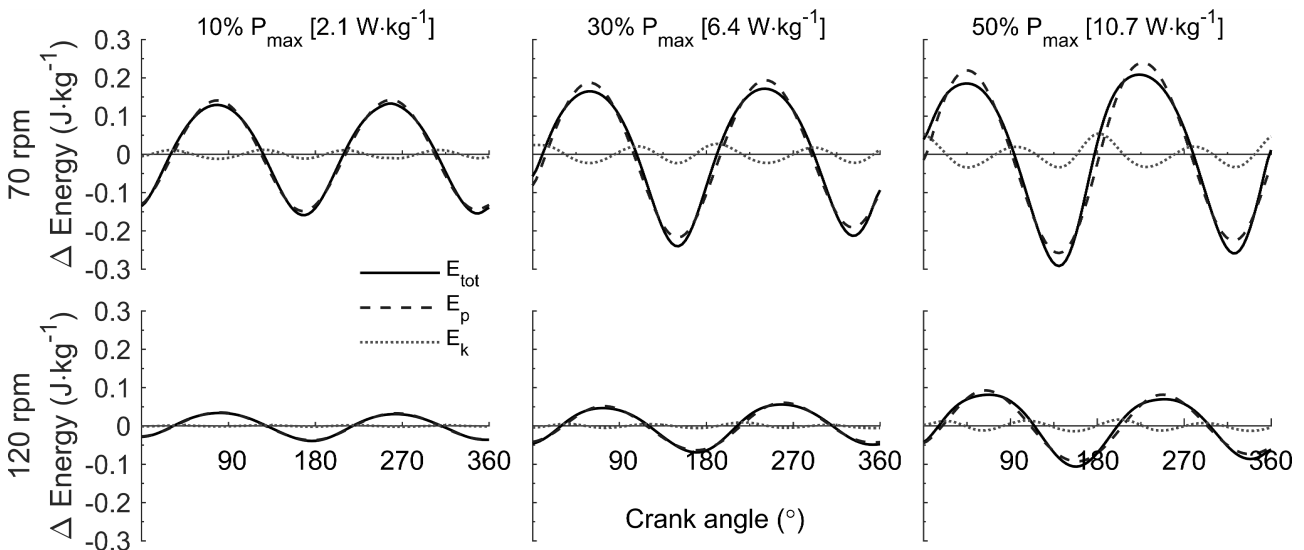


Figure 4.2: Changes in kinetic energy of the rider's CoM had little impact on the overall total mechanical energy changes. Group mean mechanical energy changes of the rider's CoM with respect to crank angle (0° ; top dead centre) during non-seated cycling at a range of power outputs (10%, 30%, and 50% $P_{max,i}$) at 70 rpm (A-C) and 120 rpm (D-F). The changes in energy have been normalised to body mass. The continuous lines in each plot indicate the total mechanical energy $E_{tot} = E_P + E_k$. The rate of energy gain and loss by the CoM (i.e. power) can be inferred by the slope of E_{tot} in each plot. The dashed lines indicate the gravitational potential energy $E_P = M_b g s_v$ (g = acceleration of gravity, s_v = vertical displacement of the CoM of the body). The dotted lines, indicate the kinetic energy of motion in all axes $E_k = \frac{1}{2} M_b v^2$ (v = resultant velocity of the CoM in x, y and z axes). The changes in kinetic energy had only a small influence on the total change in mechanical energy and were barely distinguishable from zero when generating low crank power at 120 rpm. Note that the total mechanical energy of the CoM is unchanged over the whole crank cycle, therefore only the change in energy is relevant to the quantity of mechanical energy that can be transferred to the crank or stored in elastic structures (i.e. when the change in mechanical energy is below zero) or the amount of work generated by muscle or elastic structures to raise the CoM (i.e. when the change in mechanical energy is above zero).

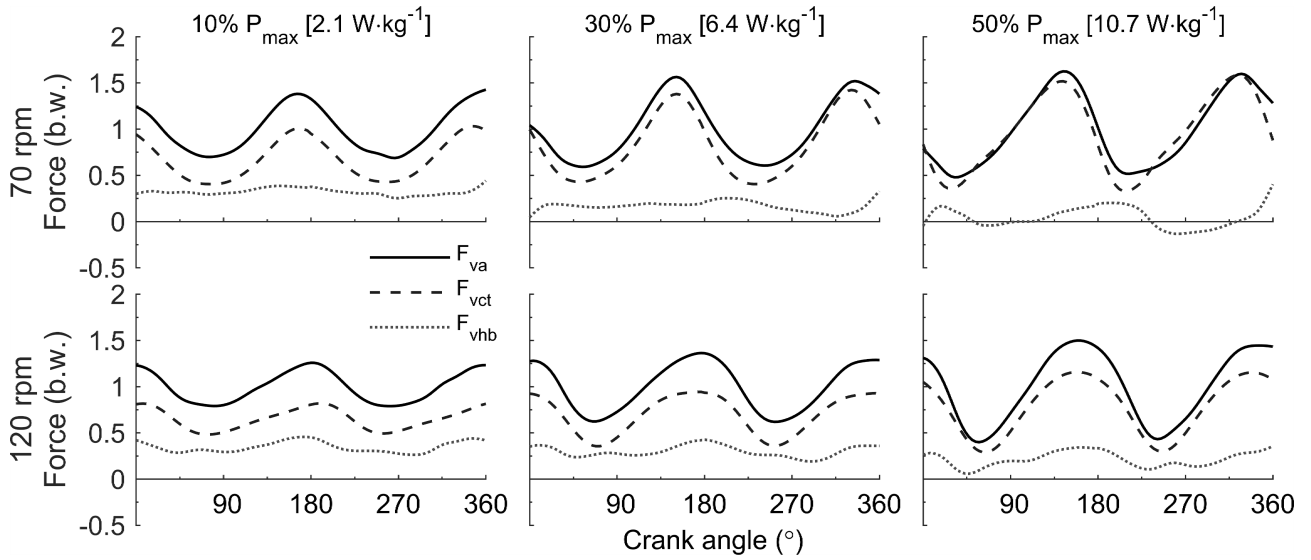


Figure 4.3: Net upward vertical handlebar forces decrease substantially as power output increases and are much lower at 70 rpm than 120 rpm, especially at 70 rpm. Group mean vertical forces during non-seated cycling at a range of power outputs (10%, 30% and 50% $P_{max,i}$) at 70 rpm (A-C) and 120 rpm (D-F). Forces have been normalised to bodyweight (i.e. $M_{bg} = 1$; g = acceleration of gravity). F_{va} (continuous lines) indicates the net vertical interaction forces between the bicycle and rider necessary to cause the measured accelerations of the rider's CoM. F_{vct} (dashed lines) indicates the total vertical force at the cranks ($F_{vct} =$ vertical force at right crank + vertical force at left crank). F_{vhb} (dotted lines) indicates the calculated net vertical force acting at the handlebar ($F_{vhb} = F_{va} - F_{vct}$). The mean level of F_{vhb} clearly decreased as power output increased at each cadence. When generating 50% $P_{max,i}$ at 70 rpm, participants generated a net pulling force at the handlebar (i.e. $\dot{L}\ddot{S}F_{vhb}$) during the power phase of each leg, resulting in an 18% (2.13 ± 0.75 W·kg $^{-1}$) contribution to net crank power by the upper body.

In combination, the phasing and magnitude of changes in E_{tot} appear to confirm our final hypothesis that mechanical energy gained by the CoM can be used later in the crank cycle to contribute to positive crank power. Figure 4 shows how mechanical energy lost by the CoM altered the joint power requirements at each instant of the crank cycle. The peak rate of CoM energy loss at each respective power output (10%, 30%, and 50% $P_{max,i}$) was equal to 50% (2.66 ± 0.85 W·kg $^{-1}$), 25% (3.50 ± 0.70 W·kg $^{-1}$), and 18% (3.87 ± 0.93 W·kg $^{-1}$) of peak crank power at 70 rpm; and equal to 26% (1.21 ± 0.34 W·kg $^{-1}$), 13% (1.73 ± 0.78 W·kg $^{-1}$), and 13% (2.88 ± 1.58 W·kg $^{-1}$) at 120 rpm. Although the work performed on the CoM is net zero across a complete crank cycle, the timing of changes in E_{tot} dictate whether energy is either absorbed as negative work by muscle, stored as energy in elastic elements, or transferred to the crank. Interestingly, as power output required at the crank increased, the peak rate of CoM energy loss occurred at crank angles closer to horizontal at 70 rpm (10% = $134 \pm 11^{\circ}$, 30% = $122 \pm 6^{\circ}$, 50% = $107 \pm 10^{\circ}$) and 120 rpm (10% = $134 \pm 16^{\circ}$, 30% = $131 \pm 14^{\circ}$, 50% = $123 \pm 13^{\circ}$). These results suggest that the absolute magnitude of power amplification at the crank due to the rate of energy loss by the rider's CoM becomes greater at higher power outputs and at lower cadence.

Additionally, it made conceptual sense that the effects of power output and cadence on

changes in E_{tot} would be reflected by changes in the pattern of joint power production. Thus, we predicted that changes in power output and cadence would also influence the net power contributed by the lower and upper body. Figure 4.5 shows the pattern of lower and upper body power production with respect to crank angle in each condition and highlights the simultaneous generation and dissipation of power by the lower and upper body. Figure 4.6 shows the net contribution of lower and upper body power to total joint power in each condition. The net contribution of upper body power increased with power output under both cadence conditions and was greater at low cadence compared to high cadence. Statistical analysis showed large main effects of power output ($F=69$, $\rho<0.001$, $\eta_G^2=0.42$), cadence ($F=37$, $\rho<0.001$, $\eta_G^2=0.31$), and a moderate interaction effect ($F=35$, $\rho<0.001$, $\eta_G^2=0.11$) on net upper body power. Net upper body power increased significantly with power output at 70 rpm ($10\% = 0.12 \pm 0.26$, $30\% = 1.02 \pm 0.38$, and $50\% = 2.13 \pm 0.75 \text{ W}\cdot\text{kg}^{-1}$) and at 120 rpm ($10\% = -0.34 \pm 0.67$, $30\% = 0.30 \pm 0.89$, and $50\% = 0.54 \pm 1.02 \text{ W}\cdot\text{kg}^{-1}$) and was significantly greater at 70 rpm than at 120 rpm at each power output. At 70 rpm, the relative contribution of net upper body power to total net joint power increased by 13%, from 5% at the lowest power output to 18% at the highest power output. At 120 rpm, the relative contribution of net upper body power to total net joint power was -15% at the lowest power output and only 5% at the highest power output. These results provide evidence that muscles in the upper body contribute significant amounts of power to raise the CoM and to generate crank power during non-seated cycling at high power outputs.

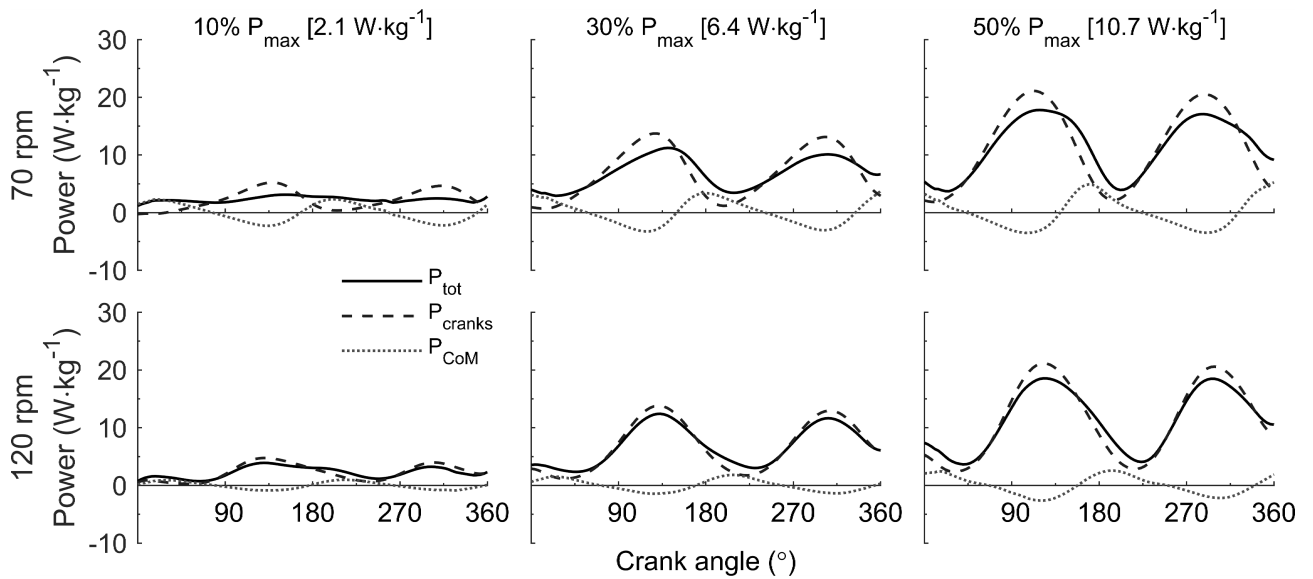


Figure 4.4: Changes in CoM power are deliberately out of phase with crank power during the period of peak crank power production, meaning that peak joint power requirements are reduced. Group mean total joint power generated by the rider normalised to body mass (P_{tot} , continuous line) separated into the measured power at both cranks (P_{cranks} , dashed line) and the rate of energy gained and lost by the rider's CoM (P_{CoM} , dotted line) over a complete a crank cycle during non-seated cycling at each power output (10%, 30%, and 50% $P_{max,i}$) at 70 rpm (A-C) and 120 rpm (D-F). N.B.: Four distinct phases appear during the crank cycle, whereby the CoM is either reducing or increasing the requirement of joint power in relation to crank power. Downward CoM velocity (negative P_{CoM}) occurs at specific times during the crank cycle to decrease the instantaneous maximal joint power requirement, while power is generated on the CoM during periods of low crank power output.

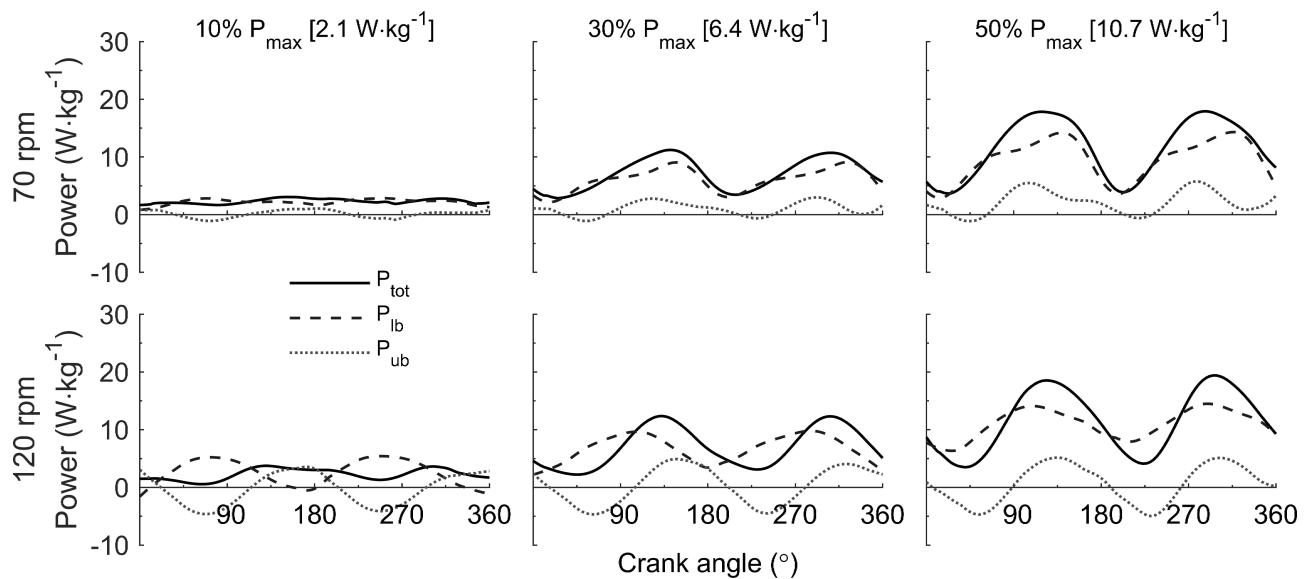


Figure 4.5: Using a non-seated posture at high cadence resulted in theoretically costly periods of simultaneous power generation and dissipation by the lower body and upper body, respectively. Group mean patterns of total joint power output (continuous line) are shown along with the pattern of power production and absorption by the lower body (dashed line) and upper body (dotted line) during non-seated cycling at each power output (10%, 30% and 50% $P_{max,i}$) at 70 rpm (A-C) and 120 rpm (D-F). N.B.: The upper body generates power in all conditions, but simultaneously absorbs greater amounts of power while the legs are generating power at 120 rpm. These results point towards the inefficiency of having to support bodyweight in the non-seated posture under conditions of lower power and high cadence.

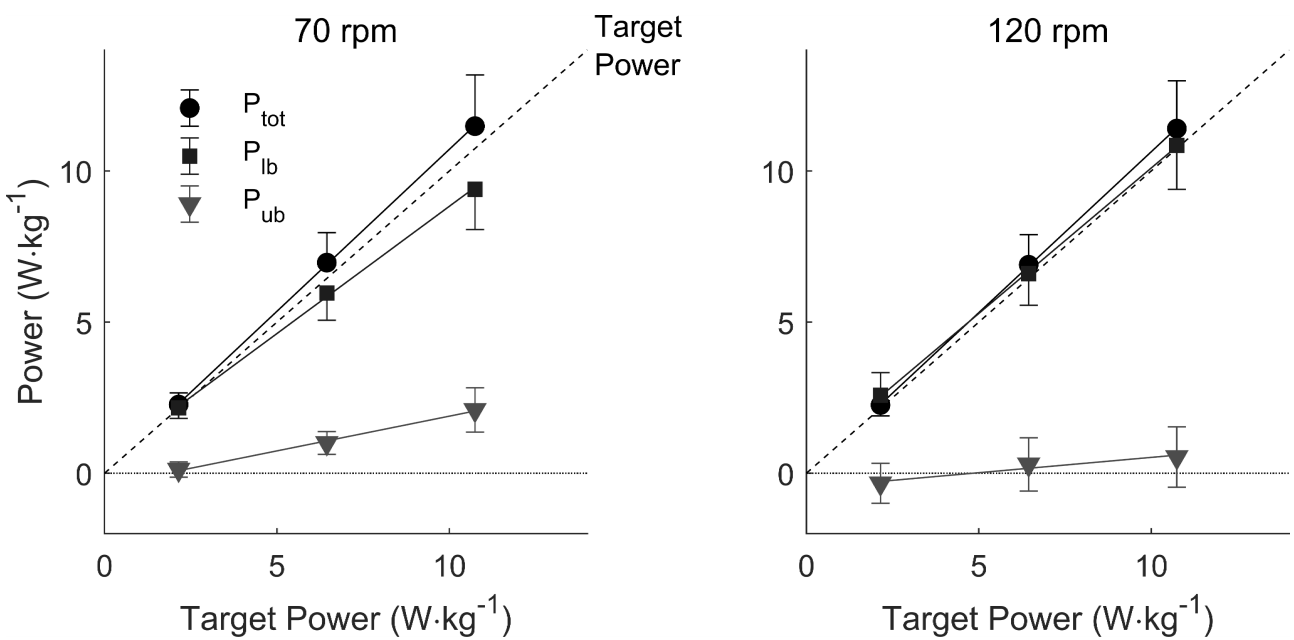


Figure 4.6: Riders use their upper body to contribute greater amounts of power as power output increases. Group mean net power contributions of the lower (P_{lb}) and upper body (P_{ub}) to total power output (P_{tot}) during non-seated cycling at each power output (10%, 30% and 50% $P_{max,i}$) and cadence (70 rpm and 120 rpm). Power has been normalised to body mass (kg). Pub at each respective power output (10%, 30% and 50% $P_{max,i}$) was equal to 5% ($0.12 \pm 0.25 \text{ W}\cdot\text{kg}^{-1}$), 14% ($1.00 \pm 0.38 \text{ W}\cdot\text{kg}^{-1}$), and 18% ($2.09 \pm 0.73 \text{ W}\cdot\text{kg}^{-1}$) of total power output at 70 rpm and equal to -15% ($-0.34 \pm 0.66 \text{ W}\cdot\text{kg}^{-1}$), 4% ($0.29 \pm 0.88 \text{ W}\cdot\text{kg}^{-1}$), and 5% ($0.54 \pm 1.00 \text{ W}\cdot\text{kg}^{-1}$) at 120 rpm. The contribution of upper body power increases roughly linearly as total power output requirements increase, with a seemingly steeper increase at 70 rpm.

4.5 Discussion

Our results confirmed that significant vertical oscillations of the rider's CoM occurred during non-seated cycling and caused equivalently scaled oscillations in total CoM mechanical energy. Greater amounts of energy were gained and lost by the CoM at higher power outputs and when cadence was decreased. This increase was a result of an increase in the time over which forces above bodyweight were applied to the CoM. When people are able to freely choose their motion during cycling on an ergometer, power generated by muscle was required to raise the CoM to increase its potential energy, while energy lost by the CoM was due to an exchange of energy with the crank. In all but the low power, fast cadence condition (10% $P_{max,i}$ at 120 rpm), potential energy gained by the CoM was used in the crank cycle to decrease the peak instantaneous joint power requirements. These results provide preliminary mechanical evidence that inertia forces due to vertical acceleration of the CoM can help riders achieve crank forces greater than bodyweight, which adds to the existing body of evidence pertaining to the benefits of foregoing bodyweight support at the saddle when trying to sustain or produce near maximal power outputs (Stone and Hull 1993; Caldwell et al. 1998; Reiser II et al. 2002; Hansen and Waldeleand 2008; Turpin et al. 2016; Soden and Adeyefa 1979; Costes et al. 2015; Hug et al. 2011).

Work generated by muscle raised the potential energy of the CoM, which was used later in the crank cycle to reduce the peak instantaneous joint power requirement. We know that muscles are both force and power limited (Galantis and Woledge 2003), and high forces combined with high shortening velocities must require higher activations (Lichtwark and Wilson 2005). Different muscle fibre types also differ in the energy required to produce a unit of force (Sargeant 2007). Thus, reducing the peak joint power required during each crank cycle is likely to help riders maintain high-power outputs for a longer duration. Previous research supports this theory, showing that riders use a non-seated posture to increase time to exhaustion at high-power outputs (Hansen and Waldeleand 2008). We also predict that CoM vertical movement during non-seated cycling can be a strategy for increasing $P_{max,i}$.

Our findings agree with earlier cycling research, showing that the upper body joint power contributes significantly to crank power output (Baker et al. 2002). Greater upper body joint power contributions occurred at higher power outputs and when cadence was reduced, helping to explain why maximal power outputs are higher when riders are able to grip the handlebar (Baker et al. 2002) and, theoretically, that greater levels of crank torque could also be achieved. Force produced at the handlebar is crucial for first raising the potential energy of the CoM and then acting in the opposite direction to give the CoM downward momentum prior to when peak forces are required. As supported by previous literature (Stone and Hull 1993), the arms play an active role to ensure that lower body power contributes to crank power rather than raising the CoM against gravity. For example, maximal power output produced over one crank cycle during seated cycling is reduced by 22% when riders are not able to grip the handlebar (Baker

et al. 2002). We suspect that in this scenario, the lower limbs produce the same level of power as when gripping the handlebar, but a portion of power is lost due to no contribution of upper body muscle power and an additional portion of power is lost due to the lower limbs generating power on the CoM rather than the crank.

We can only speculate that riders may store energy in passive elastic elements of muscle during non-seated cycling. Theoretically, almost no additional energy would be required to lift the CoM if the decrements in E_{tot} could be stored in muscle's elastic elements and then re-used during a later part of the crank cycle. It seems, however, that this scenario does not occur, or is minor, as the majority of E_{tot} is transferred to the crank. Further research is required at a muscle level to determine whether there is any potential for energy not transferred to the crank to be stored as elastic energy.

It is generally accepted that the metabolic cost of positive muscular work is roughly four times that of its mechanical output (Margaria 1968). For this reason, one may theorise that the muscular work used to raise the CoM is either performed by choice or perhaps cannot be avoided. Here we have provided evidence for the former, showing that the magnitude and phasing of CoM mechanical energy changes can contribute to net positive power at the crank. If the goal of the rider is to minimise energy expenditure, then the cost of supporting extra bodyweight and producing work on the CoM must be considered against the rate and amount of mechanical energy that can be transferred between the CoM and the crank. In this regard, recent findings (Wilkinson, Lichtwark, and Cresswell 2020) suggest that riders may be able to partially offset the cost of supporting extra bodyweight in the non-seated posture by increasing effective mechanical advantage at the knee. While metabolic cost is important to the rider during steady-state cycling, it is of no concern when they are attempting to produce maximal power output i.e. during a finishing sprint. Thus, raising and lowering the CoM appears to provide a potential performance advantage to the rider during short-lasting very-high-power output cycling.

Our findings are valid only for cycling on a stationary ergometer whereby the lateral dynamics of the bicycle are constrained. Under normal cycling conditions, particularly during climbing and sprinting, the bicycle leans from side to side during each crank cycle. Although this motion occurs about the bicycle's roll axis, it may have a significant impact on gravitational potential energy changes of the rider's CoM and joint power production. The bicycle's CoM will also rise and fall as the bicycle leans from side-to-side. Although these changes are likely small due to the low mass of the bicycle, it is possible that bicycle and rider CoM mechanical energy changes may be in- or out-of-phase, which potentially impacts on mechanical energy changes of the system. Thus, there is a need for further analyses of rider kinematics and joint mechanics under conditions where lateral bicycle dynamics are unconstrained.

This study is the first to measure rider CoM movement and the associated mechanical energy changes during non-seated cycling. Mechanical energy fluctuations of the rider's CoM are primarily due to changes in gravitational potential energy during the crank cycle. These results

show that riders can utilise their body mass to significantly amplify instantaneous maximal crank power output when cycling in a non-seated posture. Under the conditions tested here, this mechanism of power amplification significantly reduced peak joint power requirements, which may underlie why using a non-seated posture can increase time to exhaustion when cycling at high power outputs. It is also possible that raising and lowering the CoM to amplify crank power underlies previous findings that maximal crank power output is higher in the non-seated posture compared to when seated. Our future focus will be to investigate whether similar CoM mechanical energy changes occur when cycling in a non-seated posture under field conditions. The trade-off between the benefits of CoM mechanical energy changes and the separate costs of supporting bodyweight, producing work on the CoM, and potential increase in frontal surface area should also be investigated.

The following submitted manuscript has been incorporated as Chapter4.

Wilkinson, R.D., Cresswell, A.G., and Lichtwark, G.A., Rock and Roll: The Influence of Bicycle Lean on the Mechanics of Non-Seated Cycling, submitted to *Journal of Biomechanics* on May 26, 2020.

Contributor	Statement of contribution	%
Wilkinson, R.D.	writing of text study design and concept data collection data analysis statistical analysis preparation of figures revision of written work supervision, guidance	80 20 90 90 100 80 40 0
Lichtwark, G.A.	writing of text study design and concept data collection data analysis statistical analysis preparation of figures revision of written work supervision, guidance	10 40 5 5 0 10 30 50
Cresswell, A.G.	writing of text study design and concept data collection data analysis statistical analysis preparation of figures revision of written work supervision, guidance	10 40 5 5 0 10 30 50

Chapter 5

The Effect of Bicycle Lean on the Mechanics of Non-Seated Cycling

5.1 Abstract

When riding off the saddle during climbing and sprinting, cyclists appear to coordinate the rhythmic, vertical oscillations of their centre of mass (CoM) with the side-to-side lean of the bicycle. Is the coordination of these two motions merely a stability requirement, or could it also be a strategy to more effectively generate crank power? Here we combined a kinematic and kinetic approach to understand how different constraints on bicycle lean influence CoM movement and limb mechanics during non-seated cycling. Ten participants cycled in a non-seated posture at a power output of $5 \text{ W}\cdot\text{kg}^{-1}$ and a cadence of 70 rpm under three bicycle lean conditions: unconstrained on rollers (Unconstrained), under instruction to self-restrict bicycle lean on rollers (Self-Restricted) and constrained in a bicycle trainer (Trainer). Bicycle lean angle in the Unconstrained condition was greater than Self-Restricted and in the Trainer. Vertical CoM displacement, peak vertical crank force, and peak instantaneous crank power in the Unconstrained condition were greater than Self-Restricted but similar to in the Trainer. The amount and rate of energy lost and gained by the rider's CoM in the Unconstrained condition was greater than Self-restricted but similar to in the Trainer. The differences in joint power contributions to total joint power (hip, knee, ankle, and upper body) between conditions were inconclusive. We interpret these results as evidence bicycle lean plays an important role in facilitating the production of high crank force and power output during non-seated cycling by allowing a greater non-muscular contribution to crank power.

5.2 Introduction

During non-seated cycling, riders lean the bicycle from side to side (Soden and Adeyefa 1979; Hull, Beard, and Varma 1990) in conjunction with raising and lowering their centre of mass

(CoM) (Soden and Adeyefa 1979; Hull, Beard, and Varma 1990; Wilkinson, Cresswell, and Lichtwark 2020). The bicycle leans from side to side at the same frequency as pedalling, while the CoM rises at twice this frequency. During non-seated treadmill cycling, peak lean angles of 11° from vertical have been observed and occur when each crank is close to bottom dead centre (180°) (Duc et al. 2008; Hull, Beard, and Varma 1990). Studies of outdoor and ergometer cycling show the rider's CoM rises by up to 13 cm as the crank transitions from the downstroke to upstroke for each leg (Soden and Adeyefa 1979; Wilkinson, Cresswell, and Lichtwark 2020). The amplitude of bicycle lean and vertical CoM displacement appear to be positively related to crank torque requirements (Soden and Adeyefa 1979; Hull, Beard, and Varma 1990; Duc et al. 2008; Wilkinson, Cresswell, and Lichtwark 2020), but the relationship between these two motions remains unclear.

Bicycle lean is important for maintaining dynamic balance (Meijaard et al. 2007). In the frontal plane, greater pedal forces result in greater imbalances in the moments about the line of contact between the wheels and the ground (Soden and Adeyefa 1979). A rider can correct these imbalances using a combination of: 1) counter-steering into the fall to bring the line of contact underneath the CoM, 2) leaning the bicycle to bring the driving pedal over the line of contact, 3) generating a balancing torque at the handlebar, and 4) moving the CoM laterally (Cain, Ashton-Miller, and Perkins 2016). Thus, maintaining dynamic balance when climbing and sprinting in a non-seated posture requires coordinated motion and a complex interaction of forces between the rider and bicycle.

Evidence suggests vertical CoM motion and upper limb muscles can amplify crank power (Wilkinson, Cresswell, and Lichtwark 2020) and help riders achieve greater maximal power output (Baker et al. 2002; Doré et al. 2006). During non-seated cycling, peak pedal forces reach magnitudes close to two times bodyweight in each downstroke (Soden and Adeyefa 1979; Dorel 2018a; Wilkinson, Cresswell, and Lichtwark 2020). Without the action of the arms at the handlebar, vertical pedal forces greater than bodyweight result in positive work on the CoM rather than the pedal, which can cause a 22% decrease in maximal power output (Baker et al. 2002). The arms also act to give the CoM downward velocity, resulting in the CoM losing mechanical energy at a rate equivalent to 18% ($3.9 \pm 0.9 \text{ W}\cdot\text{kg}^{-1}$) of peak instantaneous crank power (Wilkinson, Cresswell, and Lichtwark 2020). Thus, using the arms to either resist or cause accelerations of the CoM is an important strategy for generating high pedal force and power output during non-seated cycling.

The use of cycling ergometers in research has limited our current understanding of optimal strategies to perform non-seated cycling at high power output. For instance, a recent study suggested a novel forward crouching posture known to limit bicycle lean during sprinting does not impair maximal power output (Merkes, Menaspà, and Abbiss 2020). However, the use of an ergometer ignores lateral dynamics of the bicycle which result from forces imparted by the rider at the pedals and handlebar. Given CoM movement and arm power contribute to crank power, and bicycle lean likely influences the rise and fall of the CoM, it is unknown how

self-restricting lean (e.g. by the rider) or constraining lean (e.g. by an ergometer) impacts how power is generated during non-seated cycling at high power output.

Our aim was to investigate whether changing constraints on bicycle lean would alter a rider's vertical CoM displacement and distribution of joint power during non-seated cycling. A combined kinematic and kinetic approach was used to analyse non-seated cycling at a constant power output and cadence under three bicycle lean conditions: 1) unconstrained on rollers, 2) under instruction to self-restrict bicycle lean on rollers, and 3) constrained in a bicycle trainer. Our hypothesis was formed by drawing parallels between cycling and horse riding; to reduce the amount of positive work a horse must generate during each stride cycle, jockeys reduce their own CoM displacement by performing negative work with their lower limbs (Pfau et al. 2009). In a similar manner, we predicted that when cyclists were instructed to self-restrict bicycle lean, they would adopt a more crouched, jockey-like posture, which would result in their vertical CoM displacement and net knee power being reduced from constrained in a trainer to unconstrained on rollers and further reduced from unconstrained to self-restricted on rollers.

5.3 Materials and methods

5.3.1 Experimental design

Ten recreational cyclists (9M/1F, age: 28 ± 8 years, height: 1.83 ± 0.09 m, mass: 76 ± 6 kg) cycled in a non-seated posture at a power output of $5 \text{ W}\cdot\text{kg}^{-1}$ and a cadence of 70 rpm under three bicycle lean conditions: 1) unconstrained on rollers (Unconstrained), 2) under instruction to self-restrict bicycle lean on rollers (Self-Restricted), and 3) constrained in a bicycle trainer (Trainer). The combination of power output and cadence was chosen to replicate a typical scenario for using a non-seated posture (Harnish, King, and Swensen 2007; Hansen and Waldeland 2008). All participants gave their written informed consent prior to participating in the study according to the procedures approved by the Human Ethics Committee of The University of Queensland. Each participant used the same racing bicycle (Reacto CF 907-E, Merida, Yuanlin City, Taiwan) while on the electromagnetically-braked rollers (Real E-motion B+, Elite, Fontaniva, Italy) and mounted in the trainer (Qubo Digital Smart B+, Elite, Fontaniva, Italy). The position of the handlebar relative to the bottom bracket remained constant for all participants. Before testing, participants performed several familiarisation bouts of cycling in a non-seated posture on the rollers until they gave verbal confirmation their technique felt comfortable and was similar to riding outdoors. For safety, participants wore a helmet and shoulder harness attached via a carabiner and a slack, static rope line to an overhead gantry. The setup did not hinder the participant's ability to move their CoM or lean the bicycle. Participants wore cleated cycling shoes (SH-R070, Shimano, Osaka, Japan) clipped into the pedals (SH-R540, Shimano, Osaka, Japan). Tyre pressure was kept constant at 689 kPa (100 psi). Subjects maintained the target power output and cadence using feedback from a visual

display placed in front of them. Trials were performed in a randomised order and participants were given 3-min rest between trials. For each condition, we acquired crank angle and force signals synchronously with motion capture for 10 s once the rider achieved the target power and cadence using a 16-bit A/D conversion board (USB-2533, Measurement Computing Corporation, Norton, MA) and Qualisys Track Manager software (Qualisys AB, Gothenburg, Sweden).

5.3.2 Kinematics

Three-dimensional positions of 45 passive reflective markers were collected at 200 Hz using an eight camera, opto-electronic motion capture system (Oqus, Qualisys, AB, Sweden). Reflective markers and lightweight clusters were secured to the skin using a combination of double-sided tape and self-adhesive bandage at previously described locations suitable for measuring full-body kinematics (Wilkinson, Lichtwark, and Cresswell 2020; Wilkinson, Cresswell, and Lichtwark 2020) (marker locations are shown in Figure 5.1B). For scaling purposes, a static trial was collected with the participant standing in a standard anatomical posture before commencing the trials. The heading (yaw) angle and lean of the bicycle was determined within the motion capture global coordinate system by placing three markers in a triangular pattern on the frame of the bicycle. These markers were used to create a local coordinate system for the bicycle, which allowed us to define the position and orientation of the bicycle and cranks relative to the global coordinate system. Positive lean values were defined to be counterclockwise in relation to the wheel-ground axis when viewing the bicycle from the front. A diagram of the reference coordinates and other physical quantities is provided as Figure 5.1A.

5.3.3 External forces

Tangential and radial forces at the left and right crank, as well as crank angle, were recorded at 100 Hz using pre-calibrated, wireless, instrumented cranks (Axis, SWIFT Performance, Brisbane, Australia). Digital signals were transmitted wirelessly to a base receiver before being converted to an analogue signal through the A/D Board. Crank angle and force signals were synchronised with motion capture trajectories using the internal sampling factor within Qualisys Track Manager software. A multi-axis, dynamic calibration of each crank was performed by the manufacturer. In addition, and prior to testing, the calibrated output voltage for the tangential and radial force was verified by suspending a 2.5 kg mass from each pedal spindle with the cranks in both horizontal and vertical positions.

Motion capture marker trajectories, crank forces, and crank angles were processed using custom scripts in Matlab (R2019b, MathWorks Inc., USA). These scripts filtered crank force signals and marker trajectories with a zero-lag, second-order, low-pass Butterworth filter with a cut-off frequency of 12 Hz (Kristianslund, Krosshaug, and Van den Bogert 2012). The radial and tangential forces at each crank were transformed from the crank coordinate system to the global coordinate system based on the crank orientation (Wilkinson, Cresswell, and Lichtwark

2020). Bicycle lean angle was not accounted for in these calculations. As the cranks did not measure lateral force, it is possible the true vertical crank force was greater than recorded when the bicycle was leant away from vertical, which would overestimate vertical handlebar forces. However, given peak lean angles were less than 6°, the maximum magnitude of this error is likely to be less than 1%. Net vertical handlebar force was resolved as the difference between the total vertical force required to cause the measured acceleration of the rider's CoM and the sum of vertical force at the left and right cranks. Further details of this method can be found in our previous work (Wilkinson, Lichtwark, and Cresswell 2020; Wilkinson, Cresswell, and Lichtwark 2020).

5.3.4 Mechanical energy and power

OpenSim software (Delp et al. 2007) was used to create participant-specific models by scaling segment lengths and segment masses of a previously developed generic full-body musculoskeletal model (Rajagopal et al. 2016) based on each participant's anthropometry. Inverse dynamic analysis was used to calculate hip, knee, and ankle net joint moments by combining inverse kinematic results with reaction force at the left and right cranks (Seth et al. 2011). Individual joint power contributions were calculated as a percentage of total joint power. Inclusion of data required the cyclist to simultaneously match the target power ($\pm 5\%$) and cadence ($\pm 5\%$) for a minimum of five crank cycles. Cycles containing more than five samples of outlying data (>3 Median Absolute Deviations), typically due to crank signal dropout, were detected and removed from each trial (Leys et al. 2013), resulting in an average of eight crank cycles being analysed for each participant in each condition.

At each instant, total joint power generated by the rider (P_{tot}) is equal to the sum of crank power (P_{cranks}) and the rate of mechanical energy lost or gained by the rider's CoM (P_{CoM}) (van Ingen Schenau and Cavanagh 1990).

$$P_{tot} = P_{cranks} + P_{CoM} \quad (5.1)$$

P_{cranks} was calculated as the summed product of torque and angular velocity measured at each crank. P_{CoM} was calculated using inverse kinematic results as the change in total mechanical energy (potential + kinetic) divided by the change in time. It should be noted that the test bicycle when stationary and upright has a total mechanical energy store of $\sim 43\text{J}$, which fluctuates within each crank cycle ($<0.5\text{ J}$ per crank cycle) due to the displacement of its CoM. The rate of change in total mechanical energy of the bicycle was approximated (range of lean angle = 6°, CoM height = 0.4 m, bicycle mass = 11 kg) to be less than $\pm 2\%$ ($\pm 0.1\text{ W}\cdot\text{kg}^{-1}$) of P_{cranks} . Thus, these fluctuations were deemed negligible in the context of this study and were omitted from Equation 5.1.

$$P_{lb} + P_{ub} = P_{cranks} + P_{CoM} \quad (5.2)$$

Lower-body joint power (P_{lb}) was calculated as the summed product of net joint moments and joint angular velocities at the hip, knee, and ankle of each leg. Upper-body power (P_{ub}) was assumed to be the difference between P_{tot} and P_{lb} . Further details regarding the application of power equations in cycling can be found elsewhere (van Ingen Schenau and Cavanagh 1990; Martin et al. 1998; Wilkinson, Cresswell, and Lichtwark 2020).

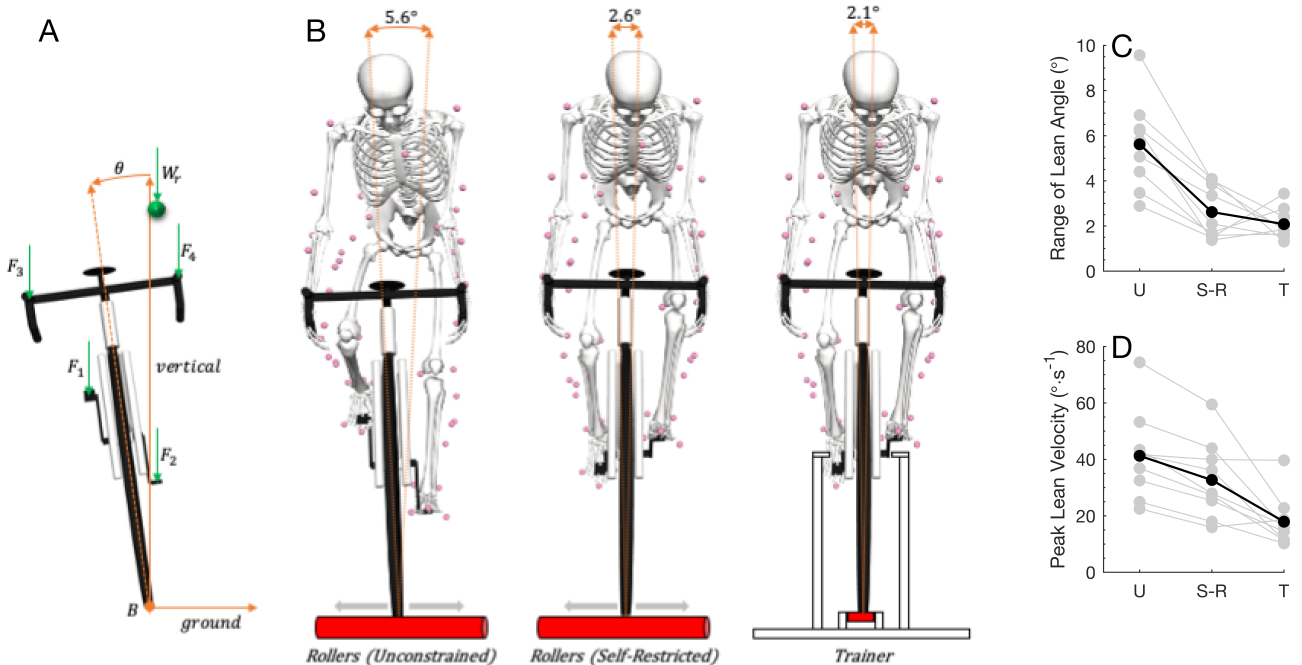


Figure 5.1: The group mean range of bicycle lean angle in the Unconstrained condition was 54% greater than Self-Restricted and 63% greater than in the Trainer.

A. Front view of reference coordinates and vertical forces imparted by the rider on the bicycle. The sum of vertical handlebar force ($F_3 + F_4$) was calculated as the difference between the force required to cause the measured accelerations of the rider's CoM and the total vertical crank force ($F_1 + F_2$). B. Diagrams depicting the musculoskeletal model cycling in a non-seated posture under the three conditions: Unconstrained, Self-Restricted, and Trainer. The group mean range of bicycle lean angle is illustrated by the arc above the rider's head. C. The group mean range of bicycle lean angle in the Unconstrained condition was 54% greater than Self-Restricted and 63% greater than in the Trainer. D. The group mean peak bicycle lean velocity in the Unconstrained condition was 20% greater than Self-Restricted and 56% greater than in the Trainer. Participant means shown in grey and the group mean in black. U, Unconstrained. S-R, Self-Restricted. T, Trainer.

5.3.5 Statistical analyses

We performed repeated-measures, one-way analyses of variance (ANOVAs) to test for main effects of bicycle lean condition on a number of variables (Table 5.1). The significance level was set at 0.008 prior to statistical analysis. This level was based on a desired false positive risk of $\leq 5\%$, prior probability of 0.5, sample size of ten, and a minimum detectable effect size of 0.8 (Colquhoun and Longstaff). The significance level was corrected for multiple comparisons using the Sidak method. The F-statistic (F), p-value (ρ), and generalised eta squared (η_G^2) are provided for main effects. For multiple comparisons the t-statistic (t), corrected p-value (ρ),

95% confidence intervals (95%CI [Low to High]), and corrected effect size (*Hedge's g_{av}*) are provided. All values are reported as mean \pm standard deviation.

5.4 Results

5.4.1 Bicycle lean

The range of bicycle lean (peak-to-peak) and peak lean angular velocity for each participant are presented in Figure 5.1C-D. The range of bicycle lean in the Unconstrained condition ($5.6 \pm 2.0^\circ$) was greater than Self-Restricted ($2.6 \pm 1.2^\circ$) and in the Trainer ($2.1 \pm 0.7^\circ$) (Table 5.1). Peak lean velocity was also greater in the Unconstrained condition ($41 \pm 16^\circ\text{s}^{-1}$) than Self-Restricted ($33 \pm 14^\circ\text{s}^{-1}$) and in the Trainer ($18 \pm 9^\circ\text{s}^{-1}$) (Table 5.1). Thus, it is likely the effects reported hereafter are predominantly due to the modification of lateral bicycle dynamics (lean) in each condition.

5.4.2 CoM motion and energetics

Figure 5.2A-C show vertical CoM displacement, vertical CoM velocity, and vertical CoM acceleration with respect to the right crank angle in each condition. The range of vertical CoM displacement in the Unconstrained condition (5.1 ± 1.2 cm) was 24% greater than Self-Restricted (3.9 ± 1.2 cm) but similar to in the Trainer (5.3 ± 1.4 cm) (Table 1). The pattern of mechanical energy gained and lost by the rider's CoM with respect to the right crank angle is shown in Figure 3A. In each condition, phases of CoM mechanical energy loss (i.e. negative power) occurred from 55° to 155° and from 235° to 335° during the right crank cycle. Figure 4A-B show the mean range of vertical CoM displacement and the peak rate of CoM mechanical energy loss for each participant and the group in each condition. The peak rate of CoM mechanical energy loss in the Unconstrained condition ($-4.0 \pm 1.1 \text{ W}\cdot\text{kg}^{-1}$) was 25% greater than Self-Restricted ($-3.0 \pm 0.9 \text{ W}\cdot\text{kg}^{-1}$) but 12.5% less than in the Trainer ($-4.5 \pm 1.3 \text{ W}\cdot\text{kg}^{-1}$). The peak rate of CoM mechanical energy gain in the Unconstrained condition ($4.9 \pm 1.2 \text{ W}\cdot\text{kg}^{-1}$) was 29% greater than Self-Restricted ($3.5 \pm 1.1 \text{ W}\cdot\text{kg}^{-1}$) but similar to in the Trainer ($4.8 \pm 1.6 \text{ W}\cdot\text{kg}^{-1}$).

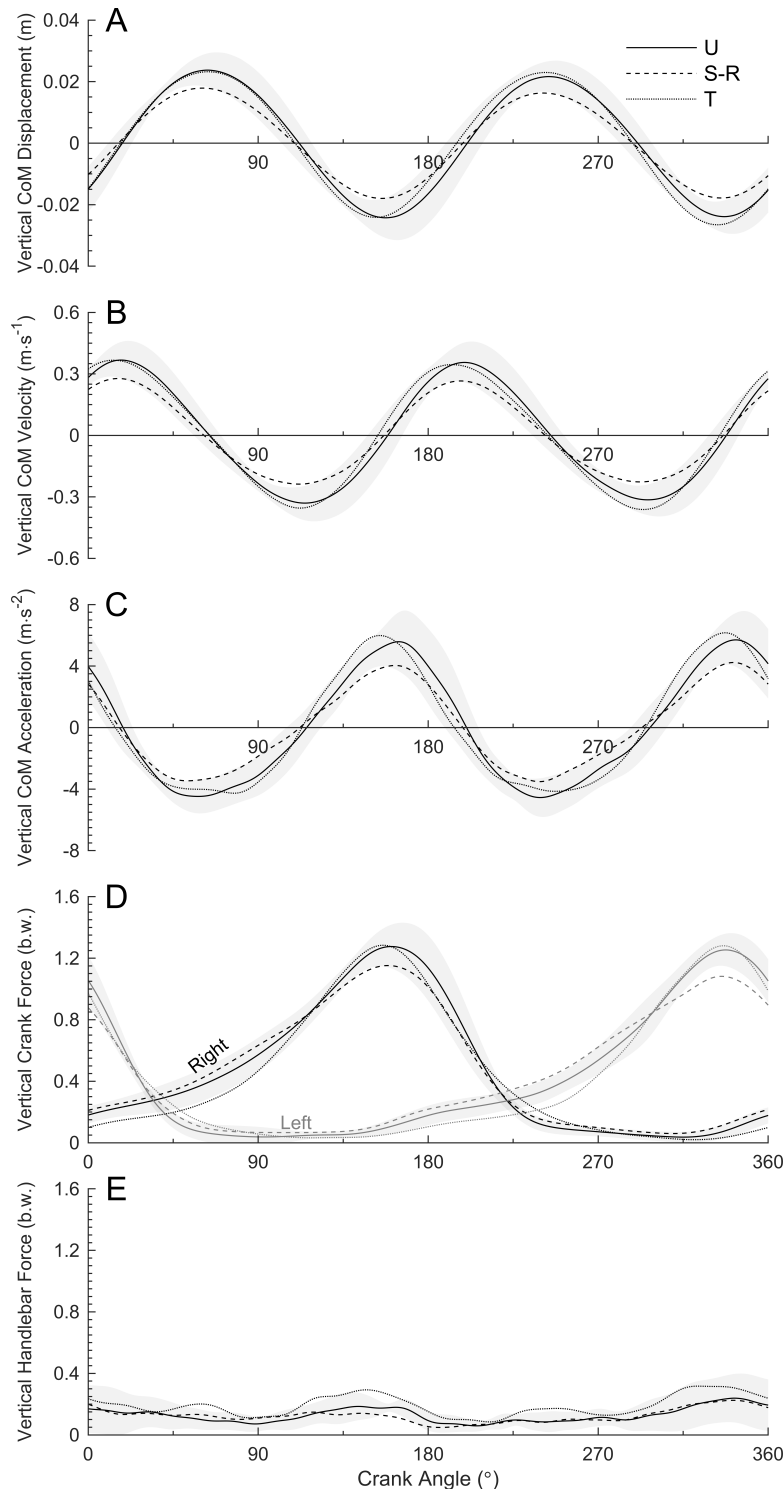


Figure 5.2: Riders self-restricted bicycle lean by reducing peak vertical forces at the crank by 15% on average. Group mean vertical CoM displacement (A), vertical CoM velocity (B), vertical CoM acceleration (C), vertical force at the left and right crank (D), and net vertical handlebar force (E) with respect to the right crank angle (0–360°) during non-seated cycling at $5 \text{ W}\cdot\text{kg}^{-1}$ at 70 rpm under each condition. Forces have been normalised to body weight (b.w.). In each axis (A–E), the shaded area denotes \pm one standard deviation from the mean in the Unconstrained condition. Crank angles of 0° and 360° represent top dead centre position of the right crank, and 180° represents the bottom dead centre position. U, Unconstrained. S-R, Self-Restricted. T, Trainer.

5.4.3 Vertical force

Figure 5.2D-E show vertical crank force and net vertical handlebar force with respect to the right crank angle in each condition. Peak vertical crank force in the Unconstrained condition ($122 \pm 7\%$ b.w.) was 13% greater than Self-Restricted ($106 \pm 6\%$ b.w.) but similar to in the Trainer ($125 \pm 11\%$ b.w.). Mean handlebar force in the Unconstrained condition ($13 \pm 4\%$ b.w.) was similar to Self-Restricted ($13 \pm 5\%$ b.w.) but 46% less than in the Trainer ($19 \pm 2\%$ b.w.).

5.4.4 Joint power

Figure 5.3B-D show the patterns of total joint power, lower and upper body power, and individual joint power with respect to the right crank angle in each condition. Net knee power was similar between all conditions (Table 5.1). A small increase in net hip power was detected in the Self-Restricted condition ($34 \pm 13\%$) compared to Unconstrained ($32 \pm 13\%$). It is possible a small increase in net ankle power occurred in the Trainer condition ($27 \pm 7\%$) compared to Unconstrained ($24 \pm 4\%$), however our study was not sufficiently powered to detect this effect. A large variation in individual joint power contributions occurred between participants (see shaded area in Figure 5.3D). Despite the variation in individual joint power contributions between participants, there was a trend towards producing less lower body power; hence more upper body power in the Unconstrained condition ($8 \pm 4\%$) compared to Self-Restricted ($7 \pm 3\%$) and Trainer ($6 \pm 1\%$), however our study was not sufficiently powered to detect this effect (Table 5.1).

5.4.5 Crank power

Figure 5.3A shows the pattern of crank power with respect to the right crank angle in each condition. Mean crank power (constrained by the task) was the same across each crank cycle (Table 5.1); hence any change in peak crank power must be compensated for at a different time during the crank cycle. For instance, peak crank power in the Unconstrained condition ($11.2 \pm 1.0 \text{ W}\cdot\text{kg}^{-1}$) was 4% higher than Self-Restricted ($10.7 \pm 0.8 \text{ W}\cdot\text{kg}^{-1}$) but similar to in the Trainer ($11.6 \pm 1.6 \text{ W}\cdot\text{kg}^{-1}$).

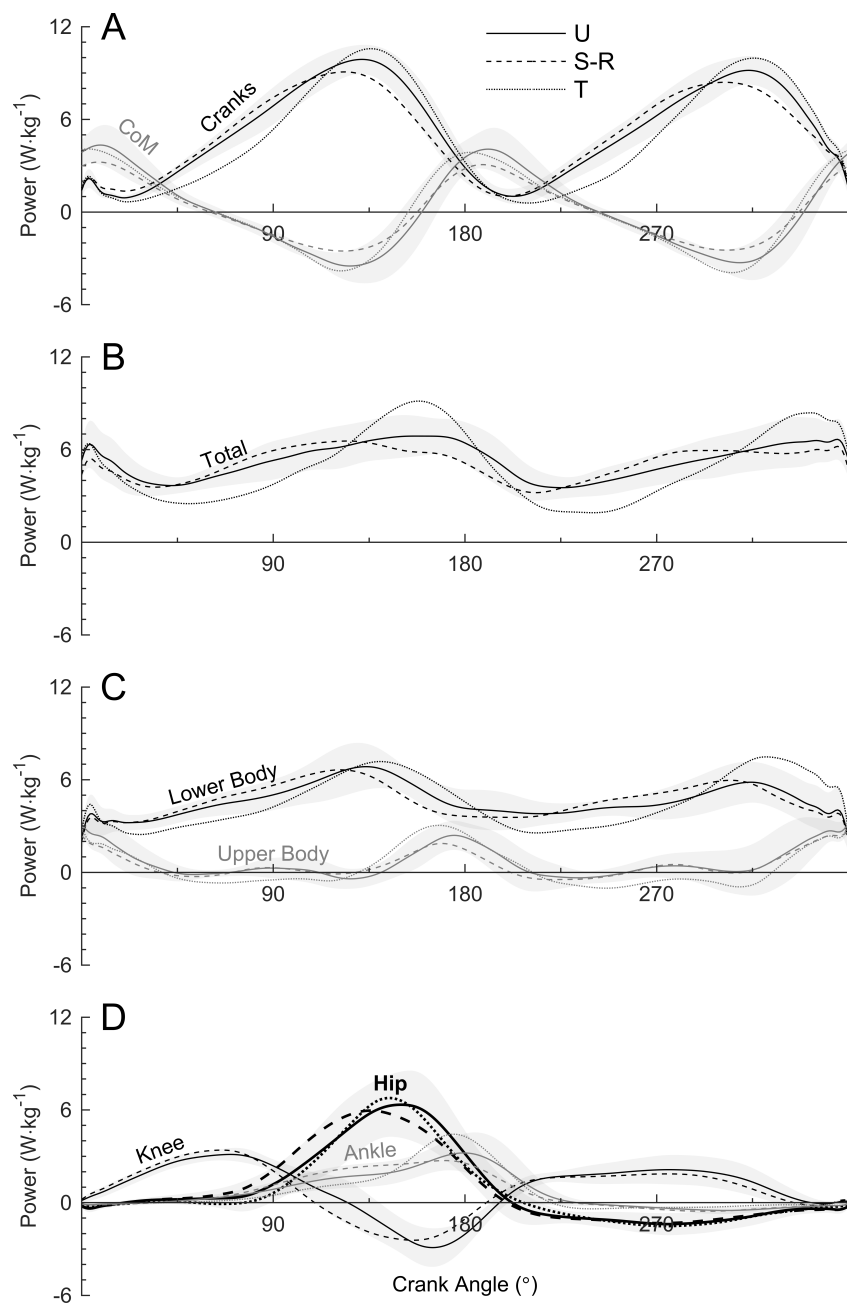


Figure 5.3: The different constraints on bicycle lean appeared to alter the pattern of total joint power production during the crank cycle. A. Group mean total crank power and CoM power normalised to body mass with respect to the right crank angle ($0-360^{\circ}$). B. Group mean total joint power normalised to body mass. C. Group mean lower body (black) and upper body power (grey) normalised to body mass. D. Group mean hip (thick black), knee (thin black), and ankle power (thin grey) of the right leg normalised to body mass. In each axis (A-D), the shaded area denotes ± 1 standard deviation from the mean in the Unconstrained condition. Crank angles of 0° and 360° represent top dead centre position of the right crank, and 180° represents the bottom dead centre position. U, Unconstrained. S-R, Self-Restricted. T, Trainer.

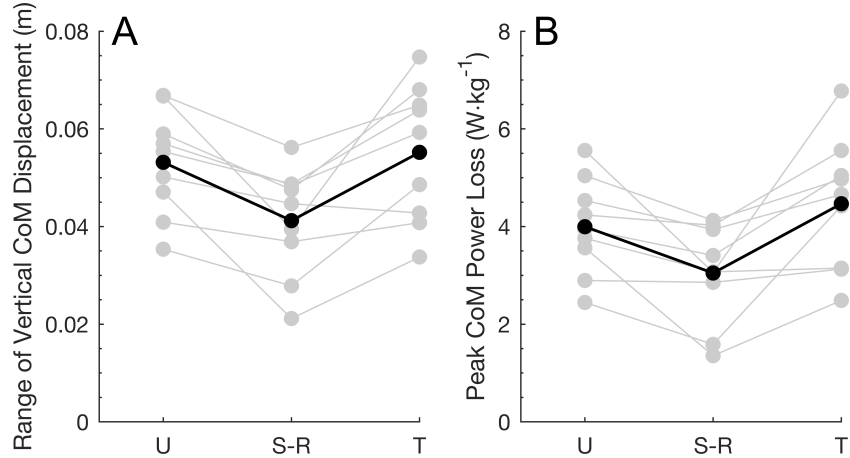


Figure 5.4: Riders increased mean and peak CoM power when lateral bicycle dynamics were constrained by a trainer, but did the opposite when having to self-restrict bicycle lean. A. The group mean range of vertical CoM displacement in the Unconstrained condition was 24% greater than Self-Restricted, but similar to in the Trainer. B. The group mean peak rate of CoM mechanical energy loss (peak negative power) in the Unconstrained condition was 25% greater than Self-Restricted, but 12.5% less than in the Trainer. Participant means shown in grey and the group mean in black. U, Unconstrained. S-R, Self-Restricted. T, Trainer.

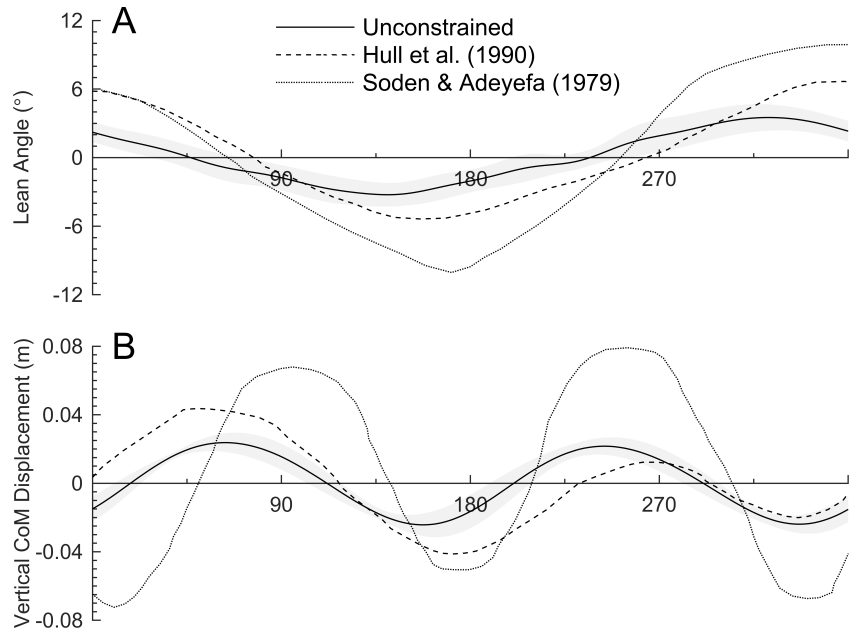


Figure 5.5: The range of bicycle lean during the unconstrained condition was less than the values reported in previous studies of non-seated cycling in the field and on a treadmill. A. Comparison of the group mean bicycle lean angle in the Unconstrained condition against data from previous literature (Soden and Adeyefa 1979; Hull, Beard, and Varma 1990). B. Comparison of the group mean vertical CoM displacement in the Unconstrained condition against a rudimentary measure of lower back displacement (Soden and Adeyefa 1979) and a measure of pelvis midpoint displacement (Hull, Beard, and Varma 1990) from previous literature. For both comparisons, data from previous literature was extracted from published figures using Web Plot Digitizer 4.2 (<https://automeris.io/WebPlotDigitizer>). In each axis, the shaded area denotes \pm one standard deviation from the mean in the Unconstrained condition.

	Conditions						One-way RM ANOVA						Multiple Comparisons (Sidak)					
	Unconstrained			Self-Restricted			Trainer			Main Effect			Unconstrained vs Self-Restricted			Unconstrained vs Trainer		
	M	SD	M	SD	M	SD	F	p	η^2_G	t	p	95% CI	Hedge's g_{av}	t	p	95% CI	Hedge's g_{av}	
Mean Crank Power (W/kg)	5.1	0.5	5	0.7	5	0.7	0.02	0.98	0.003	0.4	0.35	-0.2 to 0.3	0.05	0.4	0.35	-0.3 to 0.4	0.1	
Mean Cadence (W/kg)	69	1	69	3	70	1	0.6	0.56	0.07	1	0.22	-1 to 2	0.03	0.4	0.35	-1 to 1	0.1	
Range of Bicycle Lean (°)	5.6	2	2.6	1.2	2.1	0.7	19	<0.001	0.71	7.9	<0.001	2.1 to 3.9	1.7	7.7	<0.001	2.5 to 4.6	2.1	
Peak Lean Velocity (°·s⁻¹)	4.1	16	33	14	18	9	17	<0.001	0.68	6.8	<0.001	6 to 11	0.5	9.7	<0.001	18 to 29	1.6	
Peak Vertical Crank Force (% b.w.)	122%	7%	106%	6%	125%	11%	21	<0.001	0.72	26	<0.001	15 to 17	2.1	1.4	0.14	-2 to 7	0.3	
Mean Handlebar Force (% b.w.)	13%	4%	13%	5%	1%	2%	15	<0.001	0.65	0.7	0.3	-1 to 2	0.1	8.8	<0.001	5 to 8	1.8	
Peak Instantaneous Crank Power (W·kg⁻¹)	11.2	1	10.7	0.8	11.6	1.6	2.3	0.14	0.22	5.4	<0.001	0.3 to 0.7	0.5	1.7	0.1	-0.2 to 1	0.3	
Range of CoM Displacement (cm)	5.1	1.2	3.9	1.2	5.3	1.4	11	<0.001	0.59	12	<0.001	1 to 1.5	1	1.5	0.13	-0.1 to 0.6	0.2	
Peak CoM Power Gain (W·kg⁻¹)	4.9	1.2	3.5	1.1	4.8	1.6	9.2	0.002	0.54	14	<0.001	1.1 to 1.6	1.1	0.4	0.36	-0.3 to 0.4	0.04	
Peak CoM Power Loss (W·kg⁻¹)	-4.0	1.1	-3.0	0.9	-4.5	1.3	11	0.001	0.57	10	<0.001	0.8 to 1.3	1	3.2	0.008	0.1 to 0.8	0.3	
Mean CoM Power Gain (W·kg⁻¹)	2.3	0.6	1.7	0.6	2.3	0.7	12	<0.001	0.61	14	<0.001	0.5 to 0.7	1	0.03	0.39	-0.1 to 0.1	0.002	
Mean CoM Power Loss (W·kg⁻¹)	-2.1	0.5	-1.6	0.5	-2.3	0.6	14	<0.001	0.64	11	<0.001	0.4 to 0.6	1	3	0.01	0 to 0.3	0.3	
Net Hip Power Contribution (%)	32	13	34	13	31	15	0.7	0.51	0.08	3.3	0.008	1 to 5	0.2	0.4	0.35	-4 to 5	0.05	
Net Knee Power Contribution (%)	36	12	34	12	36	14	0.2	0.8	0.03	1.5	0.12	-1 to 5	0.2	0.4	0.35	-4 to 5	0.1	
Net Ankle Power Contribution (%)	24	4	25	5	27	7	1.1	0.36	0.12	1.3	0.16	0 to 1	0.1	1.7	0.1	-1 to 5	0.4	
Net Lower Body Power Contribution (%)	92	4	93	3	94	1	1.5	0.25	0.16	2.4	0.03	0 to 2	0.3	2.5	0.03	0 to 4	0.7	
Net Upper Body Power Contribution (%)	8	4	7	3	6	1	1.5	0.25	0.16	2.4	0.03	0 to 2	0.3	2.5	0.03	0 to 4	0.7	

M, mean. SD, standard deviation. η^2_G , generalised eta squared. Hedge's g_{av} , corrected effect size. Corrected effect size values within each multiple comparison group have been assigned a color scale from white (lowest value) to dark gray (highest value).

Table 5.1: Self-restricting bicycle lean had a large effects on vertical crank force and CoM energetics. Group results (n=10) in each condition during non-seated cycling at 5 W·kg⁻¹ at 70 rpm.

5.5 Discussion

These results demonstrate that the type of constraint on bicycle lean influences a rider's vertical CoM displacement during non-seated cycling. When lean was unconstrained on rollers, the rider's vertical CoM displacement was similar to when lean was constrained by a trainer, but was significantly reduced when lean was self-restricted by the rider on rollers. Peak vertical crank force was also reduced when self-restricting bicycle lean, meaning the decrease in vertical CoM displacement also lead to a decrease in the amount and rate of total mechanical energy gain and loss by the rider's CoM. Thus, performing non-seated cycling in a bicycle trainer decouples bicycle lean from vertical CoM displacement. Given the similarity in CoM movement between the Unconstrained and Trainer conditions it seems reasonable to suggest that using greater amounts of bicycle lean had a similar effect to having a wider base of support. While the static base of support of the trainer reduces the need for stability corrections, bicycle lean appears to allow the bicycle-rider system to dynamically recover from greater perturbations around the wheel-ground axis. Our hypothesis, which was formed by drawing parallels between riding a horse and a bicycle, correctly predicted the relationship between bicycle lean and the rider's vertical CoM displacement in the self-restricted and preferred conditions. However, it appears that lateral instability dictates a rider's vertical CoM motion when riding a bicycle, whereas reducing the whole system's vertical CoM displacement is of more concern when riding a horse. We interpret these results as evidence bicycle lean plays an important role in facilitating the production of high pedal force and power during non-seated cycling by increasing the magnitude of torque imbalances the bicycle-rider system can recover from.

Our results pertaining to the distribution of power between the lower and upper body were inconclusive, however there were important differences in peak and mean vertical forces between conditions. The between-participant variance in individual joint power contributions was likely a function of participants riding non-seated on rollers, which was a novel task for some and allowed multiple strategies to meet the power demands. Peak vertical crank force was highest in the Unconstrained and Trainer conditions, yet riders supported 6% more bodyweight at the cranks in the Unconstrained condition than in the Trainer. Peak vertical crank force in the Unconstrained condition was 13% greater than Self-Restricted, yet riders supported a similar amount of bodyweight at the cranks. Thus, determining how changes in bicycle lean and subsequent vertical CoM displacement influence the temporal nature of individual muscular force and work production remains a future goal.

Leaning the bicycle naturally resulted in greater vertical CoM displacement, which may have an impact on non-seated cycling performance. While increasing the work requirements to raise the CoM might be considered inefficient, our previous research suggests raising and lowering the CoM contributes significantly to peak crank power (Wilkinson, Cresswell, and Lichtwark 2020). Consistent with previous research (Soden and Adeyefa 1979; Hull, Beard, and Varma 1990), the results of this study show that when power output is constrained to a sub-maximal

level, riders perform extra muscular work to raise the CoM as the crank transitions between the downstroke and upstroke of each leg (Figure 5.2A). This specific phasing of CoM movement means riders use mostly radial crank force and some handlebar force to perform work on the CoM, while the arms act to facilitate power transfer between the CoM and the crank during the downstroke. Future studies should investigate the impact of constraining bicycle lean and vertical CoM displacement on maximal power output and gross efficiency during non-seated cycling.

The range of bicycle lean during the unconstrained condition ($\sim 6^\circ$) was less than the values of $16\text{--}22^\circ$ reported in previous studies of non-seated cycling in the field (Soden and Adeyefa 1979) and on a treadmill (Hull, Beard, and Varma 1990; Duc et al. 2008) (Figure 5.5A). This could be due to a number of factors. First, we conducted our study on level rollers, whereas previous studies have been on an incline. For a given power output and cadence, steeper inclines appear to result in greater amplitudes of bicycle lean (Duc et al. 2008), which we suspect is due to the reduced inertia of the system (Fregly, Zajac, and Dairaghi 1996). Second, the riding experience of our participant group was varied. Previous research shows cyclists use greater amounts of lean, rather than steering, compared to non-cyclists when on rollers (Cain, Ashton-Miller, and Perkins 2016). Finally, there are differences between lateral bicycle dynamics on rollers compared to treadmills or in the field (Kooijman and Schwab 2009; Dressel and Papadopoulos 2012), thus it would be useful to conduct this study on an inclined treadmill where greater amplitudes of lean are more likely.

In summary, we interpret our findings to suggest leaning the bicycle during non-seated cycling allows a greater non-muscular contribution to crank force and power. Further research is required to test the direct effect of bicycle lean on non-seated cycling performance.

Chapter 6

Discussion and Summary

As stated by Caldwell et al. (1999), a key aspect of the standing posture is that the rider's hips are higher and further forward in relation to the downstroke pedal. In our first experiment we attempted to uncover some clues about why cyclists transition from a seated to a non-seated posture when having to generate high torque and power on the cranks. Our analysis revealed that this postural change shifted the period of anti-gravity muscle activity (hip extensors, knee extensors, and ankle plantar flexors) later in the crank cycle. This phase shift of muscle activity redirected the pedal force vector to be more closely aligned with both the knee joint centre and the Earth's gravitational acceleration vector. Together, the more vertically aligned posture and pedal force vector meant that the internal joint moments generated by powerful anti-gravity muscles (e.g. gluteus maximus, vastus lateralis, soleus) acted to produce simultaneous propulsion and bodyweight support. These findings highlighted the likelihood of a rider's bodyweight making significant contributions to pedal force and power production during non-seated cycling.

Stone & Hull (1995) provided evidence of a strong positive relationship between a rider's static bodyweight and the peak vertical pedal force produced during non-seated cycling. Furthermore, they showed that peak instantaneous power was dictated primarily by peak vertical pedal force. However, even earlier research had provided indirect evidence that the rider's bodyweight was not static during non-seated cycling, but rather it was raised and lowered during specific phases of the pedal cycle. Our second study expanded on these findings by quantifying vertical CoM displacement and the associated changes in total mechanical energy during non-seated cycling at various combinations of cadence and power output. Our analysis confirmed that a rider's CoM gained and lost significant amounts of mechanical energy due to vertical CoM displacement. Furthermore, greater fluctuations in total mechanical energy occurred as power output increased and at lower cadence. It was apparent that the magnitude and phasing of these fluctuations was a deliberate strategy to increase the inertia of the CoM, which facilitated a greater transfer of energy to the crank during the downstroke and then a transfer of energy back to the CoM as the crank passed through bottom dead centre. This intricate flow of energy appeared to benefit the rider by decreasing instantaneous joint power but increasing instantaneous crank

power. These findings provided a more detailed insight into how cyclists are able to utilise a non-seated posture and their bodyweight to generate greater levels of pedal force and power output. However, this study was conducted on an ergometer which constrained bicycle lean. Thus, the transferability of these findings to over-ground cycling was unclear.

The use of ergometers in cycling has limited our current understanding of optimal strategies to perform non-seated cycling at high power output because they constrain the lateral dynamics of the bicycle (see Chapter 5). Capturing rider and bicycle motion over multiple cycles during over-ground cycling would be the ideal scenario, but the calibrated volume of optical motion capture systems limits the number of cycles that can be captured. Thus, our third study was conducted on a set of electromagnetically braked rollers, which allowed us to analyse multiple cycles of non-seated cycling either with or without restraints on bicycle lean. Our findings showed that vertical CoM displacement, peak vertical crank force, and instantaneous crank power when riders used a preferred amount of bicycle lean was greater than when self-restricting bicycle lean but similar to when in a bicycle trainer. Furthermore, the amount and rate of energy gained and lost by the rider's CoM when riders used a preferred amount of bicycle lean was also greater than when self-restricting bicycle lean but similar to when in a bicycle trainer. First, these results suggest that the findings from our previous studies are likely to transfer to over-ground cycling scenarios. Second, these results suggest that bicycle lean plays an important role in facilitating force and power production by allowing a greater bodyweight and inertia contribution to crank power.

In summary, this thesis has explored some of the fundamental mechanical differences between seated and non-seated cycling and demonstrated the key role that bicycle lean CoM movement play in the generation of crank power during non-seated cycling. The experiments were devised to explore how joints produce work in the different postures and whether the way in which we perform the movement, or restrictions on the interaction between bicycle and rider, can somehow enhance our ability to produce power (particularly high power). A further summary of the key findings from each study and how they build on our current understanding of cycling mechanics are provided below, along with a commentary on limitations to the studies, requirement for future research, and potential practical applications of the results.

6.1 Key findings

6.1.1 When cycling at high-power output, switching from a seated to a non-seated posture can reduce net mechanical power requirements at the knee joint.

The study in Chapter 3 provided the first evidence that the distribution of joint power within the lower limb differs between seated and non-seated cycling. Specifically, the non-seated posture results in a significant reduction in net knee power but an increase in hip and ankle

power. Our analysis of lower-limb muscle activity within the same experiment showed that the increase in hip and ankle power was achieved with similar levels of hip extensor and ankle plantar flexor muscle activity; suggesting that the action of bi-articular muscles was responsible for redistributing knee extension power to the hip and ankle. These findings confirm that the transfer of segmental energy within the lower limb is significantly altered by the change in posture, which ties together previous evidence that the change in posture alters net joint moments (Caldwell et al. 1999), joint kinematics (Caldwell et al. 1999), and muscle activity (Li and Caldwell 1998). Furthermore, our results were in agreement with previous findings (Caldwell et al. 1999) that the change in posture alters the direction of the pedal force vector during the downstroke. Our analysis was able to expand on this finding by showing that the redirection of pedal force leads to greater effective mechanical advantage at the knee joint when non-seated compared to when seated.

Based on this body of evidence, it seems reasonable to suggest that the change in posture also alters the contractile conditions under which muscles generate and dissipate mechanical energy. Gathering evidence of the contractile conditions under which certain muscles produce work (Brennan et al. 2019) would provide important insights pertaining to the effects of posture on aerobic energy expenditure (Ryschon and Stray-Gundersen 1991), time to exhaustion (Hansen and Waldeland 2008), and maximal power output (Millet et al. 2002). We interpret our first key finding as preliminary evidence that the non-seated posture allows both force and power generated from muscular and non-muscular sources to be more effectively transferred across the knee joint and subsequently to the crank. However, the limitations inherent to inverse dynamics (Zajac, Neptune, and Kautz 2002) and surface electromyography (Enoka 2008) must be acknowledged when attempting to infer muscle function. Muscle-level analyses and modelling/simulation studies are required to provide more robust evidence of the function and mechanical work performed by bi-articular muscles during non-seated cycling.

6.1.2 When cycling at high-power output in a non-seated posture, raising and lowering the CoM during specific phases of the crank cycle can amplify crank power.

The second study in this thesis quantified the mechanical energy gained and lost by the rider's CoM during non-seated cycling at different power outputs and cadences. The key finding from this study was that, at high power outputs, the rate of mechanical energy transfer between the rider's CoM and the crank could be as high as $4.5 \text{ W}\cdot\text{kg}^{-1}$. Previous research had provided rudimentary evidence that the rider's CoM gains and loses height during each crank cycle, however, the associated changes in total mechanical energy had not been quantified. Previous research (Kautz and Neptune 2002) on seated cycling showed that segmental energy of the legs is transferred to the crank resulting in external work production. Our results extend on this work by providing evidence that the amount and rate of energy transfer between the rider's

CoM and the crank is much greater during non-seated cycling. Furthermore, it was found that the rider's CoM gains and loses greater amounts of energy in response to increasing power output and time per crank cycle. This suggests that riders utilise the available time per crank cycle to increase the total mechanical energy of the CoM prior to each downstroke. This increase in CoM height and total mechanical energy provides a greater potential to increase the inertia of the CoM during the downstroke, which can then contribute greater amounts of external work at the crank.

The results of this study provide impetus to further explore the effects of raising and lowering the CoM on the efficiency of cycling. For instance, not all energy lost by the CoM is necessarily transferred to the crank. It is possible that some of this energy is absorbed by muscle performing negative work or the storage of energy within passive-elastic structures. Any energy stored within lower-limb tendons could be returned later in the crank cycle to lift the rider's CoM at a reduced metabolic cost (Wilson and Lichtwark 2011; Uchida et al. 2016; Brennan et al. 2018). The limitations of our analysis mean that we can only speculate whether energy lost by the CoM is partitioned between the crank and elastic structures. Evidence of this mechanism requires further investigation through muscle-level analyses and modelling/simulation studies and remains a goal of future work.

6.1.3 When cycling at high-power output in a non-seated posture, leaning the bicycle allows a greater non-muscular contribution to crank force and power.

The third study in this thesis investigated the effect of constraining bicycle lean on limb mechanics and CoM movement during non-seated cycling. The study showed that self-restricting bicycle lean likely reduced the amount and rate of energy transferred between the rider's CoM and the crank compared to a condition where riders were able to lean the bicycle naturally or when the bicycle was physically constrained in a trainer. This result suggests that leaning the bicycle allows riders to maximize the non-muscular contribution to crank force and power. To the best of our knowledge, this is the first study to provide a comparison of non-seated cycling under preferred and self-restricted bicycle lean conditions.

Bicycle lean occurs due to an imbalance of torque around the bicycle's wheel-ground axis, hence, attempting to restrict bicycle lean requires the rider to reduce the magnitude of these imbalances. It has been suggested by some authors that leaning the bicycle has a negative effect on non-seated cycling efficiency and performance (Bouillod et al. 2018). However, our results show that attempting to self-restrict bicycle lean reduces the amount and rate of CoM energy gained and lost, peak vertical pedal force, and peak instantaneous power output. Thus, our results suggest that bicycle lean has a significant positive influence on the temporal nature of force and power production during non-seated cycling on rollers. It is important that future investigations are designed specifically to test the effect of bicycle lean under preferred and

self-restricted cycling conditions, rather than making inferences about the effect of bicycle lean when confounding variables are present.

There are some limitations to the current study that could be addressed in future work. Cycling rollers may not accurately represent bicycle dynamics in a performance environment (Dressel and Papadopoulos 2012), which means our results may not translate to treadmill cycling or over-ground cycling. Our study was also conducted on level ground, which may alter the preferred movement pattern of the rider and range of bicycle lean compared to cycling on a sloped treadmill or uphill. Comparing preferred and self-restricted bicycle lean conditions during over-ground cycling is warranted because subtle but important differences in task constraints may affect cycling biomechanics and performance.

At this time, the scope for collecting biomechanical data during over-ground cycling is limited by equipment. Inertial sensors are a potential solution to this problem (Pfau, Witte, and Wilson 2005), but still require more thorough validation against gold standard measurement systems. Our preliminary investigation of using a single IMU placed on the lower back of the rider to track CoM motion during non-seated cycling showed promising results (See draft manuscript in Appendix B). Our findings suggest that a single IMU can track the orientation and vertical displacement of an attached cluster of reflective markers with high accuracy and precision, however, the single-IMU method overestimates vertical CoM displacement; as this displacement increases, the overestimation error increases linearly. While these results highlight that the motion of body segments other than the torso have a significant effect on whole-body CoM movement, they also show that the discrepancy between IMU and CoM movement increases systematically. Further investigation is required to assess whether linear regression can be used to account for these discrepancies and to better understand the relationship between IMU and actual CoM movement.

6.2 Future work

6.2.1 Measuring CoM mechanics in ecologically valid conditions.

It is unclear whether our findings pertaining to CoM movement and the associated changes in mechanical energy can be extrapolated to field conditions. The presence of aerodynamic resistance may alter the preferred movement pattern of the rider because raising and lowering the CoM presumably changes frontal surface area and the flow of air around the rider. Thus, measuring CoM movement under ecologically valid conditions would provide important insights into the trade-off between the benefits of non-muscular power contributions and the separate costs of aerodynamic resistance, generating work to raise the CoM, and producing force to support bodyweight. The barrier to conducting this research lies in the difficulty of measuring CoM movement in the field. The typical equipment used to measure CoM movement in laboratory settings (e.g. motion capture, instrumented cranks, and force plates) is likely to be

inadequate for high-velocity cycling scenarios or require exorbitant resources.

Upon further validation, the single-IMU method investigated in Appendix B could be used to study the preferred movement pattern of cyclists during over-ground cycling. Other potential solutions for measuring CoM movement during over-ground cycling would be to measure total vertical force produced at the pedals and handlebar or to measure the total vertical force produced on the ground. There are strengths and limitations specific to each of these approaches. The IMU approach is extremely low cost (as little as \$10) compared to either instrumenting the pedals and handlebar of a bicycle or using a series of in-ground force plates. Although the in-ground force plates would not require anything to be attached to the rider, a single IMU is unlikely to affect the rider as it is small and lightweight (~ 12 grams). Instrumenting the pedals and handlebar of a bicycle would likely require an additional power source and recording device to be mounted to the bicycle. The IMU can also be used on any rider or any bicycle and is unrestricted by location. The instrumented-bicycle and instrumented-surface approaches are likely to be more accurate and precise than the single-IMU approach because they use first principles to solve for vertical CoM acceleration. However, bicycle lean and steering may introduce errors for the instrumented-bicycle approach, unless accelerometers are used in the frame and handlebar to detect the gravity vector. The commercial appeal of integrating a wearable IMU with existing cycling computer technology should also be considered as it may provide an opportunity to collect large datasets on cyclists in any location. The IMU could be used to determine when a cyclist is either seated or non-seated and then separate analysis of cadence and power output between the two postures. It could also be used to gather data on when an individual cyclist typically transitions to a non-seated posture, which could be used as a training dataset for supervised learning algorithms to provide guidance on when that cyclist should transition. A second IMU could also be attached to the bicycle to measure bicycle lean, which would provide insights into the relationship between CoM movement and bicycle lean. Applying this novel approach to understand the importance of bicycle lean and CoM movement on non-seated cycling biomechanics and performance remains a future goal.

6.2.2 Contributions of the upper body to power production at the cranks.

The findings from Chapter 4 and 5 suggest a key contribution of the upper body to power production at the crank, but further investigation is required to quantify upper-body power production and understand its relationship to maximal power output during non-seated cycling. Previous research has provided evidence that creating a pulling force on the handlebars can facilitate a 22% increase in maximal power output during seated cycling (Baker et al. 2002). This study compared maximal power output when riders either gripped the handlebar as normal or rested their hands on the handlebar; which prevented them from generating an upward force.

The limitation of this study is that neither vertical crank force or CoM movement was measured, meaning that it is difficult to infer whether pulling on the handlebar contributes additional power at the crank or merely prevents lower-body power being wasted on lifting the rider's CoM during the downstroke. It is also likely that the effect of pulling on the handlebar will be altered by cadence, power output, and posture. For instance, under low force conditions (i.e. high cadence, low power), there may little need for the arms to resist upward acceleration of the rider's CoM, thus, the contribution of upper-body power to crank power is likely reduced. Riders tend to transition to a non-seated posture under high force scenarios (i.e. low cadence, high power) and when doing so, they support a larger portion of bodyweight at the pedals, align their posture more vertically over the downstroke pedal, and use momentum of their body mass to generate greater peak vertical force and peak instantaneous crank power compared to when seated. Hence, the effect of pulling on the handlebar will depend on pedal force requirements and posture.

Our work predicts that removing the pulling action of the arms on the handlebar is likely to affect the accelerations and subsequent movement of the CoM. It is hard to predict exactly what might happen to the CoM movement under these circumstances, but the following predictions can be made: 1) if the forces at the cranks remain similar, then the rider's CoM would have to experience more motion, 2) there may be a reduction in crank force and power output because the CoM motion becomes unfavourable (or timing is incorrect), and 3) riders may adopt a different posture to maintain high crank force and power output, but presumably with less non-muscular contributions.

6.2.3 Non-muscular contributions to instantaneous crank power.

The findings in Chapter 4 and 5, show that riders can use momentum of their body mass to amplify instantaneous crank power during sub-maximal non-seated cycling, however, further research is required to confirm the presence and extent of this mechanism during maximal cycling sprints. Based on the presence of this mechanism, I theorise that it may be possible to increase maximal power output during non-seated cycling by adding additional mass to the rider. The muscles of the human body have adapted primarily to help us stand, walk, and run against force due to gravity, however, our potential for maximal power output is often not reached until additional mass is added to the body (Baker et al. 2002; Harris, Cronin, and Hopkins 2007). Previous research on resistance trained rugby-league players performing loaded squat jumps has shown that peak instantaneous power outputs of 4110 ± 570 W can be achieved by adding loads equivalent to 21.6% of maximal squat strength ($\sim 57\%$ of body mass) (Harris, Cronin, and Hopkins 2007). These results are in line with the theoretical upper limit of human power production (Wilkie 1960a).

Our work predicts that some additional torso mass may facilitate an increase in maximal power output during non-seated cycling, but too much additional mass may be detrimental. If a

rider's lower-limb muscles have a reserve amount of force generating capacity that is not being utilised under normal body mass conditions, then a certain amount of additional torso mass could enhance their maximal power output. The additional mass could facilitate an increase in maximal power output if it prevents upward accelerations of the rider's CoM during the downstroke or if the rider is able to generate enough force to move the additional mass with the same velocity as during normal body mass conditions. Thus, the optimal amount of additional mass will depend on the force generating capacity of the rider's legs. Too much additional mass may result in the rider being unable to generate enough force to move the mass, which would negate any benefits that CoM momentum may provide. It is also possible that additional mass may not affect maximal power output, which would suggest that the rider's lower-limb muscles are already operating at their maximum force generating capacity. This null effect of additional mass would point toward the pulling action of the arms at the handlebar as a mechanism for ensuring that the maximal force and power generating capacity of the lower-limb muscles is reached. Our understanding of the relationship between body mass, arm action, and maximal power output during non-seated cycling would be greatly enhanced by investigating a rider's maximal power output in response to a spectrum of reduced and additional body mass conditions.

6.2.4 The influence of bicycle lean and vertical CoM displacement on gross efficiency and maximal power output during non-seated cycling.

Further research is required to answer the question of whether leaning the bicycle and CoM movement directly affect climbing and sprint performance. The conditions used in Chapter 5 to investigate the effects of bicycle lean (preferred, self-restricted, and trainer) provided a necessary experimental design to answer this question, however there were some major limitations in the implementation; namely that the rollers we used were restrictive and likely didn't faithfully simulate real-world conditions. To increase the ecological validity of the experiment, it may be more practical to implement the preferred and self-restricted conditions on an inclined treadmill or during uphill cycling, rather than on rollers. To gain insights into climbing performance, expired-gas analysis could be used to measure gross efficiency while cyclists ride in a non-seated posture at an aerobic intensity during preferred and self-restricted conditions. Bicycle lean and CoM movement could be assessed using either motion capture, crank force, or IMUs, to confirm the differences in bicycle lean and CoM movement between the conditions and provide further evidence of their relationship. It may also be useful to request that riders change the magnitude of bicycle lean to more directly determine whether there is an optimal strategy. Such a study would increase our understanding of the optimal bicycle lean and CoM movement strategies during uphill cycling in a non-seated posture.

A similar experimental paradigm could be implemented to understand the influence of

bicycle lean and CoM movement on maximal power output during non-seated cycling. The preferred and self-restricted conditions in this case could be conducted in a laboratory or over ground. The laboratory setting has the potential to provide a more controlled comparison of the preferred and self-restricted conditions to a trainer condition, through the use of a single ergometer which can be adjusted to either allow or constrain bicycle lean. I plan to build this device because, to the best of my knowledge, one does not exist. The ergometer would require a hinged platform to allow the ergometer to lean from side to side and a spring-like mechanism to provide a restoring force proportional to the lean angle. This design would provide a suitable replication of the lateral dynamics of a bicycle, which can be reduced to the equations of motion of an under-damped simple harmonic oscillator. This device could be validated by comparing maximal power output to that achieved during over-ground conditions, however, this comparison may be confounded by the difference in aerodynamic resistance between the two settings. Nevertheless, the comparison of preferred and self-restricted conditions in either a laboratory or outdoor environment would provide valuable insights into the optimal bicycle lean and CoM movement strategies for achieving maximal power output and maximal velocity while sprinting in a non-seated posture.

6.2.5 The influence of bicycle lean and vertical CoM displacement on muscle function and mechanical work.

The major limitation of the methodologies used in this thesis is the lack of inference that can be drawn regarding muscle function and muscular work. Inverse dynamic analysis does not provide any indication of the role of individual muscles during movement due to the action of biarticular muscles and the storage and return of elastic energy (Zajac, Neptune, and Kautz 2002). Besides *in vivo* and *in situ* techniques, this type of insight regarding the contribution of individual muscles to multi-joint human movements can only be achieved through simulations derived from muscle-based dynamical models of the body. For example, simulations of seated cycling that replicate the kinematics, kinetics, and EMG activity have been used to understand the role of individual muscles in accelerating segments, redistributing segmental energy, and delivering energy to the cranks (Neptune and Bogert 1998; Martin and Nichols 2018). These simulation-based studies have provided evidence of causal relationships between the measured kinematics, kinetic, and EMG activity during seated cycling and are therefore the best approach for furthering our understanding of non-seated cycling biomechanics. The challenge in simulating non-seated cycling is the additional degrees of freedom of the movement compared to when seated, however, similar muscle-driven modelling approaches have been successfully applied to complex movements such as walking (Neptune, Zajac, and Kautz 2004) and running (Hamner and Delp 2013).

Modern imaging techniques, such as magnetic resonance imaging and ultrasonography, have provided unprecedented knowledge on the structure and function of individual muscles and

tendons in vivo during complex movements, but have yet been applied to non-seated cycling. Previous research has implemented B-mode ultrasound to measure the effects of workload and cadence on knee-extensor and ankle plantar flexor muscle fascicle dynamics during seated cycling (Brennan et al. 2019; Dick, Biewener, and Wakeling 2017). Brennan et al. (2019) showed that although cadence did not influence the distribution of lower-limb joint power during constant-power seated cycling, it did affect vastus lateralis fascicle shortening velocities and operating lengths; leading to important differences in muscle efficiency and muscle power capacity. Integration of this information with our results showing that CoM mechanical energy fluctuations increase in response to power output and time per crank cycle, provides a reasonable basis to expect that the efficiency and power capacity of individual muscles could be altered by the transition to a non-seated posture during cycling. Investigating the differences in contractile dynamics at an individual muscle level between seated and non-seated cycling remains a future goal, as these differences likely dictate the preferred movement strategy of riders and are extremely relevant for cycling performance.

6.3 Potential Translation of Work and Thesis Reflections

There are many practical applications of the work in this thesis for rider and bicycle performance. Riders can utilise the knowledge that raising and lowering their CoM while standing may be an optimal strategy for producing maximal impulse and power on the crank. First, finding postures and movement patterns that optimise the trade-off between non-muscular power contribution and aerodynamic drag would allow riders to achieve the highest possible average and peak velocities during climbing and sprints. Second, riders can interpret our findings as evidence that leaning the bicycle is a beneficial strategy, or at least not a detrimental strategy, for increasing non-seated cycling performance. Leaning the bicycle allows a greater contribution from non-muscular sources to crank impulse and power. Equipment manufacturers can use this knowledge to understand how shifting from a seated to non-seated posture is likely to affect stresses experienced by different components of the bicycle and how shifting the CoM position is likely to affect vehicle dynamics.

The work in this thesis also has a role in better understanding how the body optimises movement to meet task demands (i.e. increasing gross efficiency or maximal power output). These insights have the potential to contribute to robotic and prosthetic design and help find solutions for neurological conditions where control is hindered. For example, this work has provided valuable information regarding the mechanical requirements of individual joints within the lower limb during non-seated cycling. This information could be used to design orthotic and prosthetic devices that maximise power output during non-seated cycling. Our results have also shown that the mechanical requirements at an individual joint level differ markedly between seated and non-seated cycling, which may provide the impetus for creating orthoses and prostheses that are either specifically designed for non-seated cycling or can be tuned for a

given riding posture.

Reflecting on upon my candidature, I am grateful to have progressed from a know-it-all bicycle shop manager to someone who is willing to admit they know very little about a subject area. As a recreational cyclist, my anecdotal understanding of why I adopted a non-seated posture and leaned the bicycle from side to side was both an opportunity and a threat to my research. At the start of my candidature I was quick to develop and proclaim universal theories of why people transitioned off the saddle and why they leaned the bicycle. Nowadays, these ideas go into a notebook of possible future studies; often being crossed off the list after further critical thought. I have come to recognise that my eagerness to confidently answer problems without sufficient evidence was bred out of insecurity. My initial expectations that completing a PhD would be the hardest thing I have ever done were not wrong. However, it was not my perceived lack of intelligence that was the major source of difficulty, but rather the ability to persevere through the days of confusion, technical problems, and seemingly endless revisions. At first, it can be scary to admit that we know very little about our own research topic, but eventually the ability to admit when we don't know something becomes empowering. Having the analytical skills to differentiate between evidence and speculation and acknowledging that gathering thorough evidence takes time has helped me to develop confidence and curiosity. I now recognise the complexities of human movement and acknowledge the amount of work that is still required to better understand the control and mechanics of non-seated cycling.

After reviewing cycling literature over the last four years, it is evident that many biomechanical aspects of seated cycling that have been investigated remain unresolved for the non-seated posture. For instance, many cyclists know that the non-seated posture used during uphill climbs is very different from that used during sprints on level terrain. Yet, there is limited evidence regarding preferred movement patterns during non-seated cycling when the nature and motivation of the task vary. The biomechanical difference between these two non-seated techniques could be just as varied, if not more so, than that seen between endurance and time trial seated techniques. The geometry of endurance road bicycles and time trial bicycles are markedly different; thus, it seems reasonable to suggest that bicycles could be designed specifically to enhance either climbing or sprinting performance in a non-seated posture.

During the initial stages of my candidature, I was often drawn to the intrigue and speculation surrounding the mechanism that may trigger the transition from a seated to a non-seated posture. The intrigue and speculation regarding this topic remain, but one must recognise that it may be extremely difficult to generalise a study's findings outside of the exact conditions tested. In this case, I believe my personal experience of transitioning off the saddle merely due to saddle soreness serves as a helpful reminder that there are many unpredictable factors that may determine a rider's choice of posture. Nevertheless, it may still be useful to use the experimental paradigm of eliciting a transition response to understand why a non-seated posture becomes preferable under different task demands.

I believe that future biomechanical research can play a large role in improving non-seated

cycling performance. It is encouraging to see recent evidence showing that cycling equipment which was deemed to have no effect on steady-state seated cycling (Straw and Kram 2016) can increase maximal power output in a non-seated posture (Burns and Kram 2020). These findings provide support for revisiting other cycling equipment to understand their effects on maximal power output in a non-seated posture. Thus, many exciting opportunities exist for future work into the biomechanics of non-seated cycling and the effects of bicycle lean, which will not only inform the refinement of cycling training and techniques, but potentially lead to the re-introduction of existing technology and new innovations in equipment design.

A final word on the phenomenon of non-seated cycling: for many of us, cycling in a non-seated posture is instinctive, however, given the relative novelty of the task in terms of the evolution of human movement, it is amazing that the dynamics of the human body and the bicycle can interact so elegantly to generate power output effectively and efficiently.

Bibliography

- Alexander, R. McNeill. 1991. Energy-saving mechanisms in walking and running. *The Journal of experimental biology* 160:55–69.
- Anderson, Dennis E., Michael L. Madigan, and Maury A. Nussbaum. 2007. Maximum voluntary joint torque as a function of joint angle and angular velocity: Model development and application to the lower limb. *Journal of Biomechanics* 40 (14): 3105–3113. doi:10.1016/j.jbiomech.2007.03.022.
- Ansley, Les, and Patrick Cangley. 2009. Determinants of “optimal” cadence during cycling. *European Journal of Sport Science* 9 (2): 61–85. ISSN: 1746-1391. doi:10.1080/17461390802684325.
- Astrand, Per-Olof, Kaare Rodahl, Hans A. Dahl, and Sigmund B. Stromme. 2003. *Textbook of work physiology : physiological bases of exercise* [in eng]. 4th ed.. Champaign, IL: Human Kinetics.
- Bakeman, Roger. 2005. Recommended effect size statistics for repeated measures designs. *Behavior Research Methods* 37 (3): 379–384. doi:10.3758/BF03192707.
- Baker, Julien S., Edward Brown, Gary Hill, Glen Phillips, Russell Williams, and Bruce Davies. 2002. Handgrip contribution to lactate production and leg power during high-intensity exercise. *Medicine and Science in Sports and Exercise* 34 (6): 1037–1040. doi:10.1097/00005768-200206000-00021.
- Barclay, C. J., J. K. Constable, and C. L. Gibbs. 1993. Energetics of fast- and slow-twitch muscles of the mouse. *The Journal of Physiology* 472 (1): 61–80. ISSN: 14697793. doi:10.1113/jphysiol.1993.sp019937.
- Barratt, Paul R., James C. Martin, Steven J. Elmer, and Thomas Korff. 2016. Effects of pedal speed and crank length on pedaling mechanics during submaximal cycling. *Medicine and Science in Sports and Exercise* 48 (4): 705–713. doi:10.1249/MSS.0000000000000817.
- Biewener, Andrew A. 1989. Scaling body support in mammals: limb posture and muscle mechanics. *Science* 245, no. 4913 (July): 45–8.

- Biewener, Andrew A., Claire T. Farley, Thomas J. Roberts, and Marco Temaner. 2004. Muscle mechanical advantage of human walking and running: implications for energy cost. *Journal of Applied Physiology* 97, no. 6 (December): 2266–2274.
- Bini, Rodrigo Rico, Patria A. Hume, and James L. Croft. 2011. Effects of bicycle saddle height on knee injury risk and cycling performance. *Sports Medicine* 41 (6): 463–476. ISSN: 01121642. doi:10.2165/11588740-00000000-00000.
- Bini, Rodrigo Rico, Patria a. Hume, and Andrew E. Kilding. 2014. Saddle height effects on pedal forces, joint mechanical work and kinematics of cyclists and triathletes. *European Journal of Sport Science* 14 (1): 44–52. doi:10.1080/17461391.2012.725105.
- Bland, J. Martin, and Douglas G. Altman. 1999. Measuring agreement in method comparison studies. *Statistical Methods in Medical Research* 8:135–160. ISSN: 02776715. doi:10.1002/sim.5955.
- . 2007. Agreement between methods of measurement with multiple observations per individual. *Journal of Biopharmaceutical Statistics* 17 (4): 571–582. ISSN: 10543406. doi:10.1080/10543400701329422.
- Bouillod, Anthony, Julien Pinot, Aurélien Valade, Johan Cassirame, Georges Soto-Romero, and Frédéric Grappe. 2018. Influence of standing position on mechanical and energy costs in uphill cycling. *Journal of Biomechanics* 72:99–105. doi:10.1016/j.jbiomech.2018.02.034.
- Brennan, Scott F., Andrew G. Cresswell, Dominic J. Farris, and Glen A. Lichtwark. 2018. The Effect of Cadence on the Mechanics and Energetics of Constant Power Cycling. *Medicine & Science in Sports & Exercise*, no. 6: 1.
- . 2019. The Effect of Cadence on the Mechanics and Energetics of Constant Power Cycling. *Medicine and Science in Sports and Exercise* 51 (5): 941–950.
- Burns, Andrew C., and Rodger Kram. 2020. The effect of cycling shoes and the shoe-pedal interface on maximal mechanical power output during outdoor sprints. *Footwear Science*: 1–8. ISSN: 1942-4280. doi:10.1080/19424280.2020.1769201. <https://doi.org/10.1080/19424280.2020.1769201>.
- Cain, Stephen M., James A. Ashton-Miller, and Noel C. Perkins. 2016. On the skill of balancing while riding a bicycle. *PLoS ONE* 11 (2): 1–18.
- Caldwell, Graham E., James M. Hagberg, Steve D. McCole, and Li Li. 1999. Lower extremity joint moments during uphill cycling. *Journal of Applied Biomechanics* 15 (2): 166–181. doi:10.1123/jab.15.2.166.

- Caldwell, Graham E., Li Li, Steve D. McCole, and James M. Hagberg. 1998. Pedal and crank kinetics in uphill cycling. *Journal of Applied Biomechanics* 14 (3): 245–259.
- Cavagna, Giovanni A. 2017. *Physiological Aspects of Legged Terrestrial Locomotion: The Motor and the Machine*. Cham, Switzerland: Springer International Publishing. doi:10.1007/978-3-319-49980-2.
- Cavagna, Giovanni A., F. P. Saibene, and Rodolfo Margaria. 1963. External work in walking. *Journal of Applied Physiology* 18:1–9.
- Cavagna, Giovanni A., Franco P. Saibene, and Rodolfo Margaria. 1964. Mechanical work in running. *Journal of Applied Physiology* 19, no. 2 (March): 249–256.
- Chang, Y.-H., H W Huang, C M Hamerski, and Rodger Kram. 2000. The independent effects of gravity and inertia on running mechanics. *Journal of Experimental Biology* 203 (Pt 2): 229–38. doi:10.1016/0021-9290(80)90019-6. <http://www.ncbi.nlm.nih.gov/pubmed/10607533>.
- Chavarren, J., and J. A.L. Calbet. 1999. Cycling efficiency and pedalling frequency in road cyclists. *European Journal of Applied Physiology and Occupational Physiology* 80 (6): 555–563. ISSN: 03015548. doi:10.1007/s004210050634.
- Coast, J R, and H G Welch. 1985. Linear increase in optimal pedal rate with increased power output in cycle ergometry. [In eng]. *European journal of applied physiology and occupational physiology* 53 (4): 339–342. ISSN: 0301-5548 (Print). doi:10.1007/bf00422850.
- Colquhoun, D., and C. Longstaff. *False positive risk calculator*. <http://fpr-calc.ucl.ac.uk/>.
- Connick, Mark J., and François Xavier Li. 2013. The impact of altered task mechanics on timing and duration of eccentric bi-articular muscle contractions during cycling. *Journal of Electromyography and Kinesiology* 23 (1): 223–229. ISSN: 10506411. doi:10.1016/j.jelekin.2012.08.012. <http://dx.doi.org/10.1016/j.jelekin.2012.08.012>.
- Costes, Antony, Nicolas A. Turpin, David Villegier, Pierre Moretto, and Bruno Watier. 2015. A reduction of the saddle vertical force triggers the sit-stand transition in cycling. *Journal of Biomechanics* 48 (12): 2998–3003. doi:10.1016/j.jbiomech.2015.07.035.
- Day, James T., Glen Anthony Lichtwark, and Andrew G. Cresswell. 2013. Tibialis anterior muscle fascicle dynamics adequately represent postural sway during standing balance. *Journal of Applied Physiology* 115 (12): 1742–1750. ISSN: 8750-7587, 1522-1601. doi:10.1152/japplphysiol.00517.2013. <http://www.ncbi.nlm.nih.gov/pubmed/24136108>.

- Delp, Scott L., Frank Clayton Anderson, Allison S Arnold, Peter Loan, Ayman Habib, Chand T John, Eran Guendelman, and Darryl G Thelen. 2007. OpenSim: Open source to create and analyze dynamic simulations of movement. *IEEE transactions on bio-medical engineering* 54 (11): 1940–1950. doi:10.1109/TBME.2007.901024.
- Dick, Taylor J.M., Andrew A. Biewener, and James M. Wakeling. 2017. Comparison of human gastrocnemius forces predicted by Hill-type muscle models and estimated from ultrasound images. *Journal of Experimental Biology* 220 (9): 1643–1653. doi:10.1242/jeb.154807.
- Dong, O., C. Graham, A. Grewal, C. Parrucci, and Andy Ruina. 2014. The bricycle: A bicycle in zero gravity can be balanced or steered but not both. *Vehicle System Dynamics* 52 (12): 1681–1694. ISSN: 17445159. doi:10.1080/00423114.2014.956126.
- Doré, Eric, Julian S. Baker, Alban Jammes, Mike Graham, Karl New, and Emmanuel Van Praagh. 2006. Upper body contribution during leg cycling peak power in teenage boys and girls. *Research in Sports Medicine* 14 (4): 245–57. ISSN: 1543-8627.
- Dorel, Sylvain. 2018a. Maximal Force-Velocity and Power-Velocity Characteristics in Cycling: Assessment and Relevance. In *Biomechanics of training and testing: innovative concepts and simple field methods*, edited by Jean-Benoit Morin and Pierre Samozino, 7–31. Springer International Publishing. doi:10.1007/978-3-319-05633-3_2.
- . 2018b. Mechanical Effectiveness and Coordination: New Insights into Sprint Cycling Performance. In *Biomechanics of training and testing: innovative concepts and simple field methods*, edited by Jean-Benoit Morin and Pierre Samozino, 33–62. Springer International Publishing.
- Dorel, Sylvain, Christophe A. Hautier, O. Rambaud, David M. Rouffet, Emmanuel Van Praagh, J. R. Lacour, and M. Bourdin. 2005. Torque and Power-Velocity Relationships in Cycling: Relevance to Track Sprint Performance in World-Class Cyclists. *International Journal of Sports Medicine* 26 (9): 739–746.
- Dressel, Andrew, and Jim M. Papadopoulos. 2012. Comment on 'On the stability of a bicycle on rollers'. *European Journal of Physics* 33 (4).
- Duc, Sébastien, William M. Bertucci, J. N. Pernin, and Frédéric Grappe. 2008. Muscular activity during uphill cycling: Effect of slope, posture, hand grip position and constrained bicycle lateral sways. *Journal of Electromyography and Kinesiology* 18 (1): 116–127. doi:10.1016/j.jelekin.2006.09.007.
- Elmer, Steven J., Paul R. Barratt, Thomas Korff, and James C. Martin. 2011. Joint-specific power production during submaximal and maximal cycling. *Medicine and Science in Sports and Exercise* 43 (10): 1940–1947. doi:10.1249/MSS.0b013e31821b00c5.

- Eng, J J, and D A Winter. 1993. Estimations of the horizontal displacement of the total body centre of mass: considerations during standing activities. *Gait & Posture* 1:141–144.
- Enoka, Roger M. 2008. *Neuromechanics of human movement*. 4th Ed. Champaign, IL: Human Kinetics.
- Enoka, Roger M., and Jacques Duchateau. 2019. Muscle Function: Strength, Speed, and Fatigability. Chap. 7 in *Muscle and exercise physiology*, 129–158. Elsevier Inc. doi:10.1016/B978-0-12-814593-7.00007-4. <http://dx.doi.org/10.1016/B978-0-12-814593-7.00007-4>.
- Ericson, Mats O., åke Bratt, Ralph Nisell, Ulf P. Arborelius, and Jan Ekholm. 1986a. Power output and work in different muscle groups during ergometer cycling. *European Journal of Applied Physiology and Occupational Physiology* 55 (3): 229–235. ISSN: 03015548. doi:10.1007/BF02343792.
- . 1986b. Power output and work in different muscle groups during ergometer cycling. *European Journal of Applied Physiology and Occupational Physiology* 55 (3): 229–235. ISSN: 03015548. doi:10.1007/BF02343792.
- Esser, Patrick, Helen Dawes, Johnny Collett, and Ken Howells. 2009. IMU: Inertial sensing of vertical CoM movement. *Journal of Biomechanics* 42 (10): 1578–1581. ISSN: 00219290. doi:10.1016/j.jbiomech.2009.03.049.
- Faria, Erik W., Daryl L. Parker, and Irvin E. Faria. 2005. The science of cycling: factors affecting performance - part 2. *Sports Medicine* 35 (4): 313–337.
- Fonda, Borut, and Nejc Sarabon. 2012. Biomechanics and energetics of uphill cycling: A review. *Kinesiology* 44 (1): 5–17. ISSN: 13311441. <http://www.scopus.com/inward/record.url?eid=2-s2.0-84865245088%7B%5C%7DpartnerID=tZOTx3y1>.
- Fregly, Benjamin J., Felix E. Zajac, and Christine A. Dairaghi. 1996. Crank inertial load has little effect on steady-state pedaling coordination. *Journal of Biomechanics* 29 (12): 1559–1567. ISSN: 00219290.
- Galantis, Apostolos, and Roger C. Woledge. 2003. The theoretical limits to the power output of a muscle-tendon complex with inertial and gravitational loads. *Proceedings of the Royal Society B: Biological Sciences* 270 (1523): 1493–1498. doi:10.1098/rspb.2003.2403.
- Galilei, Galileo. 1967. *Dialogue concerning the two chief world systems, ptolemaic copernican* [in English]. 2d. Berkeley: University of California Press.
- Gardner, A. Scott, James C. Martin, David T. Martin, Martin Barras, and David G. Jenkins. 2007. Maximal torque- and power-pedaling rate relationships for elite sprint cyclists in laboratory and field tests. *European Journal of Applied Physiology* 101 (3): 287–292.

- Gordon, Keith E., Daniel P. Ferris, and Arthur D. Kuo. 2009. Metabolic and Mechanical Energy Costs of Reducing Vertical Center of Mass Movement During Gait. *Archives of Physical Medicine and Rehabilitation* 90 (1): 136–144. ISSN: 00039993. <http://dx.doi.org/10.1016/j.apmr.2008.07.014>.
- Gottschall, Jinger S., and Rodger Kram. 2005. Energy cost and muscular activity required for leg swing during walking. *Journal of Applied Physiology* 99 (1): 23–30. ISSN: 87507587. doi:10.1152/japplphysiol.01190.2004.
- Gregor, Robert J., Peter R. Cavanagh, and M. A. Lafontaine. 1985. Knee flexor moment during propulsion in cycling - a creative solution to Lombard's Paradox. *Journal of Biomechanics* 18 (5): 307–316.
- Gregor, Robert J., and W Lee Childers. 2011. Neuromechanics of the Cycling Task. Chap. 4 in *Neuromuscular aspects of sport performance*, XVII, 52–77. Blackwell Publishing Ltd.
- Hamner, Samuel R., and Scott L. Delp. 2013. Muscle contributions to fore-aft and vertical body mass center accelerations over a range of running speeds. *Journal of Biomechanics* 46 (4): 780–787. doi:10.1016/j.jbiomech.2012.11.024. arXiv: NIHMS150003. <http://dx.doi.org/10.1016/j.jbiomech.2012.11.024>.
- Hansen, Ernst Albin, and Harry Waldegaard. 2008. Seated versus standing position for maximization of performance during intense uphill cycling. *Journal of Sports Sciences* 26 (9): 977–984. doi:10.1080/02640410801910277.
- Harnish, Chris, Deborah King, and Tom Swensen. 2007. Effect of cycling position on oxygen uptake and preferred cadence in trained cyclists during hill climbing at various power outputs. *European Journal of Applied Physiology* 99 (4): 387–391. doi:10.1007/s00421-006-0358-7.
- Harris, Nigel K., John B. Cronin, and Will G. Hopkins. 2007. Power outputs of a machine squat-jump across a spectrum of loads. *Journal of Strength and Conditioning Research* 21 (4): 1260–1264. ISSN: 10648011. doi:10.1519/R-21316.1.
- Harrison, J. Y. 1970. Maximizing Human Power Output by Suitable Selection of Motion Cycle and Load. *Human Factors: The Journal of Human Factors and Ergonomics Society* 12 (3): 315–329. ISSN: 15478181. doi:10.1177/001872087001200308.
- Hayot, Chris, Arnaud Decatoire, Julien Bernard, Tony Monnet, and Patrick Lacouture. 2012. Effects of 'posture length' on joint power in cycling. *Procedia Engineering* 34:212–217.
- Herzog, Walter, Evelyne Hasler, and Sheila K. Abrahamse. 1991. A comparison of knee extensor strength curves obtained theoretically and experimentally. *Medicine & Science in Sports & Exercise* 23 (1): 108–114.

- Hicks, Jennifer L, Thomas K Uchida, Ajay Seth, and Scott L Delp. 2015. Is My Model Good Enough? Best Practices for Verification and Validation of Musculoskeletal Models and Simulations of Movement. *Journal of Biomechanical Engineering* 137 (February): 1–24. doi:10.1115/1.4029304.
- Hill, A. V. 1922. The maximum work and mechanical efficiency of human muscles, and their most economical speed. *Journal of physiology* 14 (56): 19–41.
- Hof, A.L., M. G J Gazendam, and W. E. Sinke. 2005. The condition for dynamic stability. *Journal of Biomechanics* 38 (1): 1–8. doi:10.1016/j.jbiomech.2004.03.025.
- Hug, François, and Sylvain Dorel. 2009. Electromyographic analysis of pedaling: A review. *Journal of Electromyography and Kinesiology* 19 (2): 182–198. ISSN: 10506411. doi:10.1016/j.jelekin.2007.10.010.
- Hug, François, Nicolas A. Turpin, Antoine Couturier, and Sylvain Dorel. 2011. Consistency of muscle synergies during pedaling across different mechanical constraints. *Journal of neurophysiology* 106 (1): 91–103. ISSN: 0022-3077. doi:10.1152/jn.01096.2010.
- Hull, Maury L., Andrew Beard, and Hemant Varma. 1990. Goniometric measurement of hip motion in cycling while standing. *Journal of Biomechanics* 23 (7): 687–703.
- Jones, David E H. 1970. The stability of the bicycle. *Physics Today* 23 (4): 34–40.
- Kautz, Steven A., and Maury L. Hull. 1993. A theoretical basis for interpreting the force applied to the pedal in cycling. *Journal of Biomechanics* 26 (2): 155–165.
- Kautz, Steven A., and Richard R. Neptune. 2002. Biomechanical determinants of pedaling energetics: internal and external work are not independent. *Exercise and sport sciences reviews* 30 (4): 159–65. ISSN: 0091-6331. doi:10.1097/00003677-200210000-00004. <http://www.ncbi.nlm.nih.gov/pubmed/12398112>.
- Kipp, Shalaya, Alena M. Grabowski, and Rodger Kram. 2018. What determines the metabolic cost of human running across a wide range of velocities? *The Journal of Experimental Biology* 221 (18): jeb184218. doi:10.1242/jeb.184218.
- Kooijman, J. D.G., and A. L. Schwab. 2009. Experimental Validation of the Lateral Dynamics of a Bicycle on a Treadmill. In *Asme*, 2029–2034. doi:10.1115/DETC2009-86965.
- Kram, Rodger, and Terence J. Dawson. 1998. Energetics and biomechanics of locomotion by red kangaroos (*Macropus rufus*). *Comparative Biochemistry and Physiology - B Biochemistry and Molecular Biology* 120 (1): 41–49.
- Kram, Rodger, and C R Taylor. 1990. Energetics of Running. *Nature* 346:265. doi:10.1017/CBO9781107415324.004.

- Kristianslund, Eirik, Tron Krosshaug, and Antonie J. Van den Bogert. 2012. Effect of low pass filtering on joint moments from inverse dynamics: Implications for injury prevention. *Journal of Biomechanics* 45 (4): 666–671. doi:10.1016/j.jbiomech.2011.12.011.
- Kuo, Arthur D. 2001. THE ACTION OF TWO-JOINT MUSCLES: THE LEGACY OF W. P. LOMBARD. Chap. 10 in *Classics in movement science*, 1st ed., edited by Mark L. Latash and Vladimir M. Zatsiorsky, 289–315. Human Kinetics Publishers Inc.
- Lakens, Daniel. 2013. Calculating and reporting effect sizes to facilitate cumulative science: A practical primer for t-tests and ANOVAs. *Frontiers in Psychology* 4 (NOV): 1–12. doi:10.3389/fpsyg.2013.00863.
- Leys, Christophe, Olivier Klein, Philippe Bernard, and Laurent Licata. 2013. Detecting outliers: Do not use standard deviation around the mean, use absolute deviation around the median. *Journal of Experimental Social Psychology* 49 (4): 764–766. ISSN: 00221031.
- Li, Li, and Graham E. Caldwell. 1998. Muscle coordination in cycling : effect of surface incline and posture. *Journal of Applied Physiology* 85 (3): 927–934.
- Lichtwark, Glen A., and Alan M. Wilson. 2005. Effects of series elasticity and activation conditions on muscle power output and efficiency. *Journal of Experimental Biology* 208 (15): 2845–2853. doi:10.1242/jeb.01710.
- Lieber, Richard L., and S C Bodine-Fowler. 1993. Skeletal muscle mechanics: implications for rehabilitation. *Physical Therapy* 73 (12): 844–56.
- Lieber, Richard L., and Samuel R. Ward. 2011. Skeletal muscle design to meet functional demands. *Philosophical Transactions of the Royal Society B: Biological Sciences* 366:1466–1476.
- Lintmeijer, Lotte L., Gert S. Faber, Hessel R. Kruk, A. J.Knoek van Soest, and Mathijs J. Hofmijster. 2018. An accurate estimation of the horizontal acceleration of a rower's centre of mass using inertial sensors: a validation. *European Journal of Sport Science* 18 (7): 940–946. ISSN: 15367290. doi:10.1080/17461391.2018.1465126.
- Loeb, G. E. 1995. Control implications of musculoskeletal mechanics. *Annual International Conference of the IEEE Engineering in Medicine and Biology - Proceedings* 17 (2): 1393–1394.
- Loram, Ian D., Constantinos N. Maganaris, and Martin Lakie. 2004. Paradoxical muscle movement in human standing. *Journal of Physiology* 556 (3): 683–689. ISSN: 00223751. doi:10.1113/jphysiol.2004.062398.

- Lucia, Alejandro, Conrad Ernest, and Carlos Arribas. 2003. The Tour de France: a physiological review. *Scandinavian Journal of Science and Medicine in Sports* 13:275–283.
- Lucia, Alejandro, J. Hoyos, and J. L. Chicharro. 2001. Preferred pedalling cadence in professional cycling. *Medicine and Science in Sports and Exercise* 33 (8): 1361–1366.
- MacIntosh, Brian R., Richard R. Neptune, and John F Horton. 2000. Cadence, power, and muscle activation in cycle ergometry. *Medicine and Science in Sports and Exercise* 32 (7): 1281–1287.
- Madgwick, Sebastian O.H., Andrew J.L. Harrison, and Ravi Vaidyanathan. 2011. Estimation of IMU and MARG orientation using a gradient descent algorithm. *IEEE International Conference on Rehabilitation Robotics*: 1–7. ISSN: 19457898. doi:10.1109/ICORR.2011.5975346.
- Margaria, Rodolfo. 1968. Positive and negative work performances and their efficiencies in human locomotion. *Internationale Zeitschrift für Angewandte Physiologie Einschließlich Arbeitsphysiologie* 25 (4): 339–351. doi:10.1007/BF00699624.
- Marsh, Anthony P., and Philip E. Martin. 1993. The association between cycling experience and preferred and most economical cadences. *Medicine and Science in Sports and Exercise* 25 (11): 1269–1274.
- Marsh, Anthony P., Philip E. Martin, and David J. Sanderson. 2000. Is a joint moment-based cost function associated with preferred cycling cadence? *Journal of Biomechanics* 33 (2): 173–180. ISSN: 00219290.
- Martin, James C., and Nicholas A. T. Brown. 2009. Joint-specific power production and fatigue during maximal cycling. *Journal of Biomechanics* 42:474–479. doi:10.1016/j.jbiomech.2008.11.015.
- Martin, James C., Douglas L. Milliken, John E. Cobb, Kevin L. McFadden, and Andrew R. Coggan. 1998. Validation of a mathematical model for road cycling power. *Journal of Applied Biomechanics* 14:276–291.
- Martin, James C., and Jennifer A. Nichols. 2018. Simulated work loops predict maximal human cycling power. *The Journal of Experimental Biology* 221 (13). doi:10.1242/jeb.180109. <http://jeb.biologists.org/lookup/doi/10.1242/jeb.180109>.
- McCartney, N., G. J.F. Heigenhauser, and N. L. Jones. 1983. Power output and fatigue of human muscle in maximal cycling exercise. *Journal of Applied Physiology Respiratory Environmental and Exercise Physiology* 55 (1 I): 218–224. ISSN: 01617567.

- McDaniel, John, N Scott Behjani, Steven J. Elmer, Nicholas A. T. Brown, and James C. Martin. 2014. Joint-Specific Power-Pedaling Rate Relationships During Maximal Cycling. *Journal of Applied Biomechanics* 30 (3): 423–430. doi:10.1123/jab.2013-0246.
- McLester, John R, James M Green, and Jeremy L Chouinard. 2004. Effects of standing vs. seated posture on repeated wingate performance. *Journal of Strength and Conditioning Research* 18 (4): 816–820.
- McMahon, Thomas A., Gordon Valiant, and Edward C. Frederick. 1987. Groucho running. *Journal of Applied Physiology* 62 (6): 2326–2337.
- Meijaard, J. P., Jim M. Papadopoulos, Andy Ruina, Schwab A.L., and A. L. Schwab. 2007. Linearized dynamics equations for the balance and steer of a bicycle: A benchmark and review. *Proceedings of the Royal Society A: Mathematical, Physical and Engineering Sciences* 463 (2084): 1955–1982. doi:10.1098/rspa.2007.1857.
- Merkes, Paul F.J., Paolo Menaspà, and Chris R. Abbiss. 2020. Power output, cadence, and torque are similar between the forward standing and traditional sprint cycling positions. *Scandinavian Journal of Medicine and Science in Sports* 30:64–73. ISSN: 16000838.
- Millet, Grégoire P, Cyrille Tronche, Nicolas Fuster, and Robin Candau. 2002. Level ground and uphill cycling efficiency in seated and standing positions. *Medicine and Science in Sports and Exercise* 34 (10): 1645–1652. doi:10.1249/01.MSS.0000031482.14781.D7.
- Müller, Wolfram, and Peter Hofmann. 2008. Performanc factors in bicycling: Human power, drag, and rolling resistance. *Sport Aerodynamics: CISM Courses and Lectures* 506:49–91. doi:10.1007/978-3-211-89297-8.
- Neptune, Richard R., and Ton van den Bogert. 1998. Standard mechanical energy analyses do not correlate with muscle work in cycling. *Journal of Biomechanics* 31:239–245.
- Neptune, Richard R., and Walter Herzog. 2000. Adaptation of muscle coordination to altered task mechanics during steady-state cycling. *Journal of Biomechanics* 33:165–172.
- Neptune, Richard R., Felix E. Zajac, and Steven A. Kautz. 2004. Muscle mechanical work requirements during normal walking: The energetic cost of raising the body's center-of-mass is significant. *Journal of Biomechanics* 37 (6): 817–825. doi:10.1016/j.jbiomech.2003.11.001.
- Nickleberry, Ben L., and George A. Brooks. 1996. No effect of cycling experience on leg cycle ergometer efficiency. *Medicine and Science in Sports and Exercise* 28 (11): 1396–1401. ISSN: 01959131.

- Nordeen-Snyder, Katherine S. 1977. The effect of bicycle seat height variation upon oxygen consumption and lower limb kinematics. *Medicine and Science in Sports and Exercise* 9 (2): 113–117.
- Pfau, Thilo, Andrew Spence, Sandra Starke, Marta Ferrari, and Alan M. Wilson. 2009. Riding style improves horse racing times. *Science* 325 (5938): 289. <http://www.jstor.org/stable/2893079%7B%5C%7D0Ahttp://about.jstor.org/terms>.
- Pfau, Thilo, Thomas H Witte, and Alan M. Wilson. 2005. A method for deriving displacement data during cyclical movement using an inertial sensor. *The Journal of experimental biology* 208 (Pt 13): 2503–14. ISSN: 0022-0949. doi:10.1242/jeb.01658. <http://www.ncbi.nlm.nih.gov/pubmed/15961737>.
- Poirier, E, M Do, and Bruno Watier. 2007. Transition from seated to standing position in cycling allows joint moment minimization. *Science & Sports* 22 (5): 190–195. doi:10.1016/j.scispo.2007.08.002.
- Raasch, Christine C, and Felix E. Zajac. 1999. Locomotor Strategy for Pedaling : Muscle Groups and Biomechanical Functions. *Journal of Neurophysiology* 82:515–525.
- Rajagopal, Apoorva, Christopher Dembia, Matthew DeMers, Denny Delp, Jennifer Hicks, and Scott Delp. 2016. Full body musculoskeletal model for muscle-driven simulation of human gait. *IEEE Transactions on Biomedical Engineering* 63 (10): 2068–2079. doi:10.1109/TBME.2016.2586891.
- Rankin, Jeffery W, and Richard R. Neptune. 2010. The Influence of Seat Configuration on Maximal Average Crank Power During Pedaling: A Simulation Study. *Journal of Applied Biomechanics* 26:493–500.
- Reiser II, Raoul F, Joseph M Maines, Joey C Eisenmann, and John G Wilkinson. 2002. Standing and seated Wingate protocols in human cycling. A comparison of standard parameters. *European Journal of Applied Physiology* 88 (1-2): 152–157. doi:10.1007/s00421-002-0694-1.
- Riddick, Ryan C., and Arthur D. Kuo. 2016. Soft tissues store and return mechanical energy in human running. *Journal of Biomechanics* 49 (3): 436–441. ISSN: 18732380. doi:10.1016/j.jbiomech.2016.01.001.
- Ryschon, Timothy W., and James Stray-Gundersen. 1991. The effect of body position on the energy cost of cycling. *Medicine and Science in Sports and Exercise* 23 (8): 949–953. ISSN: 15300315.

- Saini, Meera, D. Casey Kerrigan, Mandyam A. Thirunarayan, and M. Duff-Raffaele. 1998. The vertical displacement of the center of mass during walking: A comparison of four measurement methods. *Journal of Biomechanical Engineering* 120 (1): 133–139. ISSN: 15288951. doi:10.1115/1.2834293.
- Sargeant, Anthony J. 2007. Structural and functional determinants of human muscle power. *Experimental Physiology* 92 (2): 323–331. doi:10.1113/expphysiol.2006.034322.
- Saunders, J B, V T Inman, and H D Eberhart. 1952. The major determinants in normal and pathological gait. *The Journal of Bone and Joint Surgery* 35 (3): 543–558.
- Seth, Ajay, Michael Sherman, Jeffrey A. Reinbolt, and Scott L. Delp. 2011. OpenSim: a musculoskeletal modeling and simulation framework for in silico investigations and exchange. *Procedia IUTAM* 2 (January): 212–232. doi:10.1016/J.PIUTAM.2011.04.021.
- Sharp, Archibald. 1977. *Bicycles and tricycles : an elementary treatise on their design and construction / by archibald sharp.* [in eng]. Cambridge, Mass.: MIT Press.
- Simón Mata, Antonio, Alex Bataller Torras, Juan Antonio Cabrera Carrillo, Francisco Ezquerro Juanco, Antonio Jesús Guerra Fernández, Fernando Nadal Martínez, and Antonio Ortiz Fernández. 2016. *Fundamentals of Machine Theory and Mechanisms*. 40:415. Mechanisms and Machine Science. Springer International Publishing. doi:10.1007/978-3-319-31970-4.
- Soden, P.D., and B.A. Adeyefa. 1979. Forces applied to a bicycle during normal cycling. *Journal of Biomechanics* 12 (7): 527–541. doi:10.1016/0021-9290(79)90041-1.
- Stone, Cal, and Maury L. Hull. 1993. Rider/Bicycle Interaction Loads During Standing Treadmill Cycling. *Journal of Applied Biomechanics* 9 (3): 202–218. doi:10.1123/jab.9.3.202.
- . 1995. The Effect of Rider Weight on Rider-Induced Laods During Common Cycling Situations. *Journal of Biomechanics* 28 (4): 365–375.
- Straw, Asher H., and Rodger Kram. 2016. Effects of shoe type and shoe-pedal interface on the metabolic cost of bicycling. *Footwear Science* 8 (1): 19–22.
- Tanaka, Hirofumi, David R Bassett, Shane K Best, and Kenny R Baker. 1996. Seated Versus Standing Cycling in Competitive Road Cyclists: Uphill Climbing and Maximal Oxygen Uptake. *Canadian Journal of Applied Physiology* 21 (2): 149–154.
- Taylor, C. Richard, Norman C Heglund, Thomas A Mcmahon, and Todd R Looney. 1980. Energetic Cost of Generating Muscular Force During Running: A Comparison of Large and Small Animals. *Journal of Experimental Biology* 86 (1): 9–18. ISSN: 0022-0949.

- Telli, Riccardo, Elena Seminati, Gaspare Pavei, and Alberto Enrico Minetti. 2016. Recumbent vs. upright bicycles: 3D trajectory of body centre of mass , limb mechanical work , and operative range of propulsive muscles. *Journal of Sports Sciences*. doi:10.1080/02640414.2016.1175650.
- Thirunarayan, Mandyam A., D. Casey Kerrigan, Marco Rabuffetti, Ugo Della Croce, and Meera Saini. 1996. Comparison of three methods for estimating vertical displacement of center of mass during level walking in patients. *Gait and Posture* 4 (4): 306–314. ISSN: 09666362. doi:10.1016/0966-6362(95)01058-0.
- Toft Nielsen, Emil, Peter Bo Jørgensen, Inger Mechlenburg, and Henrik Sørensen. 2019. Validation of an inertial measurement unit to determine countermovement jump height. *Asia-Pacific Journal of Sports Medicine, Arthroscopy, Rehabilitation and Technology* 16:8–13. ISSN: 22146873. doi:10.1016/j.aspmart.2018.09.002. <https://doi.org/10.1016/j.aspmart.2018.09.002>.
- Too, Danny, and Gerald E Landwer. 2003. The biomechanics of force and power production in human powered vehicles. *Human Power*, no. 55: 3–6. ISSN: 08986908.
- Turpin, Nicolas A., Antony Costes, Pierre Moretto, and Bruno Watier. 2016. Upper limb and trunk muscle activity patterns during seated and standing cycling. *Journal of Sports Sciences* 35 (6): 557–564.
- Uchida, Thomas K., Jennifer L. Hicks, Christopher L. Dembia, and Scott L. Delp. 2016. Stretching your energetic budget: How tendon compliance affects the metabolic cost of running. *PLoS ONE* 11 (3): 1–19. doi:10.1371/journal.pone.0150378.
- van Ingen Schenau, Gerrit J., and Peter R. Cavanagh. 1990. Power equations in endurance sports. *Journal of Biomechanics* 23 (9): 865–881.
- van Ingen Schenau, Gerrit J., W W van Woensel, P J M Boots, R W Snackers, and G de Groot. 1990. Determination and interpretation of mechanical power in human movement: application to ergometer cycling. *European journal of applied physiology and occupational physiology* 61 (1-2): 11–19. doi:10.1007/BF00236687.
- Vandewalle, Henry, G. Peres, J. Heller, J. Panel, and H. Monod. 1987. Force-velocity relationship and maximal power on a cycle ergometer. *European Journal of Applied Physiology and Occupational Physiology* 56:650–656.
- Wilkie, D. R. 1950. The relation between force and velocity in human muscle. *Journal of Physiology* 110:249–280. ISSN: 0022-3751. doi:10.1113/jphysiol.1949.sp004437.
- . 1960a. Man As a Source of Mechanical Power. *Ergonomics* 3 (1): 1–8. ISSN: 0014-0139. doi:10.1080/00140136008930462. <http://www.tandfonline.com/doi/abs/10.1080/00140136008930462>.

- Wilkie, D. R. 1960b. Man as an Aero Engine. *Journal Of The Royal Aeronautical Society* 64 (596).
- Wilkinson, Ross D., Andrew G. Cresswell, and Glen A. Lichtwark. 2020. Riders Use Their Body Mass to Amplify Crank Power during Nonseated Ergometer Cycling. *Medicine and Science in Sports and Exercise*, no. Published Ahead of Print.
- Wilkinson, Ross D., Glen A. Lichtwark, and Andrew G Cresswell. 2020. The Mechanics of Seated and Nonseated Cycling at Very-High-Power Output: A Joint-level Analysis. *Medicine and Science in Sports and Exercise* 52 (7): 1585–1594. ISSN: 0195-9131.
- Wilson, Alan M., and Glen A. Lichtwark. 2011. The anatomical arrangement of muscle and tendon enhances limb versatility and locomotor performance. *Philosophical Transactions of the Royal Society B: Biological Sciences* 366 (1570): 1540–1553. doi:10.1098/rstb.2010.0361. <http://rstb.royalsocietypublishing.org/cgi/doi/10.1098/rstb.2010.0361>.
- Wilson, Alan M., J. C. Lowe, K. Roskilly, P. E. Hudson, K. A. Golabek, and J. W. McNutt. 2013. Locomotion dynamics of hunting in wild cheetahs. *Nature* 498 (7453): 185–189. ISSN: 0028-0836. doi:10.1038/nature12295. <http://www.nature.com/doifinder/10.1038/nature12295>.
- Winter, David A. 1990. *Biomechanics and motor control of human movement*. 4th Ed. New York: Wiley.
- Yamaguchi, G. T., A. G. U. Sawa, D. W. Moran, M. J. Fessler, and J. M. Winters. 1990. A Survey of Human Musculotendon Actuator Parameters. Chap. Appendix in *Multiple muscle systems*, 717–773. Springer-Verlag.
- Zajac, Felix E., Richard R. Neptune, and Steven A. Kautz. 2002. Biomechanics and muscle coordination of human walking Part I : Introduction to concepts, power transfer, dynamics and simulations. *Gait and Posture* 16:215–232.
- Zelik, Karl E., and Arthur D. Kuo. 2012. Mechanical work as an indirect measure of subjective costs influencing human movement. *PLoS ONE* 7 (2). doi:10.1371/journal.pone.0031143.

Appendix A

A Theoretical Comparison of the Effect of Bicycle Lean on the Travel Path of the Bicycle

A.1 Introduction

Bicycles don't travel along a perfectly straight line. Even when in a seated posture riders make regular small adjustments to keep the system's CoM above the base of support. When shifting to a non-seated posture these adjustments become much larger but less frequent. The lean angle of the bicycle will cause the path of the bicycle to arc away from the imaginary straight line connecting the point from which you start to where you finish. The magnitude and frequency of these deviations may combine to impact performance depending on whether resistance to forward motion is due to conservative forces (i.e. gaining potential energy) or non-conservative forces (i.e. air resistance). We can see in Figure A.1 that the smooth periodic oscillations resemble that of a sine wave.

One argument against using bicycle lean is that it may increase the path length that a rider must travel between two points. Let's use an example of two common scenarios where riders use a non-seated posture to examine the possible effect of this increase in path length (See Table A.1).

A.2 Theoretical evaluation of path length

Our two scenarios are a 250 m low-velocity uphill climb and a 250 m high-velocity level sprint for the finish line. We will assume in both scenarios that the amplitude (A) of the sine wave is 0.25 m (See Figure A.1). This means the peak perpendicular distance the bicycle deviates away from the straight path in either direction is ± 0.25 m. To calculate the wave length (λ) we need to know the circumference of the bicycle tyre and the gain ratio of the drive train. The

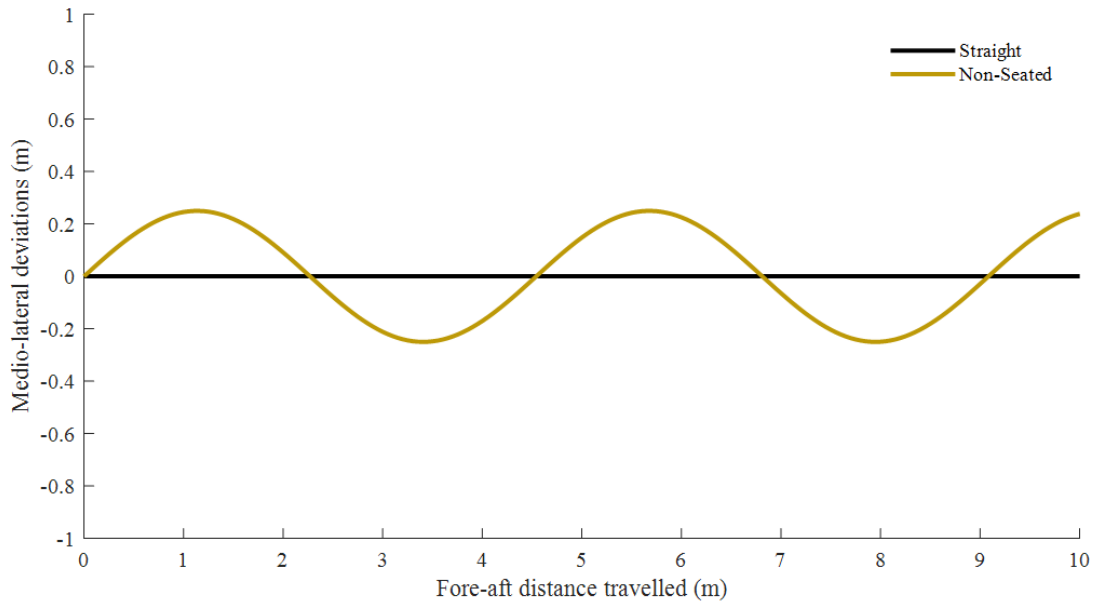


Figure A.1: Leaning and steer of the bicycle increases the path length between two points. Shown here is an aerial view of the theoretical travel path of a bicycle due to lean and steer compared to a straight path. In reality the front and rear wheels do not take the same path, therefore this example would perhaps be more representative of the path taken by the bicycle's CoM. *Data calculated using Equation A.1 and the hypothetical level sprinting scenario outlined in Table A.1.*

typical tyre size used in road racing is known as a “700x23C”, which has a circumference of 2.096 m. The gain ratio of the drive train is calculated by dividing the number of teeth on the front chain ring by the number of teeth on the rear sprocket connected by the chain. If cadence is known we can calculate the velocity of the bicycle by dividing the wave length by the time taken to complete one crank revolution. The time taken to complete one crank revolution can be calculated by dividing the number of seconds per minute by the number of crank revolutions per minute. Next we use the amplitude (A) and wave length (λ) to create our function with respect to the distance travelled (Equation A.1). Once we have our function we can then use numerical integration to find the length of a curve using the arc length formula (Equation A.2).

$$f(x) = A \cdot \sin\left(\frac{2\pi}{\lambda} \cdot x\right) + d \quad (\text{A.1})$$

$$L = \int_a^b \sqrt{1 + [f'(x)]^2} dx \quad (\text{A.2})$$

Finally, we can use the results of our integration to speculate about the impact of this increase in path length on many outcomes such as the increase in time taken to travel a set distance. The increase in time is simply calculated by dividing the increase in path length (250–L) by velocity.

These results (See Table A.1) suggest that leaning the bicycle causes a much greater increase in the path travelled at low velocity. This is due to the decrease in the wave length of the path taken. The lower velocity when climbing causes far more oscillations to occur over 250 m

	Scenario	
	Uphill climb	Level sprint
Straight line distance (m)	250	250
Wheel circumference (m)	2.096	2.096
Number of teeth on front chain ring	39	53
Number of teeth on rear sprocket	25	11
Pedalling cadence (rpm)	70	120
Amplitude of deviations (m)	0.25	0.25

	Result	
	Uphill climb	Level sprint
Total path length (m)	263.86	251.51
Increase in path length (m)	13.86	1.51
Relative increase in path length (%)	5.54	0.60
Velocity ($\text{m}\cdot\text{s}^{-1}$)	3.81	20.20
Time taken to travel new path length (s)	69.17	12.45
Increase in time versus straight line (s)	3.63	0.075

Table A.1: Leaning the bicycle at low velocity increases path length more so than at high velocity. Shown here is a comparison of the increase in path length due to the amplitude of the sinusoidal path taken by the bicycle during a hypothetical low-velocity climb and a high-velocity sprint. This comparison shows that for the same amplitude of lean and steer, the path length at low velocity is $\sim 5\%$ greater than at high velocity. *Data calculated using Equations 2.6–2.14*

than when at high velocity. Of course, there are many other variables that must be taken into account when trying to make exact predictions about the impact of bicycle lean on performance. However, if we assume our hypothetical scenarios are realistic then the increase in path length due to bicycle lean during high-velocity sprinting seems negligible compared to the $\sim 5\%$ increase in path length during low-velocity climbs.

A.3 Effect of path length on power output during uphill cycling

If using bicycle lean during certain uphill climbing scenarios increases the distance travelled by $\sim 5\%$ then it is important to consider how an increase in path length may affect uphill cycling performance. This effect is not as obvious as it seems, because the main resistance to forward motion during uphill cycling is the increase in gravitational potential energy, which is a non-conservative force. Thus, if air resistance is negligible, then the distance travelled does not affect the total amount of work that must be performed by the rider. With this in mind, we will re-visit the scenario of an uphill climb to look at how an increase in path length might affect the available options a rider has to produce the necessary amount of work against gravity to climb a set vertical height. In this example we will compare two riders climbing up a steep 180° hairpin turn who take different paths around the turn. The intuitive technique when cycling uphill is

to take the shortest route possible around corners. The theory being that this will minimise the distance that must be travelled and thus reduce the time taken to complete the climb. However, one must consider that in most cases the road has been carved out of the mountain in order to provide a level surface. Thus, before and after the hairpin turn the elevation on both sides of the road will be equal. Figure A.2 gives a schematic representation of this hairpin turn scenario.

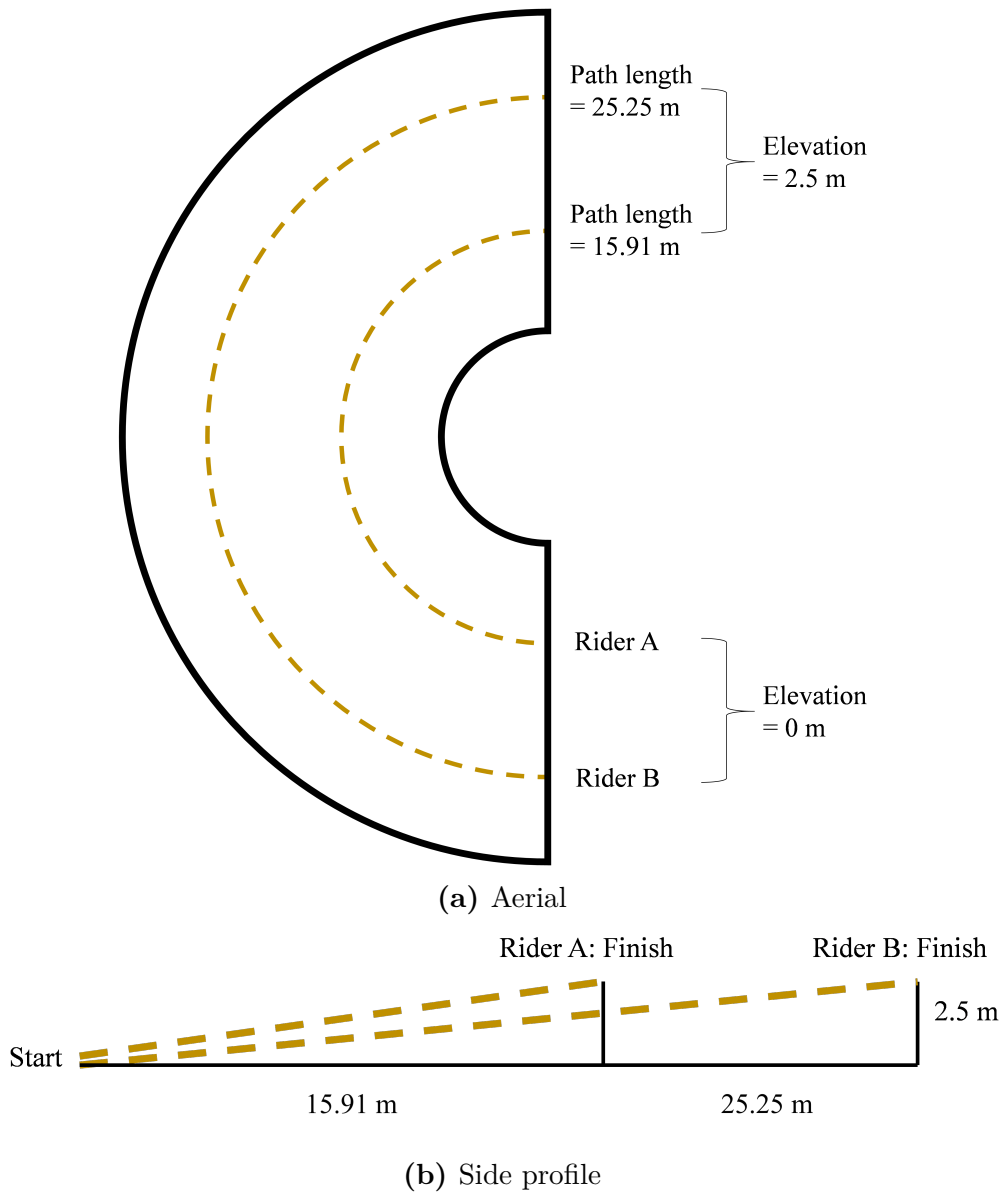


Figure A.2: Taking a wider path when climbing uphill could improve performance. A comparison of the two cornering paths taken by each rider. Because the main impedance to forward motion when climbing uphill is gravity, which is a conservative force, the distance taken by the rider does change the amount of mechanical work required. In fact, due to the decrease in slope it may be advantageous for muscular efficiency or power to take the wider path as it may allow the rider to perform the work using a higher cadence and less torque. *Data created from hypothetical scenario.*

Let's assume the following: 1) the total mass of each rider plus their respective bikes are both equal to 65 kg, 2) both riders generate the same power output, and 3) both riders are using the same gear ratio. If we negate the effects of air resistance then the total work required

to travel from the starting elevation (0 m) to the final elevation (2.5 m) will be equal to the increase in gravitational potential energy of the system calculated in Equation A.3.

$$\Delta GPE = mg\Delta h = 65 \cdot 9.81 \cdot 2.5 = 1594.13J \quad (\text{A.3})$$

If both riders are generating power (P) at 300 Watts then the time taken to travel their respective paths from start to finish will be equal to the gain in gravitational potential energy divided by the rate of generating energy calculated, which will be the same for both riders and is calculated in Equation A.4.

$$time = \frac{\Delta GPE}{P} = \frac{1594.13}{300} = 5.31sec \quad (\text{A.4})$$

Therefore, rider B covers 25.13 m in the same amount of time that rider A covers 15.71 m, and must mean that rider B travels at a greater velocity for the same power output. Given that power output is the product of force and velocity then the combination of crank torque and cadence produced by Rider B must be different to Rider A. The steps for calculating the level of crank torque, ground velocity, and cadence are shown in Table A.2. The equations used in Table A.2 are as follows:

$$\text{Distance per crank cycle (m)} = \frac{\text{wheel circumference (m)} \cdot \text{teeth on front chain ring}}{\text{teeth on rear sprocket}} \quad (\text{A.5})$$

$$\text{Time per crank cycle (s)} = \frac{\text{travel time (s)} \cdot \text{path length (m)}}{\text{Distance per crank cycle (m)}} \quad (\text{A.6})$$

$$\text{Cadence (rpm)} = \frac{60}{\text{time per crank cycle (s)}} \quad (\text{A.7})$$

$$\text{Angular velocity (rad} \cdot \text{s}^{-1}\text{)} = \frac{\text{cadence (rpm)} \cdot 2 \cdot \pi}{60} \quad (\text{A.8})$$

$$\text{Crank torque (N} \cdot \text{m}\text{)} = \frac{\text{P (W)}}{\text{angular velocity (rad} \cdot \text{s}^{-1}\text{)}} \quad (\text{A.9})$$

Rider A: Inside line		
Quantity	Calculation	Result
Distance travelled per crank cycle	$\frac{2.096 \cdot 39}{25} = 5.31 \cdot 15.91$	3.27 m
Time taken per crank cycle	$\frac{3.27}{60} = 0.0545$	1.09 sec
Cadence	$\frac{1.09}{1} = 1.09$	55.05 rpm
Angular velocity	$\frac{55.05 \cdot 2\pi}{60} = 5.76$	5.76 rad · s ⁻¹
Crank torque	$\frac{300}{5.76} = 52.08$	52.08 Nm

Rider B: Outside line		
Quantity	Calculation	Result
Distance travelled per crank cycle	$\frac{2.096 \cdot 39}{25} = 5.31 \cdot 25.25$	3.27 m
Time taken per crank cycle	$\frac{3.27}{60} = 0.0545$	0.67 sec
Cadence	$\frac{0.688}{1} = 0.688$	87.33 rpm
Angular velocity	$\frac{87.33 \cdot 2\pi}{60} = 9.14$	9.14 rad · s ⁻¹
Crank torque	$\frac{300}{9.14} = 32.83$	32.83 Nm

Table A.2: Taking a wider path around uphill corners can reduce the amount of torque required. Shown here is the effect of path length on crank torque and angular velocity when cycling uphill around a hairpin turn. This comparison is of two identical riders generating the same power output in the same gear ratio (39/25), but two different paths, one longer than the other. Taking the wider path increases cadence by 32 rpm, but reduces torque by 20 Nm. This strategy could be utilised by riders to help lower limb muscles operate closer to their optimal efficiency or power. *Data calculated using Equations 2.6–2.14*

The results (See Table A.2) show that by taking the shorter path length, rider A must generate greater crank torque at a lower cadence than rider B. These differences may have a significant impact on the metabolic energy expended by each rider during a long climb that involves multiple hairpin turns. Given that muscles are length and velocity dependent force producers, it seems reasonable to suggest that taking a longer path length around a hairpin turn would be preferable for muscle efficiency or power. It is also possible that the sinusoidal path created by steer and lean of the bicycle when riding uphill in a non-seated posture could be a deliberate strategy to allow lower limb muscles to operate closer to their optimal efficiency or power by taking a longer path length.

Appendix B

A Method for Tracking Centre of Mass Displacement During Non-Seated Cycling Using an Inertial Sensor

B.1 Abstract

Instantaneous crank power does not equal total joint power if a rider's centre of mass (CoM) gains and loses mechanical energy. Thus, estimating CoM motion and the associated energy changes can provide valuable information about cycling performance. To date, an accurate and precise method for tracking CoM motion during outdoor cycling has not been validated. **Purpose:** To assess the suitability of an inertial measurement unit (IMU) for tracking CoM motion during non-seated cycling by comparing vertical displacement derived from an inertial sensor mounted to the lower back of the rider to an attached marker cluster and to a kinematic estimate of vertical CoM displacement from a full-body musculoskeletal model (Model). **Methods:** IMU and motion capture data were collected synchronously for 10 seconds while participants ($n=7$) cycled on an ergometer in a non-seated posture at three power outputs and two cadences. A limits of agreement analysis, corrected for repeated measures, was performed on the range of vertical displacement between the IMU and the two other measures. A total of 303 crank cycles were analysed. **Results:** The IMU measured vertical displacement of the marker cluster with high accuracy (1.6 mm) and precision (3.5 mm) but substantially overestimated the kinematic estimate of rider CoM displacement. **Conclusion:** We interpret these findings as evidence that a single IMU placed on the lower back is unsuitable for tracking rider CoM displacement during non-seated cycling if the linearly increasing overestimation is unaccounted for.

B.2 Introduction

During non-seated cycling, tracking a rider's centre of mass (CoM) position can provide valuable information regarding rider and bicycle performance. At each instant during the crank cycle, the power output a rider generates is not equal to their total joint power if their CoM loses and gains mechanical energy (van Ingen Schenau and Cavanagh 1990). Previous research on non-seated cycling shows that a rider's CoM can gain and lose mechanical energy at rates of up to $4.5 \text{ W}\cdot\text{kg}^{-1}$ (Wilkinson, Cresswell, and Lichtwark 2020), which has a significant effect on peak force and power production within each crank cycle. Thus, combining crank power measurements with an estimate of CoM energy changes could provide valuable insights into how rider's maximise gross efficiency and maximal power output.

Estimating a rider's CoM position while cycling on an ergometer, treadmill, or over-ground can be done using an optical motion capture system. However, there are limitations to each of these experimental setups. Although ergometers allow multiple cycles to be collected per trial, they constrain the lateral dynamics of the bicycle, which changes the preferred movement pattern of the rider and may affect performance (See Chapter 5). Treadmills can provide a solution to ecological validity, but performing maximal sprinting is problematic due to the danger of matching the belt velocity to the rapid acceleration and high velocity of the bicycle wheels. Over-ground cycling can be captured, but the calibrated volume of the camera system will limit the number of cycles that can be collected. Thus, a method for tracking a rider's CoM motion when motion capture is not feasible would make it possible to examine the preferred movement pattern of cyclists outside of the laboratory.

Examining the interaction between a rider and their bicycle outside the laboratory is important because the preferred movement pattern of cyclists is dependent on lateral bicycle dynamics (See Chapter 5). A study of non-seated cycling on an ergometer showed that fluctuations in CoM energy increase in response to increasing power output, decreasing cadence, or both (Wilkinson, Cresswell, and Lichtwark 2020). Furthermore, a study of non-seated cycling on rollers showed that fluctuations in CoM energy are greater when riders use their preferred amount of bicycle lean compared to when self-restricting bicycle lean (See Chapter 5). Confirming whether these results extrapolate to over-ground cycling would further our understanding of the mechanics of non-seated cycling.

Total mechanical energy of the CoM is calculated as the sum of potential and kinetic energy. Calculating changes in potential energy depend on vertical displacement, while changes in kinetic energy depend on velocity in three dimensions. Traditionally, the CoM position is computed from full-body kinematic analyses using motion capture data and estimates of body segment inertial parameters (Eng and Winter 1993). To date, the best estimate of CoM displacement and velocity during non-seated cycling has been provided using this method (Wilkinson, Cresswell, and Lichtwark 2020). Because the CoM of quietly standing humans is located anterior to the lumbosacral joint, a single sacral marker has been suggested as a convenient and reliable

approximation of vertical CoM displacement during walking (Thirunarayan et al. 1996; Saini et al. 1998). This simplified method has been used to estimate the pattern of vertical CoM displacement during non-seated cycling (Soden and Adeyefa 1979) and appears to show good agreement with full-body kinematic results. Thus, tracking a single marker placed near the sacrum could provide a suitable estimate of CoM motion and associated energy changes during non-seated cycling.

Inertial measurement units (IMU), are commonly used to assess the acceleration of a single point representing the CoM (Pfau, Witte, and Wilson 2005; Esser et al. 2009; Wilson et al. 2013; Lintmeijer et al. 2018; Toft Nielsen et al. 2019). Pfau et al. (2005) have also demonstrated that this data can be processed to accurately determine displacement and orientation of a point on the trunk of a Thoroughbred horse during locomotion, when compared to optical motion capture. These results showed that the sensor error for tracking the trunk movement of the horse in each axis was less than 5% during walking and 7% during a trot or canter. Here, we assess the validity of an IMU mounted near the sacrum for measuring vertical CoM displacement and associated energy changes of cyclists while riding in a non-seated posture by comparing the derived vertical displacement of the IMU to an attached marker cluster tracked with gold-standard optical motion capture technology and to a kinematic estimate of vertical CoM displacement using a full-body musculoskeletal model.

B.3 Materials and methods

B.3.1 Participants

Seven people participated in this study (5 men and 2 women, age: 24 ± 13 yrs, height: 1.75 ± 0.07 m, mass: 71 ± 11 kg). Each participant gave written informed consent prior to participating in the study according to the procedures approved by the Human Ethics Committee of The University of Queensland.

B.3.2 Experimental design

All trials were performed on the same cycling ergometer (Excalibur Sport, Lode BV, Groningen, The Netherlands) with the saddle height and handlebar position matched to each participant's accustomed cycling position. Participants wore the same model of cycling shoes in their preferred shoe size (SH-R070, Shimano, Osaka, Japan) that clipped into the pedals (SH-R540, Shimano, Osaka, Japan). The single experimental session described below included a maximal power output test and six experimental trials in a non-seated posture.

At the beginning of the session, participants warmed-up by cycling at 100 W at their preferred cadence for 5 minutes. Participants then performed five maximal 5-s sprints in a seated posture, each separated by 3 minutes of rest, to determine their instantaneous maximal power output ($P_{max,i}$). Each participant's $P_{max,i}$ was used to individualise power output for their experimental

trials. Participant's completed six 10-second experimental trials in a non-seated posture at three different power outputs (10%, 30%, and 50% of $P_{max,i}$) and two different cadences (70 rpm and 120 rpm), each separated by 3 minutes of rest. Each participant completed the experimental trials in a randomised order. For all experimental trials, the ergometer was set to Hyperbolic mode, which ensured that the power output remained constant independent of cadence. Thus, participants were required to maintain the target cadence using feedback from the visual display on the ergometer for 10 seconds.

B.3.3 Optical motion capture

Before beginning the experimental trials, reflective markers and lightweight clusters were secured to the skin using a combination of double-side tape and self-adhesive bandage at previously described locations suitable for measuring full-body kinematics (Wilkinson, Lichtwark, and Cresswell 2020; Wilkinson, Cresswell, and Lichtwark 2020) (marker locations are shown in Figure B.1). The three-dimensional position of each marker was collected for 10 seconds at 200 Hz using an eight-camera, opto-electric motion capture system (Oqus, Qualisys AB, Gothenburg, Sweden). Motion capture data was processed using Qualisys Track Manager software (2019.1, Qualisys AB, Gothenburg, Sweden) before being exported to Matlab.

B.3.4 IMU

Before beginning the experimental trials, an IMU (BlueThunder Sensor, iMeasureU, Auckland, New Zealand) attached to a rigid cluster of reflective markers was secured to the rider's skin at the intersection of Tuffier's line and the midline of the lumbar spine (L4 spinous process) using double-sided tape (See Figure 1). The markers were attached such that the plane created by the markers corresponded to the XY plane of the IMU. A self-adhesive bandage was then wrapped around the cluster and torso of the rider to limit soft-tissue artefact. The IMU Research Application (iMeasureU, Auckland, New Zealand) was used to collect IMU data at 100 Hz via Bluetooth to an iPad (Apple, California, United States). The IMU contained a triaxial accelerometer ($\pm 16 \text{ g}$), triaxial gyroscope ($\pm 2000 \text{ }^{\circ}\text{s}^{-1}$), and triaxial magnetometer ($\pm 1200 \mu\text{T}$) with micro-electro-mechanical systems (MEMS) technology connected to a small circuit board. Thus, the sensor logged acceleration, angular velocity, and magnetic flux data in the three orthogonal planes. IMU and motion capture data were synced by lightly tapping the sensor prior to the start of the trial with a motion capture calibration wand. The collision between the sensor and wand marker provided a synchronised spike in their respective resultant accelerations.

The approach used in this study for calculating orientation and linear displacement of the IMU have been described previously (Pfau, Witte, and Wilson 2005). However, the IMU used did not output orientation, and hence we used freely available sensor fusion algorithm to determine sensor orientation (Madgwick, Harrison, and Vaidyanathan 2011). We further rotated

the IMU data about the vertical axis such that the heading direction was co-incident with the motion capture system in the static trial, thereby aligning the orientation of the two systems. During cycling trials, the quaternion orientation was used to rotate the linear acceleration and angular velocity of the IMU from its local-coordinate system to the global-coordinate system defined by gravity and due north. Acceleration due to gravity was then removed from the vertical component of the acceleration signal. The linear accelerations were then double integrated to calculate velocity and displacement. A short window (one cycle) was implemented for drift correction under the assumption that there would be small cycle-to-cycle variations in movement pattern because subjects were cycling at a constant power output and cadence. At each time point, the position of the rigid cluster was approximated by creating a virtual marker in the centre of the cluster, which was calculated as the mean position of the cluster markers.

Because different investigators use different names, symbols, and sets of rotation axes to define Euler angles, the notation used in this study has been provided in Table B.1.

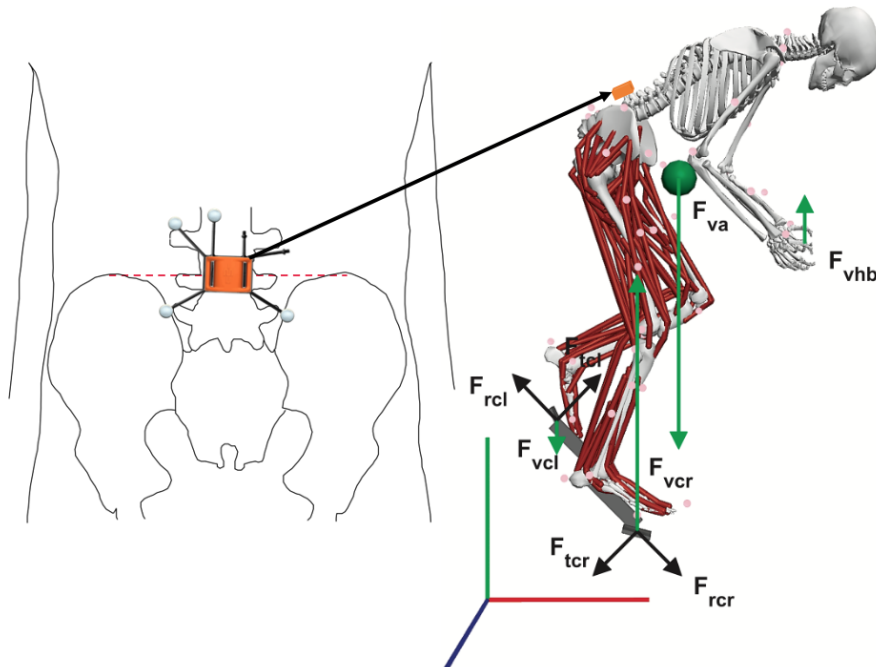


Figure B.1: A single inertial sensor was used to estimate rider CoM displacement during non-seated cycling. A. An IMU attached to a rigid marker cluster was secured to the skin at the intersection of Tuffier's line (dashed) and lumbar spine midline (\sim L4 spinous process). B. Sagittal plane view of a scaled musculoskeletal model cycling in a non-seated posture. The kinematic estimate of the rider's CoM position is represented by the green sphere.

B.3.5 Musculoskeletal model

Kinematic analysis was performed using a previously developed full-body musculoskeletal model (Rajagopal et al. 2016) within OpenSim software (Delp et al. 2007). A static trial was collected with each participant standing in a standard-anatomical posture to scale the model to each participant's anthropometry. Segment length of the arms, trunk, and legs were scaled in all

Local and global-coordinate systems	Right-handed cartesian
Global x, y, and z axis definitions	+x to the right, +y straight up, +z toward viewer (See Figure 1B)
Euler angles	Angular position about local x, y, and z axes defined as bank, heading, and attitude, respectively.
Symbols	$\psi = \text{bank}, \theta = \text{heading}, \phi = \text{attitude}$
Angular velocity	Angular velocity about local x, y, and z axes defined as roll (ψ_e), yaw (θ_e), and pitch (ϕ_e), respectively.
Euler angle rotation order	Heading, attitude, then bank
Angle units	Radians, radians per second

Table B.1: Notation, reference coordinates, and definitions used in this study.
Notation, reference coordinates, and definitions used to describe the orientation and motion of the IMU and marker cluster body in this study.

three axes using the distance between nominated marker pairs. Scaling factors were calculated by comparing these distances to that of the generic model. The mass of the participant was then used in combination with these scaling factors to distribute segment masses. The scaled model and motion capture data were used to run inverse kinematics via the Application Programming Interface between OpenSim and Matlab. The inverse kinematics tool within OpenSim calculates the position of each segment at each time step by using a weighted-least-squares fit to minimise errors between the experimental and the model markers. Segment positions as calculated by the inverse kinematic analysis are then combined with segment masses to determine the whole-body CoM location.

B.3.6 Statistical analysis

Sensor performance was quantified for each experimental condition as the root-mean-square (RMS) error in each Euler parameter describing the yaw, pitch, and roll components of the IMU angular velocity compared to the attached marker cluster body. For each trial, the mean error was calculated from the absolute error in each frame over the 10 seconds of data. The range of vertical IMU displacement within each crank cycle was compared across all experimental conditions to an attached marker cluster tracked with an optical motion capture system and to a kinematic estimate of vertical CoM displacement using a full-body musculoskeletal model.

Agreement between the IMU and the two other measures was assessed by applying a Limits of Agreement (LoA) approach (Bland and Altman 1999). LoA analyses were corrected for repeated measures and encompassed accuracy (Bias), precision (standard deviation), average error (bias/range), and maximum error (standard deviation/range). Different LoA calculations were carried out depending on whether a significant linear trend was identified in the distribution of differences between the IMU and the two other measures (IMU –measure) as a function of

the mean range of vertical displacement ($(\text{IMU} + \text{measure}) \div 2$). If a linear trend was identified, bias was calculated as the equation of the linear model, rather than a constant value (Bland and Altman 2007). Sphericity of the data was checked using Mauchly's test and non-parametric analyses were used when necessary. For non-parametric analyses, LoA were calculated as the median difference \pm 1.45 times the interquartile range of differences, rather than the mean difference \pm 1.96 times the standard deviation of differences. A simple linear regression was performed across all experimental conditions to identify the linear trend between the range of vertical IMU displacement to the two other measures. All statistical analyses were performed in Matlab. Normally distributed data are presented as mean \pm standard deviation (SD), whereas non-normally distributed data are presented as median \pm median absolute deviation (MAD).

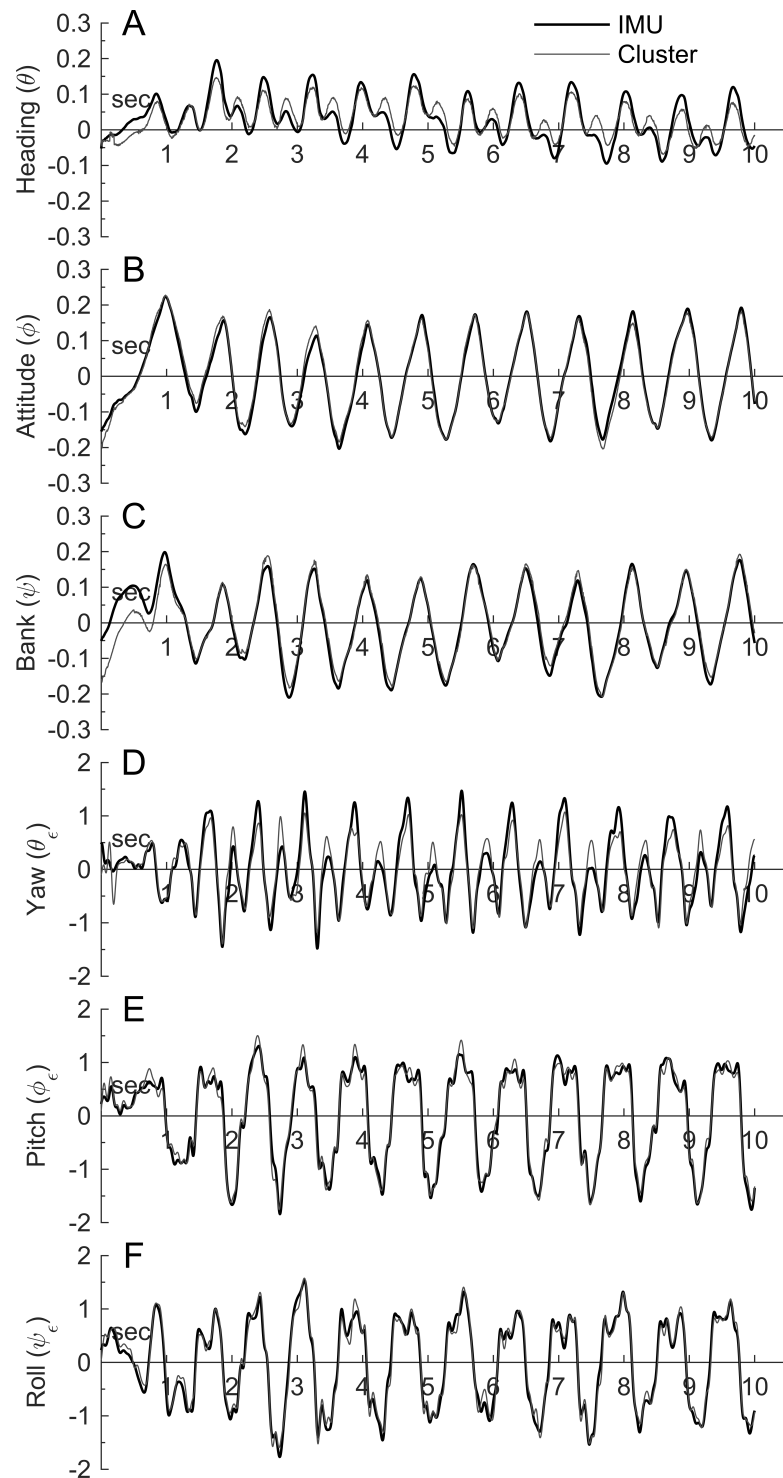


Figure B.2: The orientation of the sensor matched nicely with the attached marker cluster. Comparison of Euler angle and angular velocity parameters between the IMU and rigid marker cluster body for a single participant cycling in a non-seated posture at 30% $P_{max,i}$ at 70 rpm. All angle values are in radians and angular velocity values are in radians per second.

B.4 Results

To avoid any bias between the two cadence conditions at each power output, the number of cycles analysed from each participant was matched between each 70 rpm and 120 rpm condition. This meant that eight crank cycles were processed for each of the seven participants in each of the six conditions. Due to data dropout, 12 cycles were discarded, while a further 21 cycles were identified as outliers (>3 scaled median absolute deviations from the median) (Leys et al. 2013) and removed from the analysis. Thus, a total of 303 cycles were analysed (~ 7 cycles per condition per participant). The distribution of differences between the IMU and the two other measures violated Mauchly's test for sphericity, thus non-parametric analyses were used for all statistical comparisons.

B.4.1 Sensor Performance

The results of the sensor performance analysis are summarised in Table B.2. Group mean (\pm standard deviation) RMS errors between the IMU and marker cluster body are reported for each condition. The data shown in Figure B.2 illustrates how well the IMU was able to track the orientation and motion of the marker cluster body in all three axes.

B.4.2 IMU vs Optical motion capture

Differences between the IMU and marker cluster's range of vertical displacement were non-normally distributed with no significant linear trend. As such, a non-parametric, constant LoA analysis was performed. Linear regression results and Bland-Altman plots are presented in Figure B.4A and B, respectively. Across all conditions, there was high agreement between the IMU and marker cluster range of vertical displacement (See Table B.3). On average, the IMU marginally overestimated the cluster results by 1.6 ± 3.5 mm (accuracy \pm precision), which equated to an average error of $1.8 \pm 3.9\%$. Figure B.3 illustrates how well the IMU was able to track the marker cluster's vertical displacement during the crank cycle.

B.4.3 IMU vs Musculoskeletal model

Differences between the IMU and musculoskeletal model's range of vertical displacement were non-normally distributed and showed a significant linear trend. As such, a non-parametric, variable LoA analysis was performed. Linear regression results and Bland-Altman plots are presented in Figure B.4C and D, respectively. Across all conditions, the agreement between the IMU and marker cluster range of vertical displacement decreased at higher ranges of vertical displacement (See Table B.3). Across all conditions, the IMU substantially overestimated the cluster results, especially at higher ranges of vertical displacement. Figure B.3 illustrates the discrepancy between the IMU's vertical displacement and the model's vertical CoM displacement during the crank cycle.

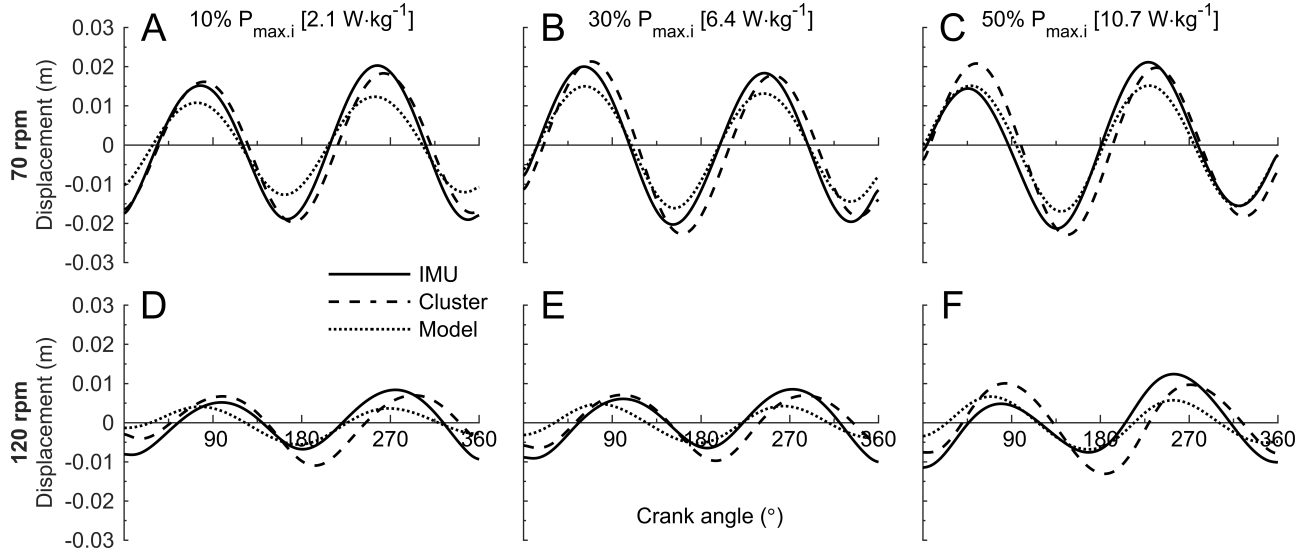


Figure B.3: The pattern of vertical IMU displacement matched well with the marker cluster and model's CoM. Group mean vertical displacement of the IMU, marker cluster body, and CoM of the musculoskeletal model with respect to crank angle (0° and 360° = top dead centre) during non-seated cycling at three power outputs (10% (A,D), 30% (B,E), and 50% (C,F) $P_{max,i}$) at 70 rpm (A-C) and 120 rpm (D-F).

	70 rpm			120 rpm		
	10% $P_{max,i}$	30% $P_{max,i}$	50% $P_{max,i}$	10% $P_{max,i}$	30% $P_{max,i}$	50% $P_{max,i}$
Yaw (θ_ϵ)	0.16 ± 0.02	0.19 ± 0.05	0.21 ± 0.02	0.22 ± 0.03	0.19 ± 0.05	0.24 ± 0.06
Pitch (ϕ_ϵ)	0.14 ± 0.02	0.15 ± 0.04	0.15 ± 0.02	0.17 ± 0.03	0.18 ± 0.08	0.19 ± 0.05
Roll (ψ_ϵ)	0.11 ± 0.03	0.15 ± 0.08	0.12 ± 0.01	0.18 ± 0.08	0.16 ± 0.02	0.17 ± 0.05

Table B.2: The sensor performance was excellent across all conditions. Group mean (\pm standard deviation) RMS error in each Euler parameter describing the yaw, pitch, and roll components of the IMU angular velocity ($\text{rad}\cdot\text{s}^{-1}$) compared to the rigid marker cluster body during non-seated cycling at three different power outputs (10%, 30%, and 50% $P_{max,i}$) and two different cadences (70 rpm and 120 rpm).

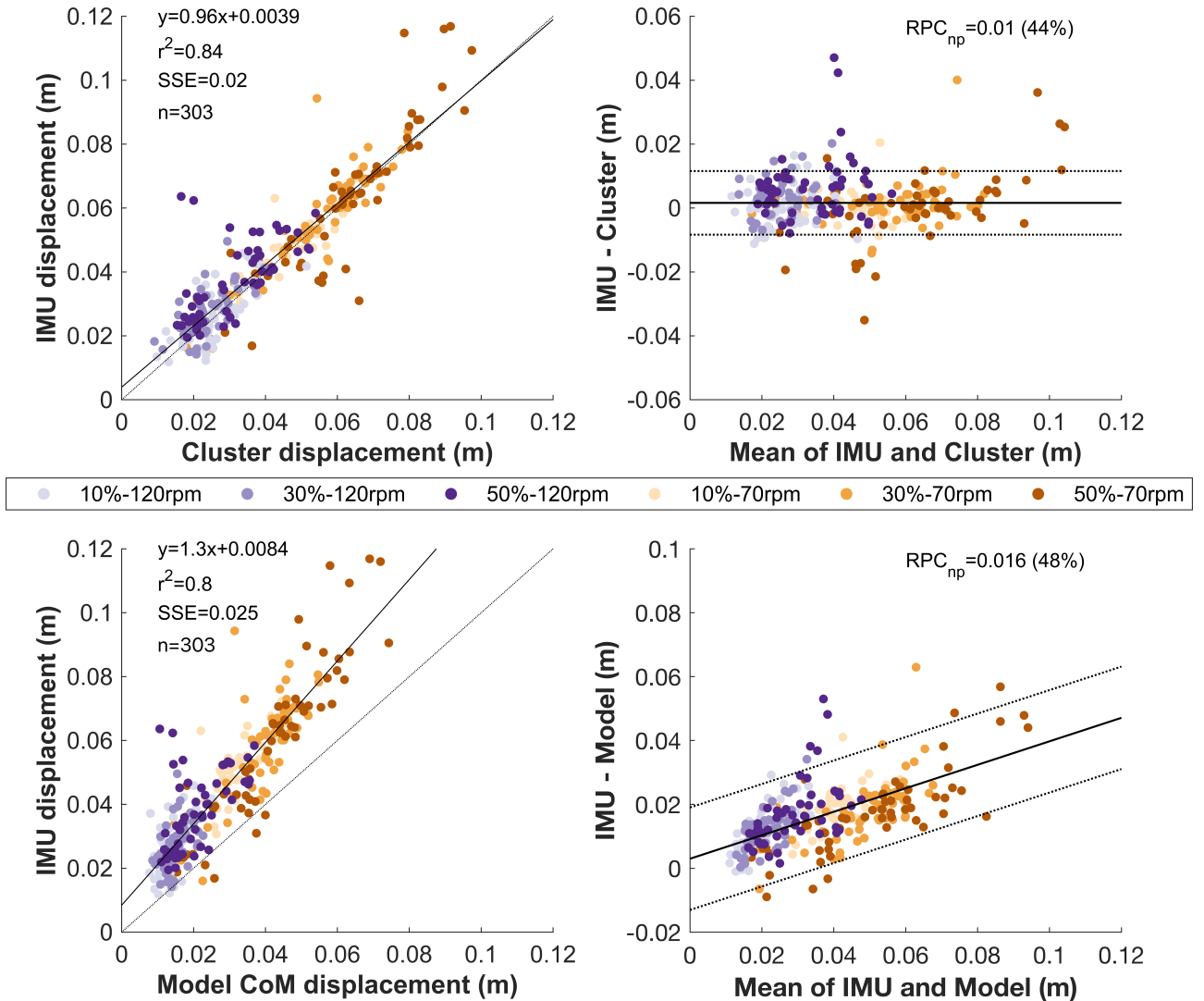


Figure B.4: The IMU tracked the cluster with high accuracy, but overestimated the model's range of vertical CoM displacement. A. Regression (left) and Bland-Altman plots (right) of the range IMU vertical displacement within each crank cycle as a function of Cluster vertical displacement (top) and Model CoM vertical displacement (bottom). The non-parametric repeatability coefficient (RPC_{np}) is also shown as a percentage of mean displacement.

	Agreement				Descriptive statistics		
	LloA	UloA	Accuracy (Bias)	Precision (MAD)	Range	Average error	Maximum error
IMU vs Cluster	-8.3	11.6	1.6	3.5	88.3	1.8%	±3.9%
IMU vs Model	0.37x -13.1	0.37x +19.0	0.37x+3.0	5.6	-	-	-

LloA, lower limit of agreement; UloA, upper limit of agreement; MAD, median absolute deviation; Average error = bias/range; Maximum error = precision/range.

Table B.3: There was good agreement between the IMU and cluster, but not between the IMU and model. A fixed limits of agreement analysis was used to compare the range of vertical displacement derived from an IMU to a rigid marker cluster. Positive values indicate an overestimation of the marker cluster's vertical displacement by the IMU (IMU –Cluster). All measures are in millimetres. A variable limits of agreement analysis was used to compare the range of vertical displacement derived from an IMU to the musculoskeletal model. All measures are in millimetres.

B.5 Discussion

The present study aimed to assess the suitability of a single IMU for tracking the vertical displacement of a rider's CoM displacement during non-seated cycling at three power outputs and two cadences. We found that the IMU overestimated the kinematic estimate of vertical CoM displacement and that this overestimation increased linearly with respect to the measured range of vertical CoM displacement. The IMU was able to identify the trend that the range of a rider's vertical CoM displacement during non-seated cycling increases in response to increasing power output and time per crank cycle, however, it underestimated the rate of this increase. The lowest power output trial in this study was approximately $2.1 \text{ W}\cdot\text{kg}^{-1}$, which is typical of steady-state cycling in a seated posture, suggesting that the IMU is likely to be more accurate during steady-state conditions compared to very-high-power output conditions. However, it should be noted that the non-seated posture is typically used for producing high-power outputs during climbing and sprinting.

We interpret our findings as evidence that a single IMU can track the vertical displacement of an attached marker cluster with high accuracy and precision, but unacceptable discrepancies exist between the vertical displacement of the IMU and the kinematic estimate of rider CoM displacement. While discrepancies between the single IMU and rider CoM increased with increasing power output and decreasing cadence, these increases were systematic and may be able to be accounted for using linear regression.

Across all trials, the IMU tracked the attached marker cluster with high accuracy and precision, but substantially overestimated the kinematic estimate of rider CoM displacement. This suggests that a rider's lower back goes through a larger range of vertical displacement during each crank cycle than their CoM. This makes intuitive sense as the motion of body segments other than the torso have a significant influence on the whole-body CoM. For example, previous research on seated cycling shows that the total segmental energy of the legs fluctuates during each crank cycle, predominantly due to changes in potential energy (Kautz and Neptune 2002). However, just as the range of CoM displacement increased in response to increasing power output, so too did the absolute difference between lower back and CoM displacement. This suggests that negative work done by the arms (Turpin et al. 2016; Wilkinson, Cresswell, and Lichtwark 2020) likely acts on the torso to decouple lower back movement from the torso CoM. Thus, it is evident that a single IMU on the lower back cannot account for the entirety of changes in CoM position due to motion of the legs and rotation of the torso during non-seated cycling.

We cannot rule out that a portion of the disagreement between the IMU and model was due to the processing of the IMU data, however, the accuracy between the IMU and cluster suggests the portion of disagreement due to processing errors was minimal. It is possible that small offsets were present due to the manual synchronisation process between the IMU and motion capture data, which could be avoided in future studies by using hardware-synchronised

systems. Another possible source of error was the misalignment between the IMU and marker cluster. The IMU was attached using a silicone putty which prevented any relative movement but does not guarantee that the alignment to the plane created by the marker clusters was exact. A misalignment between the IMU and marker cluster would cause a constant offset in the orientation data, however, small errors in orientation are known to have a minimal influence on linear displacements in a global-coordinate system (Pfau, Witte, and Wilson 2005).

Our data suggest that a single IMU placed on the lower back is not sufficient for tracking a rider's CoM displacement during non-seated cycling. It is possible that multiple IMUs would provide a solution to this problem, however, any additional weight or restriction of movement due to such a system would likely prevent its widespread use during cycling. It is possible that another location on the body may provide superior tracking of the CoM compared to the lower back. In general, the location of the CoM during non-seated cycling is in front of the pelvis and outside the body (See Figure B.1). Thus, an IMU placed on the front of the pelvis would be closer to the CoM, however, this location would still be unable to account for the influence of leg motion on CoM movement. Furthermore, we suspect that this location may be more likely to suffer from greater soft-tissue movement not related to the CoM movement (Riddick and Kuo 2016).

A single IMU placed on the lower back may still be suitable for other applications in the analysis of cycling. For example, a single IMU is lightweight and relatively low-cost, meaning it could provide a low-cost solution for identifying when a cyclist changes their posture from seated to non-seated. Our data suggest that the precision of the IMU would be adequate for providing within-condition comparisons. Our findings are in agreement with previous research that IMUs provide an accurate and precise measure of orientation and displacement of attached objects. Thus, a single IMU attached to the frame of a bicycle would be suitable for measuring the angular displacement and velocity of the bicycle frame; this and many other analytics could be provided by integrating an IMU with a cycling computer.

In summary, we found that, during non-seated cycling, a single IMU placed on the lower back overestimates a rider's vertical CoM displacement: as this displacement increases, the overestimation error increases linearly. Further development of a single-IMU method for measuring a rider's CoM displacement and associated mechanical energy fluctuations during over-ground cycling remains a future goal.

Appendix C

Supplementary Figures

C.1 Supplementary figures for study in Chapter 3

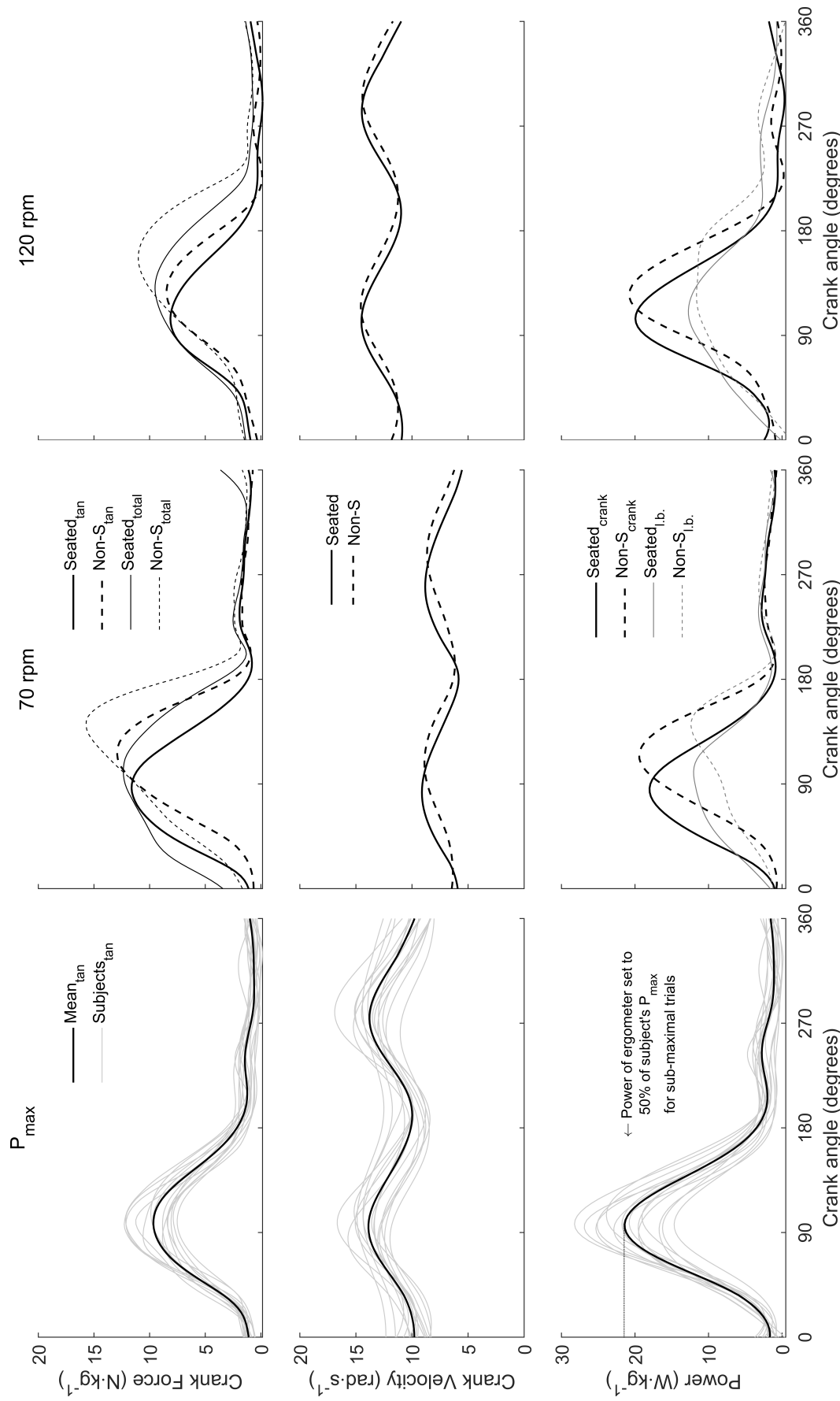


Figure C.1: Peak crank power far exceeds peak power generated by the leg during seated and non-seated cycling, suggesting that additional power is generated by muscles in the upper body or the rider's CoM. Participant and group mean crank force, velocity and power during the $P_{max,i}$ trials (left column) as well as a comparison of crank and leg power during the sub-maximal trials at 70 rpm (centre) and 120 rpm (right).

Supplementary Table 1. Group mean (\pm SD) peak angle (deg), velocity (deg·s $^{-1}$) and joint moments (Nm·kg $^{-1}$) at the hip, knee and ankle during high power output cycling (10.74 W·kg $^{-1}$) at low (70 rpm) and high (120 rpm) cadence.

	70 rpm		120 rpm	
	Seated	Non-Seated	Seated	Non-Seated
Hip extension				
Angle*†‡	43 \pm 5	30 \pm 5 ^a	42 \pm 5	32 \pm 5 ^a
Velocity†	-177 \pm 34	-167 \pm 26	-328 \pm 36 ^b	-315 \pm 38 ^b
Moment*†‡	-3.67 \pm 0.52	-4.25 \pm 0.68 ^a	-3.02 \pm 0.52 ^b	-3.11 \pm 0.57 ^b
Hip flexion				
Angle*†‡	89 \pm 6	79 \pm 4 ^a	92 \pm 5	84 \pm 4 ^{ab}
Velocity*†	155 \pm 33	185 \pm 35	259 \pm 33 ^b	294 \pm 36 ^{ab}
Moment*†‡	1.10 \pm 0.35	1.03 \pm 0.30	0.81 \pm 0.29 ^b	0.98 \pm 0.22
Knee extension				
Angle*†‡	23 \pm 6	14 \pm 3 ^a	33 \pm 6 ^b	21 \pm 5 ^{ab}
Velocity*†‡	-294 \pm 28	-295 \pm 24	-507 \pm 53 ^b	-548 \pm 42 ^{ab}
Moment*†‡	-1.49 \pm 0.41	-1.16 \pm 0.44 ^a	-0.81 \pm 0.10 ^b	-0.75 \pm 0.08 ^b
Knee flexion				
Angle*†‡	109 \pm 3	109 \pm 3	114 \pm 2 ^b	109 \pm 3 ^a
Velocity*†‡	324 \pm 56	417 \pm 43 ^a	497 \pm 46 ^b	520 \pm 38 ^b
Moment‡	1.68 \pm 0.34	1.58 \pm 0.25	1.52 \pm 0.21	1.70 \pm 0.27
Ankle plantar flexion				
Angle*†‡	-26 \pm 9	-32 \pm 5 ^a	-20 \pm 8 ^b	-26 \pm 7 ^{ab}
Velocity*†‡	-240 \pm 33	-316 \pm 55 ^a	-251 \pm 65	-259 \pm 54
Moment*†‡	-1.54 \pm 0.21	-2.02 \pm 0.22 ^a	-1.18 \pm 0.25 ^b	-1.37 \pm 0.25 ^{ab}
Ankle dorsiflexion				
Angle*†‡	25 \pm 5	20 \pm 5 ^a	11 \pm 6 ^b	9 \pm 6 ^b
Velocity‡	282 \pm 91	209 \pm 60 ^a	237 \pm 77	265 \pm 66
Moment‡	0.24 \pm 0.09	0.24 \pm 0.09	0.11 \pm 0.08 ^b	0.16 \pm 0.06 ^b

*Main effect of posture. †Main effect of cadence. ‡Interaction effect. ^aNon-Seated significantly different to Seated. ^b120 rpm significantly different to 70 rpm.

Table C.1: Peak knee extension moments decreased, while range of motion at the knee increased when non-seated at 70 rpm compared to when seated. Group mean (\pm SD) peak angle (°), velocity (°s $^{-1}$) and joint moments (Nm·kg $^{-1}$) at the hip, knee, and ankle during high power output cycling (10.74 W·kg $^{-1}$) at low (70 rpm) and high (120 rpm) cadence.

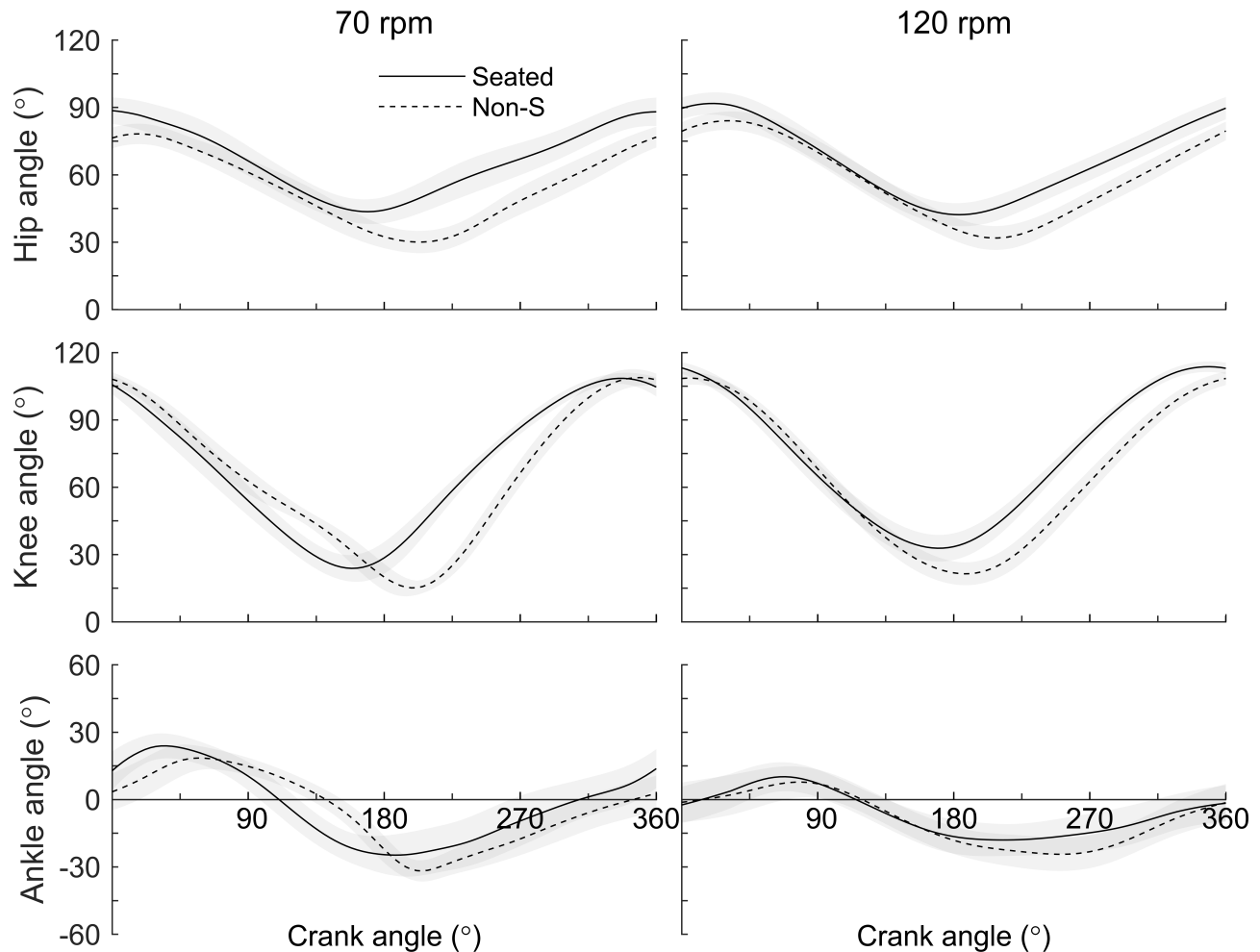


Figure C.2: The hip, knee, and ankle extend later in the crank cycle and to a greater extent when non-seated compared to when seated. Group mean (\pm SD, shaded area) joint angle with respect to crank angle at the hip, knee and ankle during each condition.

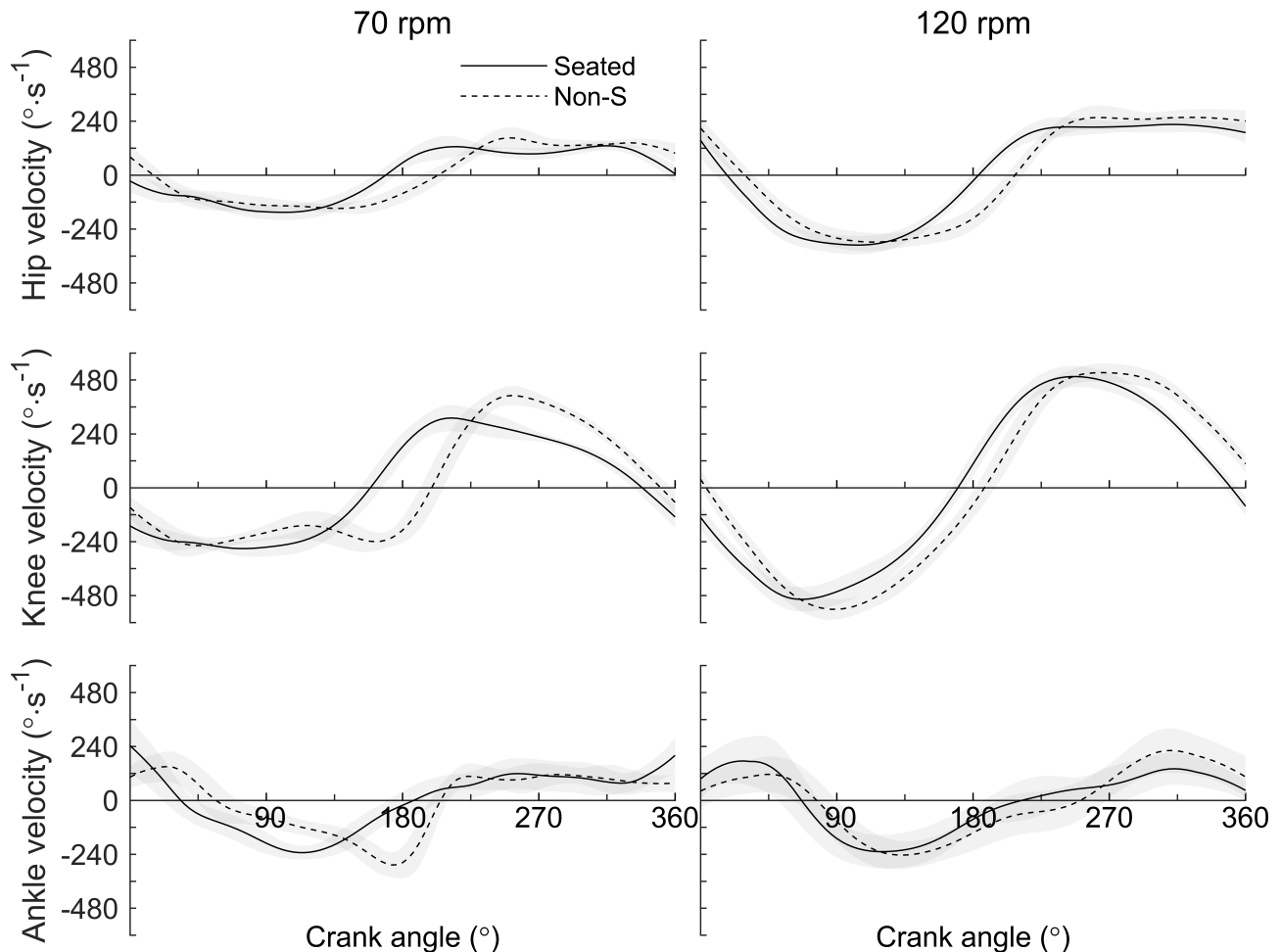


Figure C.3: Duty cycle of the knee increased at 70 rpm when non-seated compared to when seated, which also resulted in greater peak knee flexion velocity. Group mean ($\pm SD$, shaded area) joint velocity with respect to crank angle at the hip, knee and ankle during each condition.

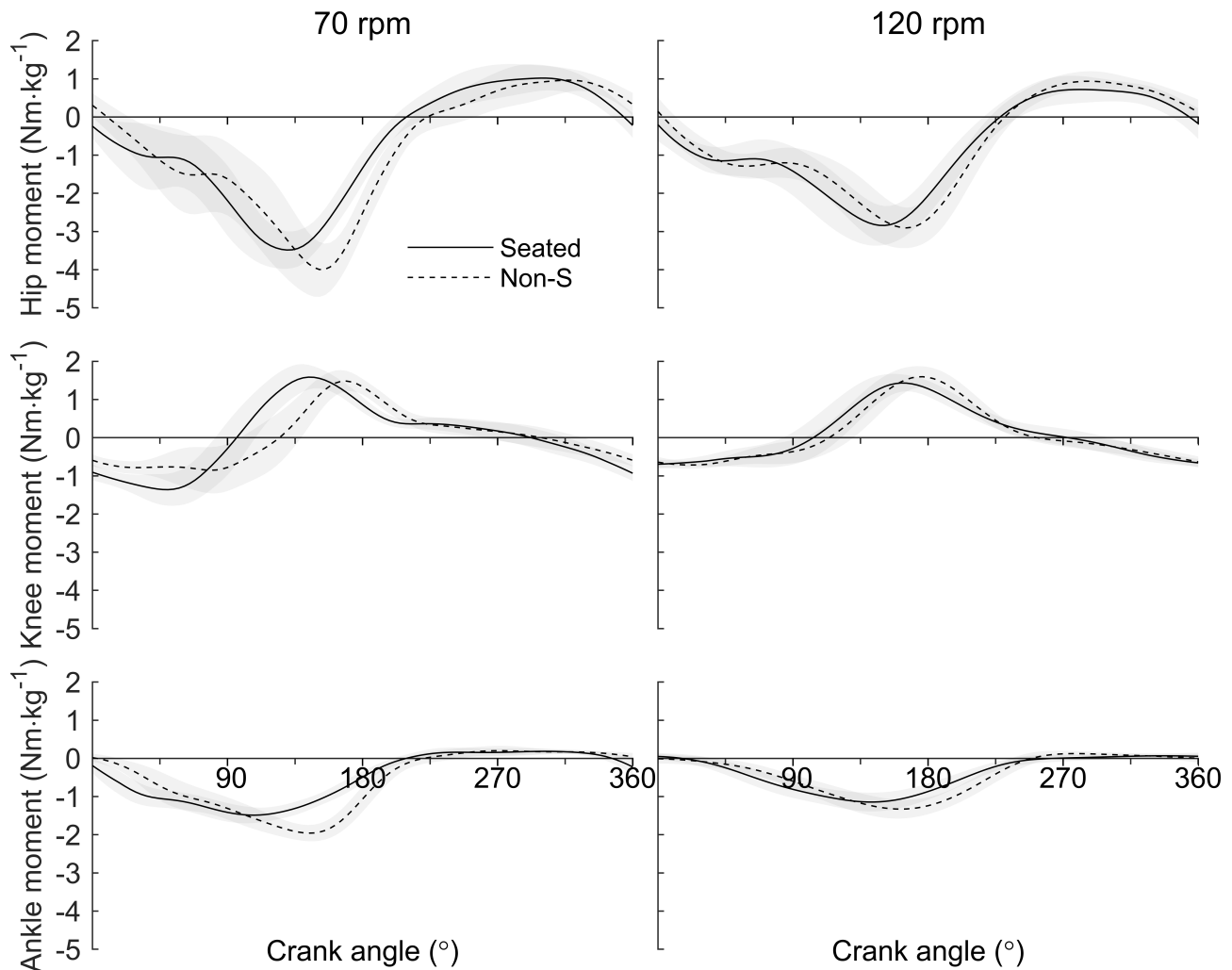


Figure C.4: Peak hip extension moments and ankle plantar flexion moments increased when non-seated at 70 rpm, likely due to an increased redistribution of net joint moments by bi-articular muscles. Group mean ($\pm\text{SD}$, shaded area) net joint moments with respect to crank angle at the hip, knee and ankle during each condition.

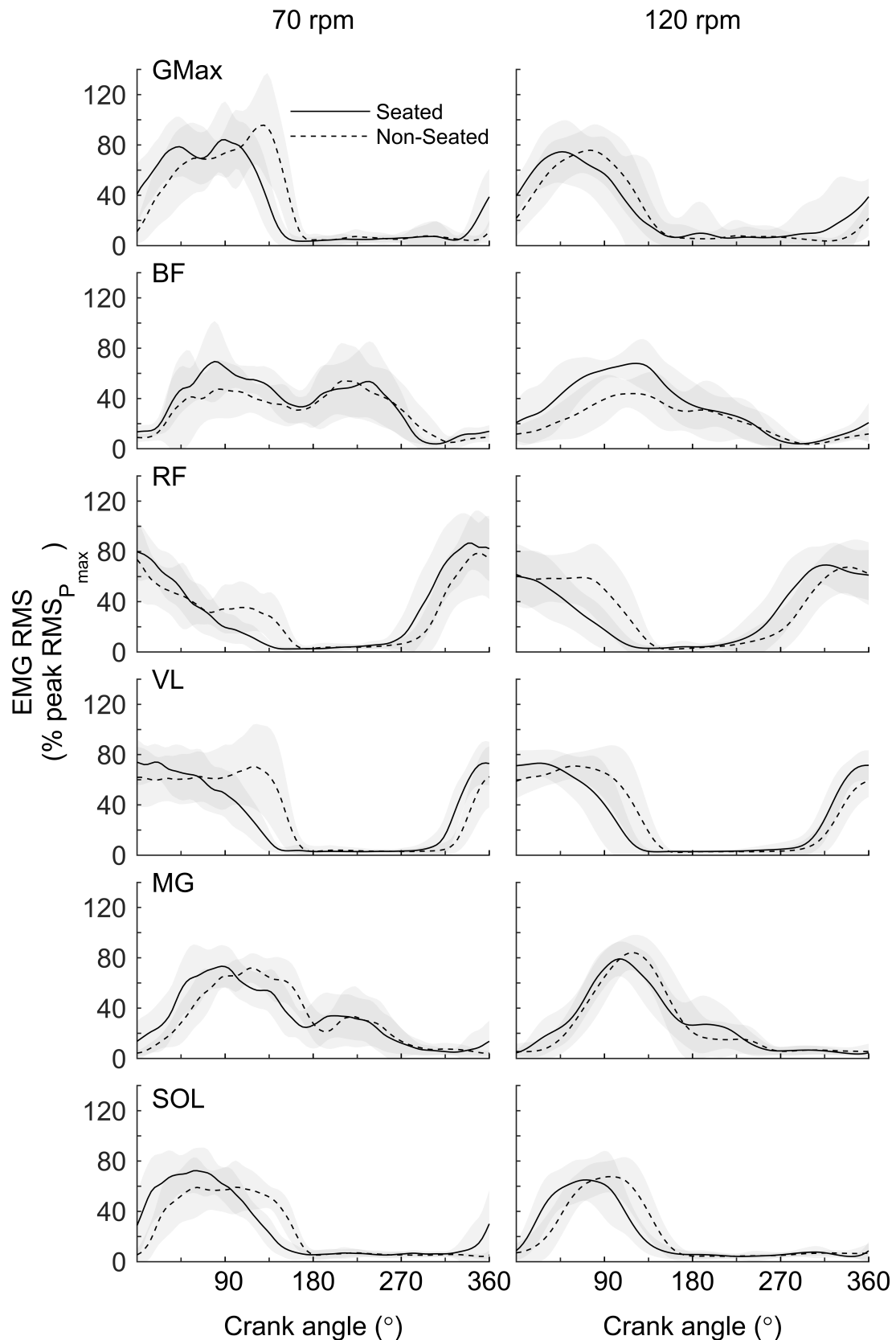


Figure C.5: The period of EMG activity of most muscles within the lower limb was shifted later in the crank cycle when cycling in a non-seated posture. Group mean (\pm SD, shaded area) EMG activity of muscles within the right lower limb with respect to crank angle during high-power output cycling at 70 rpm and 120 rpm in a seated and non-seated posture.

C.2 Supplementary figure for study in Chapter 4

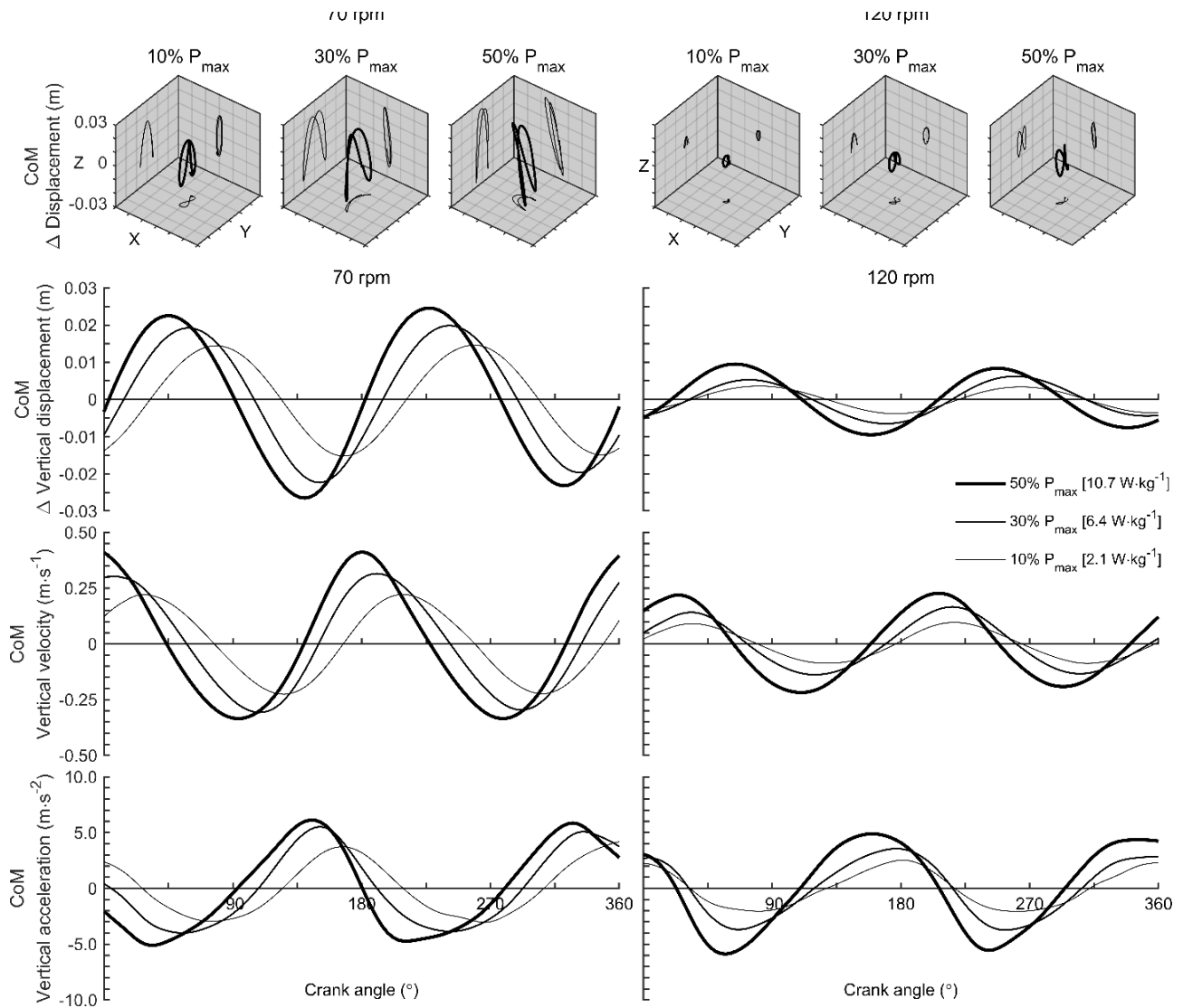


Figure C.6: Rider CoM displacement occurred predominantly in the vertical direction during non-seated cycling. Data in the cubes show the group mean CoM trajectory (green) projected onto three planes (black) during non-seated cycling under different power outputs (10%, 30%, and 50% $P_{max,i}$) at 70 rpm (left) and 120 rpm (right). The X, Y, and Z axes relate to CoM movement in the anterior-posterior, medio-lateral and vertical directions, respectively. Cartesian plots show the group mean CoM vertical displacement, velocity and acceleration with respect to crank angle (0° ; top dead centre) under the same conditions. Note that displacement is the result of work done on, or by, the CoM. Velocity is the result of power generated on, or by, the CoM. Acceleration is the result of vertical interaction force between the bicycle and the rider.

C.3 Supplementary figures for study in Chapter 5

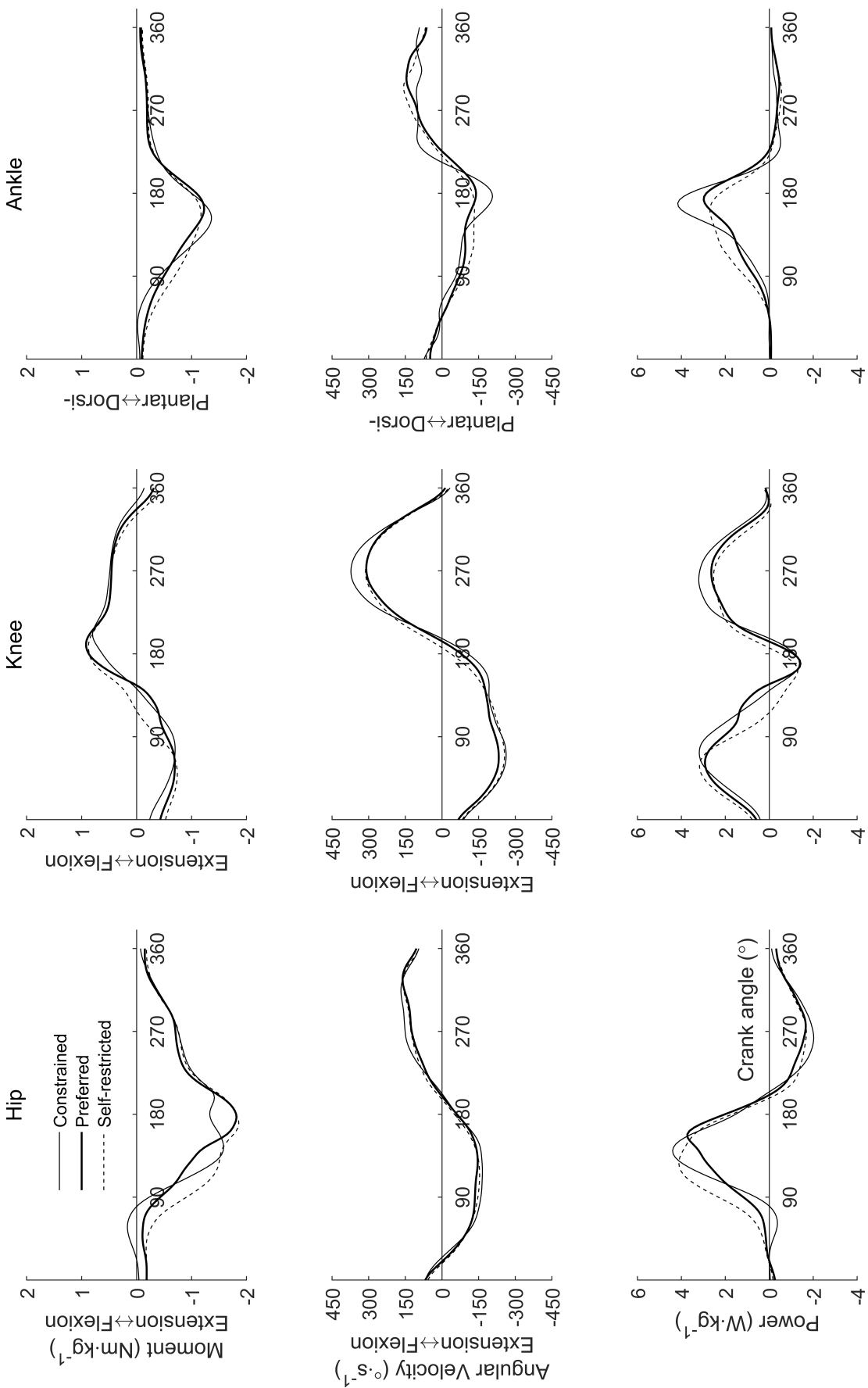


Figure C.7: Riders appeared to dissipate power at the knee much earlier in the crank cycle when self-restricting bicycle lean. Group mean net joint moments, joint velocities, and joint power at the hip, knee, and ankle in each condition. The altered pattern of power generation and dissipation within the right lower limb in the self-restricted condition points toward a greater demand on bi-articular knee extensors and flexors to transfer power from the knee to hip and ankle during the downstroke.

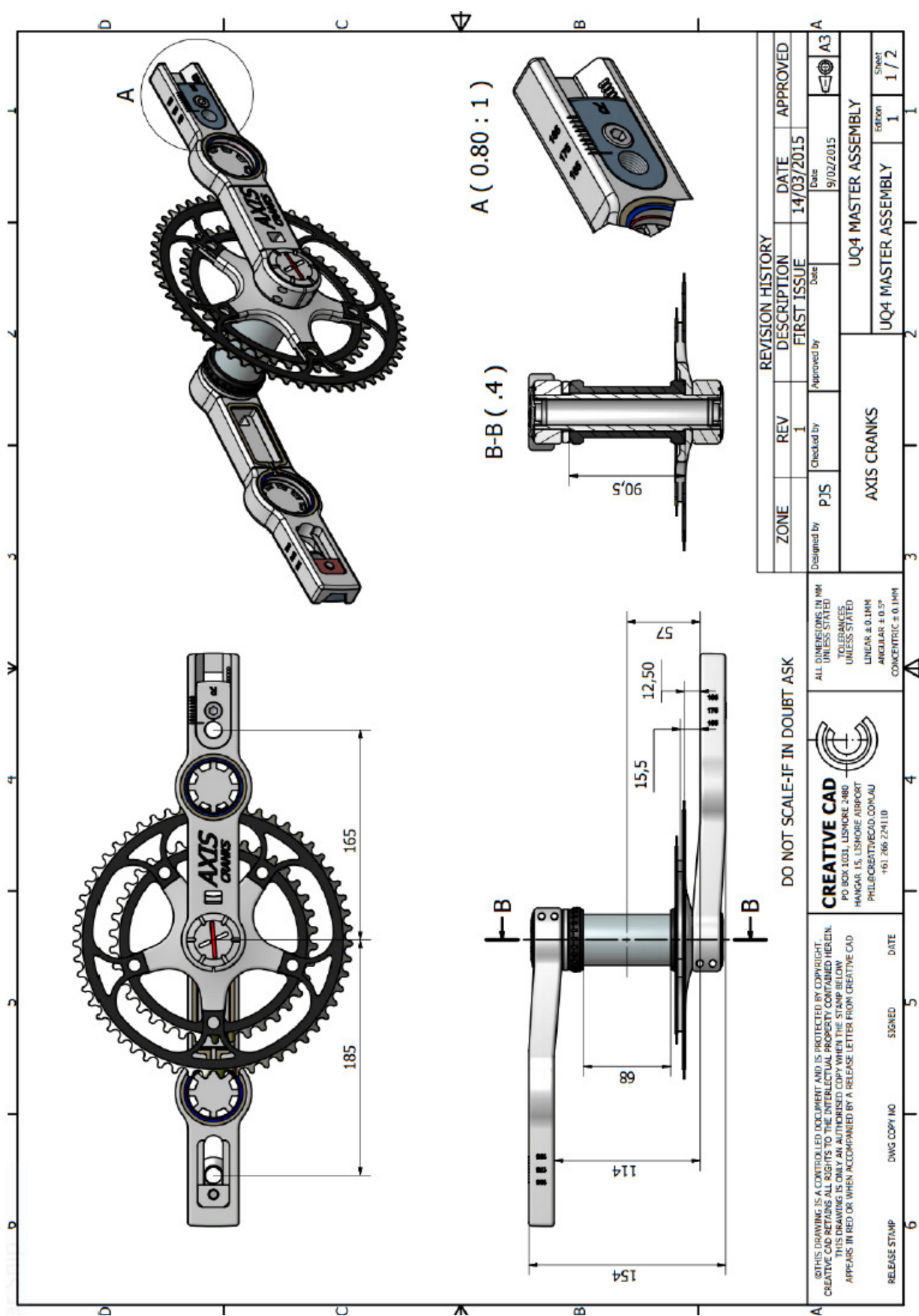


Figure C.8: Technical drawing of instrumented cranks used for study in Chapter 5.

Appendix D

Ethical Approval Forms

D.1 Ethical approval for studies in Chapters 3 and 4, and Appendix B



THE UNIVERSITY
OF QUEENSLAND
AUSTRALIA

School of Human Movement and Nutrition Sciences

HEAD OF SCHOOL
Professor Andrew Cresswell

The University of Queensland
Brisbane Qld 4072 Australia
Telephone (07) 3365 6241
International +61 7 3365 6241
Facsimile (07) 3365 6877
Email secretary@hms.uq.edu.au
Internet www.hms.uq.edu.au
CRICOS PROVIDER NUMBER 00025B

14th September, 2016

Mr Ross Wilkinson

School of Human Movement and Nutrition Sciences,
Connell Building
The University of Queensland
St Lucia QLD 4072

Dear Mr Wilkinson

Re: ethical review of the following project:

Effect of body position on muscle activity patterns during high-intensity cycling

Thank you for the opportunity to review your proposal. I am pleased to let you know that your project has been cleared in accordance with the ethical review guidelines at The University of Queensland. Your approval number is: HMS16/1409.

Please note that:

- (i) Amendments to any part of the approved protocol (however minor) should be submitted to me for consideration.
- (ii) Signed statements of informed consent should be kept secure in case we need to access them in the future.
- (iii) Any adverse side-effects or outcomes should be reported to me.

I wish you well with your research.

Yours sincerely,

Guy Wallis
Chair of the School of Human Movement and Nutrition Sciences Ethics Committee

D.2 Ethical approval for study in Chapter 5



THE UNIVERSITY
OF QUEENSLAND
AUSTRALIA

School of Human Movement and Nutrition Sciences

HEAD OF SCHOOL
Professor Andrew Cresswell

The University of Queensland
Brisbane Qld 4072 Australia
Telephone (07) 3365 6241
International +61 7 3365 6241
Facsimile (07) 3365 6877
Email secretary@hms.uq.edu.au
Internet www.hms.uq.edu.au
CRICOS PROVIDER NUMBER 00025B

4th August 2017

Mr Ross Wilkinson

School of Human Movement and Nutrition Sciences,
Connell Building
The University of Queensland
St Lucia QLD 4072

Dear Mr Wilkinson

Re: ethical review of the following project:

Effect of body position on muscle activity patterns during high-intensity cycling

Thank you for the opportunity to review your proposal. I am pleased to let you know that your project has been cleared in accordance with the ethical review guidelines at The University of Queensland. Your approval number is: HMS17/0908.

Please note that:

- (i) Amendments to any part of the approved protocol (however minor) should be submitted to me for consideration.
- (ii) Signed statements of informed consent should be kept secure in case we need to access them in the future.
- (iii) Any adverse side-effects or outcomes should be reported to me.

I wish you well with your research.

Yours sincerely,

Guy Wallis
Chair of the School of Human Movement and Nutrition Sciences Ethics Committee

Appendix E

Copyright Permissions

E.1 Copyright permission for Figure 2.1

RightsLink - Your Account

1/26/20, 8:05 PM

ELSEVIER LICENSE TERMS AND CONDITIONS

Jan 26, 2020

This Agreement between Mr. Ross Wilkinson ("You") and Elsevier ("Elsevier") consists of your license details and the terms and conditions provided by Elsevier and Copyright Clearance Center.

License Number	4755191323390
License date	Jan 24, 2020
Licensed Content Publisher	Elsevier
Licensed Content Publication	Neuroscience
Licensed Content Title	The constrained control of force and position in multi-joint movements
Licensed Content Author	G.J. van Ingen Schenau,P.J.M. Boots,G. de Groot,R.J. Snacken,W.W.L.M. van Woensel
Licensed Content Date	Jan 1, 1992
Licensed Content Volume	46
Licensed Content Issue	1
Licensed Content Pages	11
Start Page	197
End Page	207
Type of Use	reuse in a thesis/dissertation
Portion	figures/tables/illustrations
Number of figures/tables/illustrations	1
Format	both print and electronic
Are you the author of this Elsevier article?	No
Will you be translating?	No
Title	The implications of lateral bicycledynamics on rider centre of massmovement and limb mechanics duringnon-seated cycling
Institution name	The University of Queensland
Expected presentation date	Jun 2020
Portions	Figure 8
Requestor Location	Mr. Ross Wilkinson 777 Broadway
Publisher Tax ID	BOULDER, CO 80302 United States Attn: Mr. Ross Wilkinson 98-0397604

E.2 Copyright permission for Figure 2.2

RightsLink - Your Account

1/26/20, 8:04 PM

THE AMERICAN PHYSIOLOGICAL SOCIETY LICENSE TERMS AND CONDITIONS

Jan 26, 2020

This Agreement between Mr. Ross Wilkinson ("You") and The American Physiological Society ("The American Physiological Society") consists of your license details and the terms and conditions provided by The American Physiological Society and Copyright Clearance Center.

License Number	4755530302035
License date	Jan 24, 2020
Licensed Content Publisher	The American Physiological Society
Licensed Content Publication	Journal of Applied Physiology
Licensed Content Title	Muscle coordination in cycling: effect of surface incline and posture
Licensed Content Author	Li Li, Graham E. Caldwell
Licensed Content Date	Sep 1, 1998
Licensed Content Volume	85
Licensed Content Issue	3
Type of Use	Thesis/Dissertation
Requestor type	author of original work
Format	print and electronic
Portion	figures/tables/images
Number of figures/tables/images	1
Will you be translating?	no
World Rights	no
Order reference number	
Title	The implications of lateral bicycledynamics on rider centre of massmovement and limb mechanics duringnon-seated cycling
Institution name	The University of Queensland
Expected presentation date	Jun 2020
Portions	Figure 2
Attachment	japp05927002x.jpeg
Requestor Location	Mr. Ross Wilkinson 777 Broadway
Billing Type	BOULDER, CO 80302 United States Attn: Mr. Ross Wilkinson Invoice

E.3 Copyright permission for Figure 2.3

RightsLink - Your Account

1/26/20, 8:05 PM

WOLTERS KLUWER HEALTH, INC. LICENSE TERMS AND CONDITIONS

Jan 26, 2020

This Agreement between Mr. Ross Wilkinson ("You") and Wolters Kluwer Health, Inc. ("Wolters Kluwer Health, Inc.") consists of your license details and the terms and conditions provided by Wolters Kluwer Health, Inc. and Copyright Clearance Center.

License Number	4755200157549
License date	Jan 24, 2020
Licensed Content Publisher	Wolters Kluwer Health, Inc.
Licensed Content Publication	Medicine & Science in Sports & Exercise
Licensed Content Title	Joint-Specific Power Production during Submaximal and Maximal Cycling
Licensed Content Author	STEVEN ELMER, PAUL BARRATT, THOMAS KORFF, et al
Licensed Content Date	Oct 1, 2011
Licensed Content Volume	43
Licensed Content Issue	10
Type of Use	Dissertation/Thesis
Requestor type	University/College
Sponsorship	No Sponsorship
Format	Print and electronic
Will this be posted on a password protected website?	Yes
Portion	Figures/tables/illustrations
Number of figures/tables/illustrations	1
Author of this Wolters Kluwer article	No
Will you be translating?	No
Intend to modify/adapt the content	No
Title	The implications of lateral bicycledynamics on rider centre of massmovement and limb mechanics duringnon-seated cycling
Institution name	The University of Queensland
Expected presentation date	Jun 2020
Portions	Figure 1
Requestor Location	Mr. Ross Wilkinson 777 Broadway

E.4 Copyright permission for Figure 2.4

RightsLink - Your Account

1/26/20, 8:05 PM

ELSEVIER LICENSE TERMS AND CONDITIONS

Jan 26, 2020

This Agreement between Mr. Ross Wilkinson ("You") and Elsevier ("Elsevier") consists of your license details and the terms and conditions provided by Elsevier and Copyright Clearance Center.

License Number	4755200824483
License date	Jan 24, 2020
Licensed Content Publisher	Elsevier
Licensed Content Publication	Journal of Biomechanics
Licensed Content Title	Goniometric measurement of hip motion in cycling while standing
Licensed Content Author	M.L. Hull, Andrew Beard, Hemant Varma
Licensed Content Date	Jan 1, 1990
Licensed Content Volume	23
Licensed Content Issue	7
Licensed Content Pages	17
Start Page	687
End Page	703
Type of Use	reuse in a thesis/dissertation
Portion	figures/tables/illustrations
Number of figures/tables/illustrations	1
Format	both print and electronic
Are you the author of this Elsevier article?	No
Will you be translating?	No
Title	The implications of lateral bicycledynamics on rider centre of mass movement and limb mechanics during non-seated cycling
Institution name	The University of Queensland
Expected presentation date	Jun 2020
Portions	Figure 11
Requestor Location	Mr. Ross Wilkinson 777 Broadway
Publisher Tax ID	BOULDER, CO 80302 United States Attn: Mr. Ross Wilkinson 98-0397604

When the spirits are low, when the day appears dark, when work becomes monotonous, when hope hardly seems worth having, just mount a bicycle and go out for a spin down the road, without thought on anything but the ride you are taking

Sir Arthur Conan Doyle,
Scientific American, Volume 74, January 18, 1896.